FROM DEPLOYMENTS OF ELDER CARE SERVICE ROBOTS TO THE DESIGN OF AFFORDABLE LOW-COMPLEXITY END-EFFECTORS AND NOVEL MANIPULATION TECHNIQUES

Caio Cesar Rodrigues Mucchiani

A DISSERTATION

in

Mechanical Engineering and Applied Mechanics

Presented to the Faculties of the University of Pennsylvania

in

Partial Fulfillment of the Requirements for the

Degree of Doctor of Philosophy

2021

Supervisor of Dissertation

Mark Yim, Director, GRASP Lab; Asa Whitney Professor, MEAM

Graduate Group Chairperson

Michelle J Johnson, Associate Professor of Physical Medicine and Rehabilitation

Dissertation Committee

Vijay Kumar, Nemirovsky Family Dean of Penn Engineering

FROM DEPLOYMENTS OF ELDER CARE SERVICE ROBOTS TO THE DESIGN OF AFFORDABLE LOW-COMPLEXITY END-EFFECTORS AND NOVEL MANIPULATION TECHNIQUES

Pai, Mãe, Camila, amo vocês!

ACKNOWLEDGEMENT

I would like to acknowledge all colleagues from Modlab and GRASP, as well as Jeremy and Terry, whose help both in terms of hardware and technical input were extremely helpful for many challenges in this thesis. A special thanks to my thesis committee Dr. Michelle J Johnson and Dr. Vijay Kumar for all the help and feedback on improving this thesis, Dr. Johnson also overseeing and actively participating in many of the studies here presented. Thanks to Dr. Cacchione for the very needed insights on studies with the elderly, and help during all field deployments. Thanks to Bruno Gabrich for the emotional support from experiments to conferences and off lab hours. Finally, thanks to Dr. Mark Yim, for his trust, support and unique creativity insights that were seed to many of the concepts here presented.

ABSTRACT

FROM DEPLOYMENTS OF ELDER CARE SERVICE ROBOTS TO THE DESIGN OF AFFORDABLE LOW-COMPLEXITY END-EFFECTORS AND NOVEL MANIPULATION TECHNIQUES

Caio Cesar Rodrigues Mucchiani

Mark Yim

This thesis proposes an investigation on both behavioral and technical aspects of human-robot interaction (HRI) in elder care settings, in view of an affordable platform capable of executing desired tasks. The behavioral investigation combines a qualitative study with focus groups and surveys from not only the elders' standpoint, but also from the standpoint of healthcare professionals to investigate suitable tasks to be accomplished by a service robot in such environments. Through multiple deployments of various robot embodiments at actual elder care facilities (such as at a low-income Supportive Apartment Living, SAL, and Program of All-Inclusive Care, PACE Centers) and interaction with older adults, design guidelines are developed to improve on both interaction and usability aspects. This need assessment informed the technical investigation of this work, where we initially propose picking and placing objects using end-effectors without internal mobility (or zero degrees-of-freedom, DOF), considering both quasi-static (tipping and regrasping as in-hand manipulation) and dynamic approaches. Maximizing grasping versatility by allowing robots to grasp multiple objects sequentially using a single end-effector and actuator is also proposed. These novel manipulation techniques and end-effector designs focus on minimizing robot hardware usage and cost, while still performing complex tasks and

complying with safety constraints imposed by the elder care facilities.

Contents

Chapter 1

Introduction

Older adults are forming a much larger percentage of the population leading to a strain in the healthcare sector. It is expected that the population aged 65 and over in the United States (US) alone will double in the next 30 years [117], and similarly worldwide [151]. Despite abundance of the facilities to accommodate the growing older adult population, there is a shortage of caregivers to staff these facilities [165]. Additionally, the current COVID-19 pandemic has greatly impacted older adults living in group settings, since the risk for severe illness from COVID-19 increases with age [139]. With the scarcity of care options available, affordable robots may be a creative solution for simple tasks that would normally be handled by a caregiver. Tasks essential to maintain older adults' independence, such as toileting, eating, or bathing are called Activities of Daily Living, or ADLs. Furthermore, tasks referred to as Instrumental Activities of Daily Living, or IADL, are tasks such as using a telephone, cooking, doing laundry or using transportation [146]. Service robots can help older adults be more independent with ADLs and IADLs. This implies the robot will not only have the ability to communicate with the older adult by voice or with an user-interface (UI) but also manipulate objects around it with a manipulator and end-effector. Given that current solutions for both mobile robots and manipulators are not affordable by most elder care facilities, low-cost solutions are necessary in order to leverage adoption and approval of these robot platforms.

This thesis proposes an investigation on both behavioral and technical aspects of human-robot interaction in elder care settings in view of an affordable platform capable of executing desired tasks. The behavioral investigation is a need assessment that combines a qualitative study with focus groups and surveys from not only the elders' standpoint, but also from the standpoint of healthcare professionals to investigate suitable tasks to be accomplished by a service robot in such environment. Through multiple deployments of the robot at actual elder care facilities (such as at a low income Supportive Apartment Living, SAL or Program of All-Inclusive Care, PACE Center) and interaction with older adults, design guidelines are developed in order to improve on both interaction and usability aspects. The

technical investigation proposes a different approach to conventional grasping and manipulation techniques. Inspired by the constraints imposed by low-income elder care community settings to the complexity of an assistive robot, novel manipulation techniques and end-effectors focusing on minimizing hardware usage and cost, along with the safety requirements are proposed: object picking through in-hand manipulation (PnP, or Pick-in-Place) using end-effectors with no internal mobility (or zero degrees-of-freedom, DOF), a low-cost manipulator for assisting older-adults in manipulation tasks and grasping of multiple objects sequentially with a serpentine-type end-effector design.

The Pick in Place (PnP) in-hand manipulation technique allows for picking objects off a flat surface with an end-effector that can be abstracted as a collection of two point fingers with fixed separation distance. The resulting operation incorporates tipping and regrasping as in-hand manipulation operations. This technique can be applied to a wide range of scenarios, (such as complement the common parallel-jaw gripping) and also be directly applied to placing objects back on a flat surface. Since most robotic grippers have their cost determined by the number of actively controllable DOF, the proposed solutions represent low-cost alternatives to more conventional ones, and suggest new approaches to well-know robotic manipulation operations, such as pick-and-place and rolling. The problem may be solved considering quasi-static (Chapter 3) or dynamic (Chapter 5) approaches.

The lack of mobility is advantageous in human interactions, as no forces can be applied directly to the object by the end-effector, and so the manipulated item be safely placed or removed by humans. The development of an affordable mobile manipulator robot for applications in low resource community based settings seeks to endow the robot with capabilities for providing walking and hydration support, basic reaching assist and game based assistance for active and frail elders who may also have motor and mild cognitive impairment. These manipulation tasks may require the robot to manipulate various objects, not necessarily in the vicinity of each other, or even multiple objects at the same time (such as a box of pills and a water bottle). The sequential grasp of multiple objects therefore aims to facilitate this object retrieval by the robot in case older adults may be physically impaired to do so. A serpentine type tendon driven underactuated design with a closing mechanism that is triggered upon contact with an object allows the end-effector to grasp multiple objects not necessarily in its vicinity. This end-effector can grasp objects without knowing the size a priori and has a single DOF for actuation. A low-cost prototype demonstrates two implementations of the end-effector (radius estimation and autonomous grasp of circular objects by torque control, and sequential grasps of multiple objects) through several experiments. A method for estimating applied internal forces is also proposed.

The outline of this thesis is as follows. Chapter 2 discusses relevant literature for the studies of social and service robots and affordable-low-complexity manipulation relevant to the context of elder care robotics. Chapter 3 presents a qualitative

study with stakeholders aimed to inform robot tasks of potential benefit to older adults, and subsequent deployments of a mobile service robot modified to perform such tasks at low-income elder care facilities. Chapter 4 proposes a novel grasping and manipulation method and hardware that can benefit previously ranked manipulation tasks during robot interactions with the older adult population. Chapter 5 investigates a more practical scenario on achieving grasps as stated on Chapter 4, using similar hardware design but relaxing some assumptions in order to increase performance in robot deployment scenarios. Chapter 6 presents additional end-effector hardware design and experimentation capable of addressing more ranked tasks from the qualitative study. Chapter 7 presents the conclusion and contributions.

Chapter 2

Related Work

2.1 Elder Care Robotics

As a recent largely explored field in robotics, there are various types of interaction found in elder care robotics research. Numerous studies considered different methods of investigation as well as types of robot interaction: Companionship [130, 9], hygiene [77] , reminders [120] , entertainment [146], among others [102, 16] . In one study [16], robots for elder care were categorized as rehabilitation robots (such as smart wheelchairs and artificial limbs) and social assistive robots (SAR) [43, 84]. In particular, SAR [44] are emerging both academically and commercially [69] and can be subdivided into service type (as Healthbot [157] capable of entertaining older adults, as well as vital sign measurement, medication management and fall detection) and companion type (such as commercially known robots, Paro and AIBO)[11, 70]. Previous work where mobile robotic applications have been deployed with active elders and elders with mental and physical impairment, different methods used to promote exercise as well as different types of robot interactions including the more recent demand for robots amidst the COVID-19 pandemic are discussed in sequence.

2.1.1 Assisting older adults with and without impairments

Improving the cognitive ability of elders with dementia by interacting with robots has been investigated by several authors using different robotic platforms such as [132], [82], [156], [155], [22] and [10]. In [154] the robot (*UMA*) was intended to assist older adults and disabled people with transportation of objects over short distances. The mobile robot recognizes a color marker held by the user and follows it while carrying the payload, However, the robot was not deployed in a real facility nor used by older adults. Walking support for older adults by a robotic platform was proposed in [149]. In [66],[65] a *Healthbot* robot was introduced as a versatile mobile base capable of assessing vital signs, facial recognition, fall detection, medication

reminding and other features. This robot did not have a manipulator. A mobile robot targeted for older adults with Mild Cognitive Impairment was developed in [49] capable of intelligent reminders, such as medications, cognitive stimulation using video calls and autonomous fall detection. In [77], a robot (*Cody*) was designed to help older adults in hygiene tasks, such as bathing, using two manipulator arms.

2.1.2 Mobile manipulators and elder care robotics

Robotic manipulation for assistance with ADLs and IADLs has also been explored in the literature. Physically Assistive Robots (PAR) are those which can perform physical interaction with the user, such as dressing, shaving or assistance with eating. A taxonomy regarding preferences for PAR was presented in [21]. SaM [126], a mobile manipulator, autonomously grasps objects for physically impaired people based on user input on the robot's screen. Other solutions for people with mobility problems included workstation systems (such as a desk mounted manipulator), stand alone manipulators (lighter versions of workstation manipulators), wheelchair mounted manipulators and mobile platforms [126], [163]. *Mary* [153], a mobile manipulator with vision capabilities, was designed to assist older adults in tasks such as fetching objects. However, the testing environment did not include real users or a Program-of-All-Inclusive-Care (PACE) center environment. A *PR-2* robot with a head tracker device was also used to perform manipulation tasks in a home environment [28]. Care-O-Bot [125] is a mobile service robot designed for interaction with older adults and capable of manipulation and navigation, using a 7 DOF manipulator arm for fetching objects. The study, however, did not consider an actual elder care scenario or elders for evaluating the proposed platform.

2.1.3 Exercise motivation for older adults

Through exercise, older adults can delay the onset of numerous diseases and consequently prevent the degradation of their independence and quality of life [12]. Extensive research have proposed different ways to motivate and promote exercise among older adults, including the use of treadmill walking [72], seated exercises [42] and gesture based games [141]. Games are a powerful context for promoting physical and cognitive exercises. Brain activity stimulation in older adults when playing physical or virtual games, in some instances, is capable of improving their cognitive ability and has been investigated in the literature [68]. Some studies considered games played individually by the older adult or with their peers [85], or promoted exercise among low-income older adults while monitoring their health activity [83], though data from real end-users was not presented.

2.1.4 Demand for COVID-19 robotic solutions

Numerous works discussing the direct impact of the COVID-19 pandemic in robotics research and development have been presented [76, 32, 41, 171, 26]. A thorough review discussing these impacts on robotic applications, along with possible solutions is found in [140]. Robotic assisted surgery (RAS) adoption has shown direct and indirect benefits towards the pandemic. Directly, as less staff (especially surgical teams at the bedside) may be needed to perform various surgeries and consequently the risk of cross contamination between staff and patients is reduced. Indirectly, robots may reduce the hospital stay in some procedures, making more rooms available for COVID-19 patients [76]. Expensive robots, however, are difficult to budget for, limiting adoption. Affordable robot solutions are preferred [75]. Stringent cleaning requirements may also impose additional challenges to the hospital staff and therefore logistical planning can become an issue. Other approaches in COVID-19 robotics response include testing for symptoms [32] temperature screening [47, 123] and a cough detection algorithm [167].

2.2 Low-Cost Low-Complexity Manipulation

An important skill for assistive robots is the ability to manipulate objects around humans, either to facilitate accomplishing a task (such as cleaning or retrieving objects) or as as an instrument for interaction (e.g. playing a game). A large variety of robotic object manipulation techniques have been developed to date. In [98], they are classified according to their models of task mechanics. Kinematic approaches to robotic manipulation include robotic caging, concerning how to bound the mobility of objects of interest without necessarily making contact. Algorithms for computing cages were presented in [162]. Low-cost Low-Complexity Manipulation, however, involves a minimalist approach in manipulation, or how could one achieve a desired task with a minimal configuration of resources [14], or least amount of hardware, and consequently less component cost. In this case, the number of actuators and sensors for a determined task can define a manipulation type as minimalist or not. Developing techniques capable of minimizing the total number of sensing and actuation, but concurrently achieving the same end result is thus proposed as low-cost manipulation.

Conventionally, notions of grasp closure (*force/form-closure*, and *immobilization* [145]) were the only factors to determine a grasp stability/feasibility. Model-based [160, 164] and data-driven [121] approaches demonstrated how to construct stable robotic grasping. Alternatively, other approaches to robot manipulation techniques such as caging [98, 162, 131, 35], pushing [89, 105, 106], sliding, toppling [88], [142] and general non-prehensile manipulation techniques [168, 91, 2, 62, 88, 6] have shown to render robotic manipulation more robust, despite not directly applicable to our problem.

2.2.1 Pick-and-Place (PnP) Manipulation

Robotic manipulation can be indeed classified through a taxonomy, including kinematic, static, quasi-static and dynamic manipulation [99]. The first refers to kinematics alone for analyzing a grasp, the second adds static forces, the third quasi-static forces (i.e. frictional forces) and finally dynamic manipulation includes all aforementioned as well as inertial forces for determining the feasibility of a grasp and manipulation task. One fundamental form of robotic quasistatic manipulation is robotic grasping and fixturing. The closure properties of robotic grasps have been investigated extensively. Important notions of grasp stability include *force-closure*, *form-closure*, and *immobilization* [145]. It has been shown that the dynamic stability of a grasp is a function of local contact geometry, contact models, and material properties [59]. Robotic pushing [89] is another practically important capability that can be achieved in a quasistatic manner. According to [97], quasidynamic manipulation is intermediate between static and dynamic manipulation as if excessive damping prevents accelerations from integrating into significant velocities. Examples in the literature include tray tilting to reorient an object using a quasidynamic mechanics model [40], identifying pushing primitives of a parallel-jaw gripper for regrasping [24], and most recently the planning of a stable pushing strategy for in-hand manipulation [25]. Recently, robotic systems that can do grasping and manipulation with some autonomy have been presented in [135, 63].

This thesis work is relevant to quasistatic object handling skills, particularly for non-prehensile manipulation. Examples in the literature include stable rotations of a polygonal object with two contacts [2], object handling with flat contact surfaces (or "palm") [62], knocking an object over with a single contact [88], and pivoting operation [6]. However, these techniques cannot be directly applied to our problem of object picking through in hand manipulation with no internal mobility. For example, compared to stably supported rotations [2], our problem is formulated with a more conservative assumption that the distance between two contacts is fixed. Our interest in keeping an object of interest within a gripper lies beyond the scope of the problem of robotic toppling [88].

Another relevant theme is robotic in-hand manipulation, which refers to the capability to move and hold an object within a robotic hand. This is an important problem related to the issue of robotic dexterity. We are particularly interested in rendering low degrees-of-freedom (DOF) end-effectors, such as the parallel-jaw gripper [147] or single rigid body end-effectors [138], more dexterous when it comes to object picking and placing. Robotic in-hand manipulation capabilities have been realized in the forms of robotic regrasping, dexterous manipulation, and finger gaiting, and are an active research area [158, 134, 52, 13]. Robotic in-hand manipulation is still a challenging problem, with a high-dimensional search space and limited robotic motor skills. The challenge here proposed is also relevant to in-hand manipulation using resources from the environment, a topic also examined in [33].

2.2.2 Dynamic Grasping

As previously mentioned, dynamic manipulation includes inertial forces for determining the feasibility of a grasp/manipulation task. It is advantageous in the sense that the manipulator does not need to come to a stop during a task, and therefore can be a much faster routine. Additionally, the dynamic motion can occur outside of the robot workspace without compromising the task (such as juggling [127]), and so simpler manipulators may accomplish complex tasks. Early demonstrations of dynamic manipulation include throwing [3], catching [133, 78] and batting [18]. More recent examples include dynamic non-prehensile manipulation for reorienting and picking [90, 91], grasping moving objects [96] and grasping objects in space using gecko-inspired end-effectors [94]. Furthermore, a grasp generally should attain desirable properties of dexterity, equilibrium, stability and dynamic behaviour [143], obtained through computational methods concerned with the contact properties (such as location or applied wrenches), known as grasp synthesis algorithms. Possibly first explored by [113], various grasp synthesis methods considered planar and spacial analysis with various contact modes adopted. A comprehensible summary of these algorithms can be found in [143] [128],[129],[67].

The proposed idea of dynamic grasping objects in this thesis considers two frictional point contacts not necessarily antipodal and two opposing edges. The concept is similar to snatching [87], however since the contacts can constrain the object of certain motions, less free space and DOFs from the manipulator may be necessary to attain a successful grasp. In addition, cylindrical type objects can also be successfully grasped if their off-plane motions are restricted by the end-effector design, which can prove more difficult with the non-prehensile snatching approach.

2.2.3 Grasping Multiple Objects

Similar to manipulators, end-effectors can be categorized as discrete, serpentine and continuum [166]. Discrete type end-effectors contains few rigid links, with limited number of degrees-of-freedom (DOF). The serpentine type end-effector has a series of chained links (mostly identical) which results in numerous degrees of freedom and the continuum type mechanisms have few or no joints and in theory infinite DOFs. The literature describes serpentine type end-effectors with a variety of applications, mechanical design and actuation methods. Perhaps the earliest and most related work to this thesis was written by Hirose and Umetani [58]. They propose a passive automatic mechanism that causes a chain of links to close on an object conforming to its shape when in contact. The mechanism uses only pulleys and a pair of wires for actuation and release and no controller is needed. Even though Hirose and Umetani refer to the gripper as "softgripper", the mechanism links are rigid. It is also noted that the pressure distribution along the entire end-effector is uniform. Various applications of serpentine manipulators were also previously explored, including inspection tasks [29], control using machine learning [148] and obstacle avoidance

[19] and more recently applications in minimally invasive robotic surgery [81]. This work addresses serpentine type end-effectors considering the numerous DOFs will enable passive compliance to the shape of the objects, but also since it still has joints, contact detection can be estimated through torque sensing at the actuation level.

Regarding the design for underactuated grippers, extensive literature proposes new approaches for grasping individual (symmetric or asymmetric) objects with underactuated end-effectors [93], [115], [7], [80], but to the authors knowledge, no published articles consider the design of end-effectors capable of grasping multiple objects. On the other hand, the dexterity problem and stability in grasping multiple objects simultaneously has been explored via rolling contacts in order to achieve enveloping grasps [53], [54], [71]. Concepts of force closure were extended to the grasp of multiple objects and discussed in [170], along with the kinematics of the manipulation. A more general analysis of grasping two objects simultaneously is found in [169]. Other techniques for grasping multiple objects include bin-picking [100] and distributed manipulation [36]. However, in all cases the end-effector proposed for experimentation was fully actuated, or objects were in the vicinity of each other, such that the interaction forces between objects had to be considered in the analysis. If an end-effector is able to grasp multiple objects sequentially, each time an object is grasped can be treated as a new grasp, and no concern with interaction forces between objects is needed, something desirable since these forces are not directly controllable [54].

Sensing the applied force in a grasp is also essential to determine the success or failure of a grasp as well as facilitate control of the internal forces applied to the objects. Numerous methods of force sensing were previously discussed, ranging from commercial force sensors in minimally invasive surgery applications [124], electroadhesive composites with elastomer actuation capable of proprioception and exteroception [50], multiaxial force sensors [159] and force sensing using load cells [17]. The method proposed in this thesis utilizes photo-reflective sensors to estimate the applied grip force to the object.This work also combines design features from [58] and self-locking constraints [4] modified such that the end-effector can attain the desired property of conforming to different object shapes while only applying forces upon contact with the object, and consequently have the ability to grasp multiple objects in a sequential manner.

Chapter 3

Need Assessment: From Task Investigation to Deployments of a Robot for Elder Care

To determine how a real world problem can be solved through robotics, a need assessment with the relevant stakeholders is necessary. Our need finding study [137] consisted of qualitative focus groups with all stakeholders (elders, clinicians and caregivers) at a Program of All-Inclusive Care for the Elderly (PACE) center. From focus groups and surveys, priority tasks emerged regarding the usability of a mobile robot, a common method of investigation in SAR. Other studies [15] have also previously used both focus groups and questionnaires to investigate possible tasks for a health care robot in a nursing home. Following this study, four deployments took place at a low income Supportive Apartment Living (SAL) and at a PACE center, consisting of mobile only ranked tasks, such as walking encouragement, hydration reminders with water delivery included [109], the screening of older adults (and healthcare workers) for COVID-19 symptoms and exposure and finally an interactive manipulation game with older adults and assisted by the robot.

3.1 A Qualitative Descriptive Study

A mixed methods approach consisting of focus groups, surveys and questionnaires informed us about elder, clinician and caregiver stakeholders' needs and priority tasks. Data collection and analysis of focus groups, member checks and confidential surveys are presented and summarized on Fig. 3.1.

3.1.1 Subjects

Elders were members at the PACE center identified as Living Independently for Elders (LIFE) and resided in a supported apartment living (SAL) (Fig. 3.2). To be

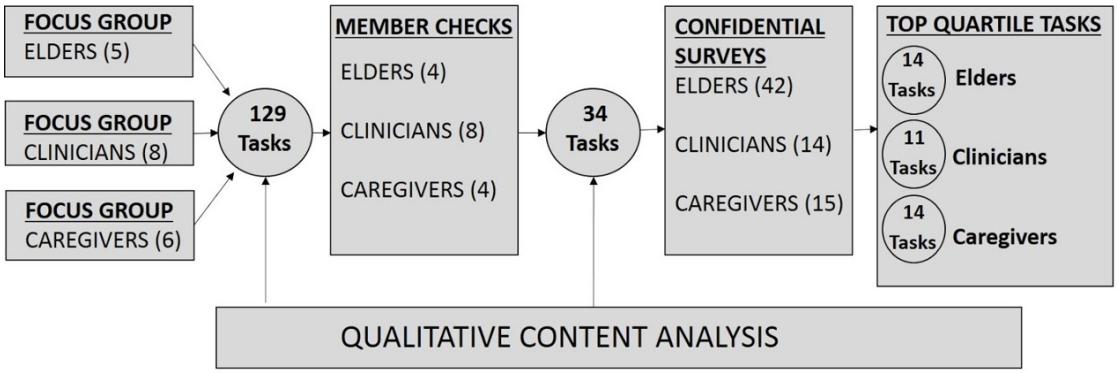

Figure 3.1: Process flow from focus groups to member checks and confidential surveys [69]

Figure 3.2: Deployment Locations: Living Independently for Elders (LIFE) Center (left) and Supportive Apartment Living (SAL) (right).

a member of LIFE, an elder must be age 55 or older, in need of medical care or supportive services, be state-certified as nursing home eligible, and live in Philadelphia County, Pennsylvania. There are approximately 456 members of LIFE. In addition to the requirements for PACE, these members typically require more assistance with physical, mobility, cognitive and social functioning provided by caregiver staff 24-hours 7 days a week when they are not at the PACE day center. Qualifications for SAL were that members had to be 62 years of age and older, in imminent risk of nursing home placement, attend the LIFE day center, able to have ADLs met by caregivers, able to pay required rent for an apartment, and able to function safely in the community with other elders. Eligible subjects were screened by the Short Blessed Concentration and Memory Test [73], a common screening tool used by clinicians and researchers to assess cognitive impairment among the geriatric population. Any potential subject scoring an 8 or greater was excluded from the study. Clinicians and caregivers were permanent or contracted employees at the PACE center. They were nurses, therapists, certified nursing assistants and home health nursing assistants who were providing services to clients at one SAL building. It is

important to note that there are significantly more LIFE members than clinicians and caregivers so as a result obtaining an equal sample of clinician/caregivers as elders was difficult.

3.1.2 Focus Group Data Collection and Analysis

One focus group per stakeholder (three in total) were conducted by an experienced interviewer member of the research team. An interview guide was developed by the research team and used during the focus group sessions. Participants were informed that the research team was interested in developing an "assistive device to aid older adults during their daily routines". The research questions for the elders focused on which tasks were of importance for them to accomplish physically, socially, and mentally on a daily basis, and associated probes directed clinicians and caregivers to identify their impressions of the elders task needs. A conventional content analysis was chosen as analytical technique to examine the focus group transcripts [39]. Several steps are involved in such analysis, including

- Initial immersion into the data, reading the transcripts word by word to derive highlighted key thoughts (known as codes)
- Sorting the codes into categories based on how the codes related, and then clustering the emergent categories into themes [48, 60]
- Use of software Atlas.ti 7.5.4 for storage, retrieval, coding and management of the qualitative data.

3.1.3 Members Check Surveys Data Collection and Analysis

A list of tasks identified in the focus groups were given back to each participant as a survey (member check) for the purpose of quality control, allowing for the verification of the accuracy and completeness of the findings from the focus groups [122, 20] and no additional items were added.

Participants were asked to score each task in terms of importance and frustration levels. The data was subsequently coded and analyzed for each group of stakeholders by "Importance of Task" with High (H) receiving a 3, Medium (M) a 2, and Low (L) a 1 (Not Applicable was coded as NA). Under the "Frustration" column, a Yes response was coded with a 1 and No with a 0. Frustration level represent elders'determination on the difficulty on completing (partially or fully) a task and for clinicians how frustrating it was to help elders with a particular task.

For each task, i , the task importance, X_i was added across columns for each respondent, and divided by the total number of respondents in that stakeholder group (Eq. 3.1.1). For NA responses, N was reduced by 1. The same method was

applied to calculate average frustration, $\overline{F_i}$ (Eq. 3.1.2). The maximum average task importance of 3 indicated all members ranked high importance for a task and the maximum average frustration of 1 indicated all members conveyed that task was frustrating. Tasks were sorted by average importance $\overline{X_i}$ and average frustration $\overline{F_i}$ to determine top quartile ranking tasks, which were subsequently used in the confidential survey per stakeholder group.

$$\overline{X_i} = \sum_{i=1}^{N} \frac{Xi}{N} \tag{3.1.1}$$

$$\overline{F_i} = \sum_{i=1}^{N} \frac{Fi}{N} \tag{3.1.2}$$

3.1.4 Confidential Surveys Data Collection and Analysis

Following the member check surveys, a confidential survey was then administered to a larger segment of the stakeholder population to determine if a prioritized subset of tasks from the member check surveys were supported by a larger segment of the stakeholder population, scoring the importance of each task and identifying whether it was frustrating. The confidential surveys were coded similarly as the member checks to determine the average task importance and average frustration across the sample size (n = 42). The series of focus groups and surveys allowed a bottom-up approach to interpreting robot task requirements. Results from Member checks and confidential surveys are presented on Tables 1, 2 and 3.

3.2 Deployments at Elder Care Community Settings

Four robot deployments involved different levels of automation: autonomous interaction with older adults by water delivery and teleoperation for walking (encouraging the older adults to exercise), health screening and manipulation tasks. The study had a total of 61 participants, of which 4 older adults participated in the water task multiple times over the span of a week, 18 older adults did the walking and game interaction over a two day period, 17 older adults and 12 staff members participated in the COVID-19 screening with the robot. Two different robot platforms were also deployed: the Savioke Relay (Fig.3.3) and Quori (Fig. 3.13). The demographics of all participants is listed in Table 3.1. Care was taken to avoid the observer (or "Hawthorne") effect during interactions, which refers to the change of behavior of the subjects in the awareness of the presence of the observers [101]. After every interaction, a post-interaction survey was conducted with the participant in order to better understand their reaction and record any change in response

over subsequent interactions, according to the parameters on Table 3.2, in accordance with the *Almere Model* [57]. Every participant gave written consent and the study was approved by the Institutional Review Board (IRB) of the University of Pennsylvania.

Table 3.1: Participant Demographics for All Deployments

Gender	Male	Female	**Total**
	22	39	**61**
Age	<65	66-79	80 or older
	25	33	3
Race	African American	Other	**Total**
	55	6	**61**

Table 3.2: Post-interaction parameters for surveying participants

Anxiety during interaction	Attitude towards technology
Intention of use	Perceived adaptiveness
Perceived ease of use	Perceived sociability
Perceived usefulness	Social influence
Social presence and trust	Perceived enjoyment

3.2.1 Water Delivery, Hydration Reminder and Walking Encouragement

Hardware

Acceptance by both staff and bystanders is a critical first step to introducing mobile robots into service industries such as in healthcare and hospitality institutions. Design goals were set to develop an embodiment that garnered trust and empathy for the robot as well as addressed ergonomics, usability, and safety requirements. This study utilized the Savioke Relay mobile robot (Figure 3.3 left). The Relay robot has been designed for indoor delivery applications, where newer versions are currently used for room service delivery in hotels. Savioke identified three attributes that would help guide the design and interaction of the robot:

- Assume that every user is a first-time user
- Generate bystander empathy to make Relay more successful

- Honest design and managing user expectations

Multiple studies were performed by Savioke to understand the relationship between screen interactions and sentiments of intimidation by the robot. Participants were shown a variety of screen examples and asked to choose the ideal size laid flat on a table. The result of this design research concluded that subjects felt more comfortable when the top of the screen was below the horizon of their sight line. The position and design for Relay's screen and payload were informed by Americans with Disabilities Act (ADA) requirements [116] and informally tested against a variety of adult subjects. It was determined a 0.8m height enabled a majority of people to interact with the robot in both seated and standing positions, with the goal of avoiding bending over or reaching out to access the payload and interact with the robot's display. The robot weighs 21kg, has a 177mm touchscreen monitor and uses arrays of Light Detection and Ranging (Lidar) and sonar sensors to navigate autonomously. It also has 21 liters of storage space, which includes a bin that is accessible by a servo-motor controlled door on the top of the robot. A pocket camera was installed on the robot to record subject interactions and a speaker was added to enhance the sound, so older adults with decreased hearing could hear instructions.

Figure 3.3: The Savioke Relay robot modified to the first and second deployments at the SAL facilities(left) and 2D occupancy grid map constructed for the deployment using Lidar SLAM.

Software

The Relay software includes a Savioke graphic programming language for creating new behaviors called *CustomPrograms*. The robot has a suite of actions, called primitives, to program user interactions [61]. These blocks can be organized in different hierarchies of menus to make the robot perform various tasks. Table 3.3

shows a few of the primitives that define the robot's movement, user interaction and set of actions.

Navigation

For the first deployment, the main floor where all participants lived was mapped using the robot's Lidar system and SLAM [37]. The 2D occupancy grid map (Figure 3.3 right) included public hallways and a lounge in front of the elevator, but did not include any older adult apartments, which the robot was not allowed to enter. Poses were defined in front of each room, so that the only requirement for navigation would be to input the room number. After completing a task, the robot returned to a home location, defined as the elevator lounge. For the second deployment, which occurred at the PACE center, the robot navigation was remotely controlled by the observer and a camera mounted on the robot was used.

Table 3.3: Example of Robot Primitives

Robot Movement	**User Interaction**	**Bin and Battery**
goTo()	displayMessage()	openBin()
move()	askMultipleChoice()	closeBin()
distanceTravelled()	askScale()	isLidOpen()
turn()	askNumber()	batteryPercentage

To help the interaction with older adults who may have poor eyesight and difficulty in reading the instructions, the robot spoke aloud any messages shown with the *displayMessage()* function with text-to-speech.

Experimental Set-up and Tasks

The first robot deployment took place at the SAL facility with older adults who were participants in the PACE program described earlier. Compared to other participants at the PACE center, the older adults in the SAL are provided with 24-hour home health care aides to assist them. The second robot deployment took place at the PACE center which includes approximately 460 older adults, most with an $8th - 12th$ grade level of education and qualify for Medicaid, impoverished with limited previous access to technology. For both deployments, the older adults were consented and instructed on the robot sequence of actions before each interaction. All interactions were recorded and the reactions of the participants were evaluated by the observer based on the following criteria:

- Initial interaction and greeting by their name

- Facial expression of older adults (smile, frown, neutral)
- Participation in the task and specific task details
- Ability to understand and follow instructions
- Interaction with the robot user interface
- Request by the older adult for robot to return
- Observer intervention during interaction (for explanation or in case of robot errors)

The robot design requirements besides the obvious functional ones were:

- Simple user interface targeted for older adults with little or no experience with computers
- Ability to operate robot remotely and adjust task details to ensure interaction without human intervention or quick intervention if required
- Safe operation while interacting with the older adults.
- Appropriate language level and choice of a robot with an appearance to promote ease and comfort.

Water Delivery and Hydration Reminders

Keeping older adults hydrated is becoming a challenging task, due to the loss of thirst receptors and short term memory loss as a result of aging [104]. For this interaction, the robot was programmed to go autonomously to the older adults' room, make a knocking sound and wait for the older adult to open the door. Once the door was opened, the robot greeted the older adult and reminded them about the importance of being hydrated. It then offered water and asked when to make another water delivery (morning or evening). After the interaction and pain assessment, the robot returned to the base and reported to the observer whether the older adult accepted the water, the requested time for the next water delivery, and the current pain level.

Pain Assessment

Pain in older adults is generally under-assessed and under-treated [95]. Thus we regularly ask for levels of pain. To evaluate pain levels, a discrete visual analog measurement scale (DVAS) [5] was used as user interface. Depending on the input value from the older adult, the robot would respond differently (see Figure 3.6). Following the pain assessment interaction, the robot returned to the base, reported

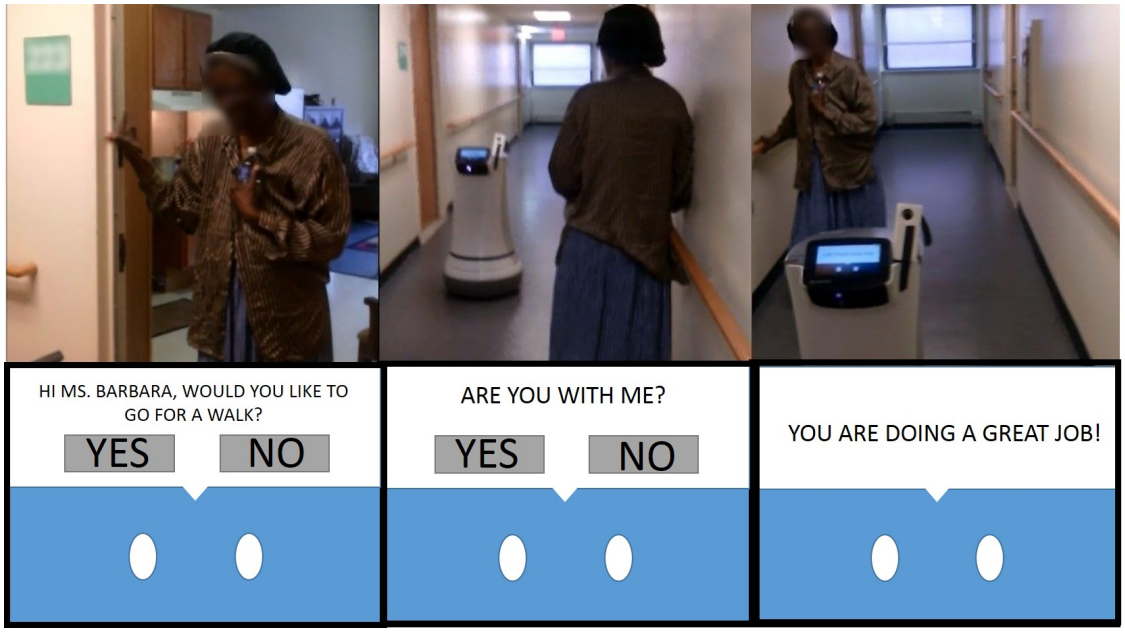

Figure 3.4: Older adult waking in the hallway with the robot. Dialogues and screen options are shown below.

the results to the observer through the screen and in the event of reported pain, the observers would notify the caregivers. A detailed description of all tasks, dialogue and screen options are shown in Figs. 3.5 and 3.6.

Walking Encouragement through Exercise

Physical activity is an important component of healthy aging [23]. In this walking task, the robot was teleoperated by the experimenter through a wireless joystick, with a camera mounted to aid navigation and to record the interaction (Figure 3.4). The robot traveled for 20 meters along the hallway, always maintaining a distance from the older adult and allowing them to dictate the walking pace.

Results

For the water delivery and hydration task, the robot interacted with four subjects at the SAL location over the span of a week. Between the four participants, the robot performed 12 autonomous water deliveries twice per day (morning and evening). Participants were often uncertain about how to interact with the robot on their first encounter. In these instances, observers intervened to encourage participants. Observer interaction also occurred due to robot errors, such as people walking too close to the robot, which affected the autonomous navigation, dialog errors and the robot not being loud enough for the older adults with hearing problems. Results of the water interactions from the observer viewpoint can be seen on Figure 3.7.

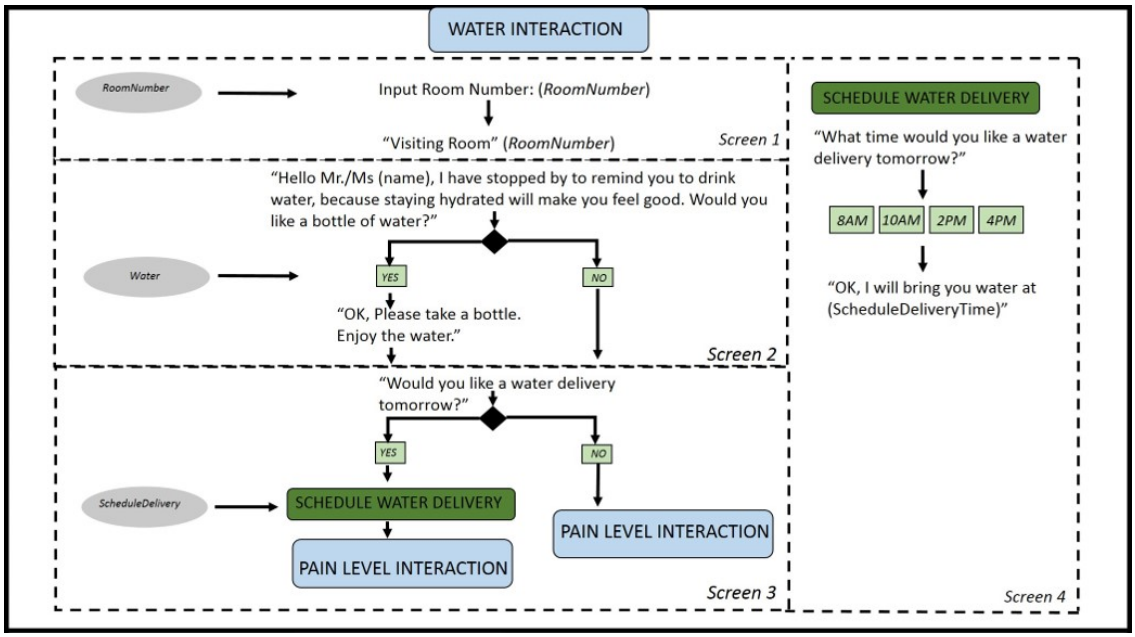

Figure 3.5: Dialogues for the hydration reminder and water delivery task. On the left, the robot reminds the older adult of the importance of hydration, offering a water bottle and a possible next delivery date. A pain assessment routine (Fig. 3.6) follows the interaction. Light green buttons represent the touch options on the screen.

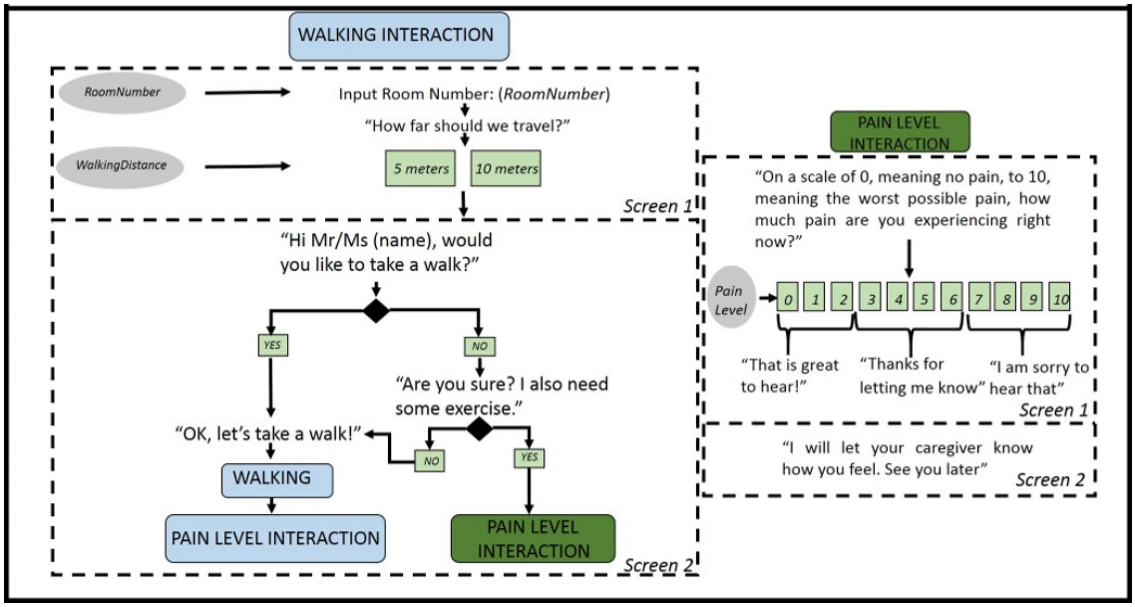

Figure 3.6: The robot proposes a walking exercise with the older adult considering two choices of travel distances (5 and 10 meters). Following the interaction, pain levels are accessed (right).

For the walking task through exercise, the robot interacted with 12 elders, through teleoperation, walking with each elder for a distance of about 5 to 10 meters. The robot operator, discretely distant from the elder and the robot, was cautious so that the robot would drive in pace with the walking elder, and would immediately stop if the elder also stopped (to catch their breath, for instance). Results are shown on Figure 3.8 .

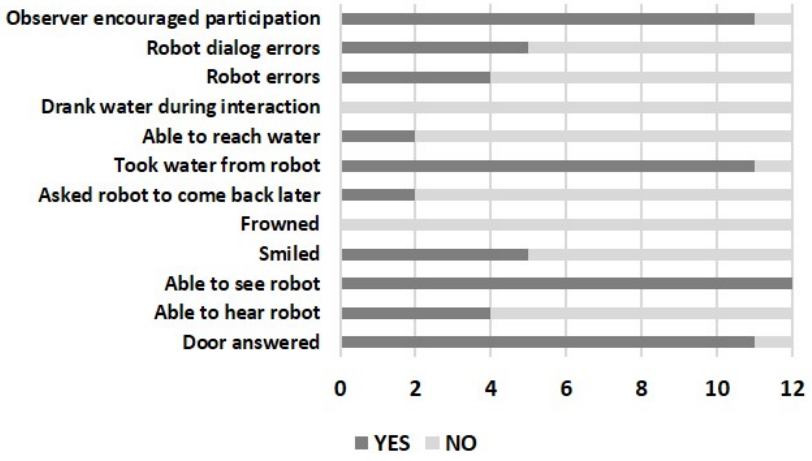

Figure 3.7: Water Interactions from Observer viewpoint.

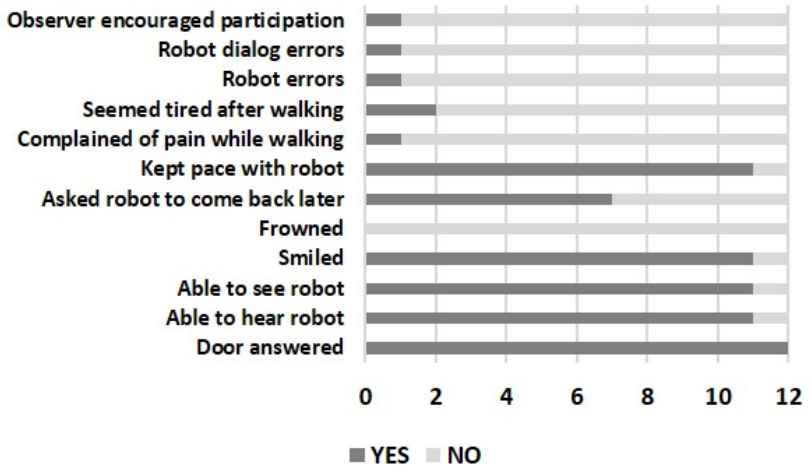

Figure 3.8: Walking interactions from Observer viewpoint.

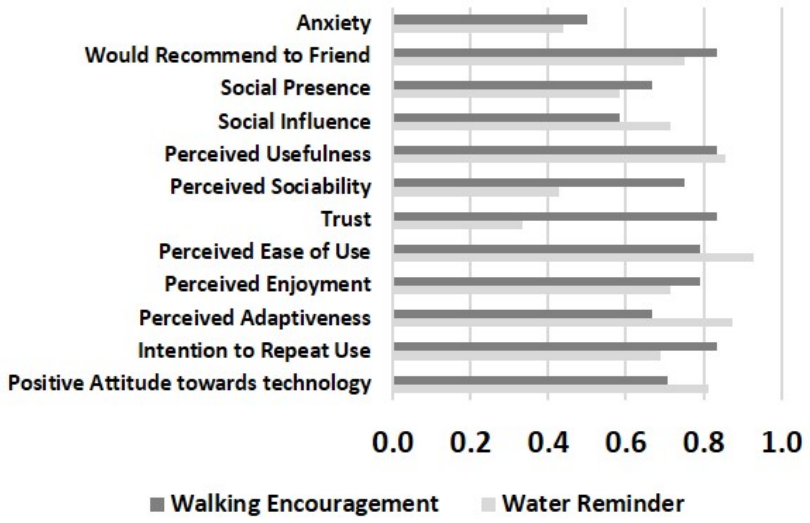

Figure 3.9: Results of post-interaction surveys for both water delivery and walking encouragement tasks.

Discussion: First and Second deployments

As a result of the deployments, some key observations, anecdotal conclusions and design guidelines regarding the robot hardware and the interaction itself are discussed. Post-interaction survey responses (Figure 3.9) were weighted as: Very little = 0, Somewhat = 0.5 and Very much = 1. The maximum possible value, divided by the number of occurrences will be unity.

Observer Viewpoint

A comparison between the water and walking tasks from the observer viewpoint (Figures 3.7 and 3.8) shows great decrease in observer encouragement for the older adult participation. One factor is that, since the water task was autonomous, the observer needed to explain to the elder how to interact with the robot for the first time. Despite instructions however, most elders would get confused and forget to interact with the robot (tapping the touchscreen). In these cases, the observer would go over the entire interaction with the elder to make sure he or she comprehended how the interaction would occur. On the other hand, since the walking task simply involved walking and no touchscreen interaction, a more natural interaction was observed.

There were fewer dialogue errors for the walking task noted, and is attributed to dialogues played remotely (through a computer paired with the bluetooth speaker), allowing control over timing and repetition. Likewise, general robot errors were also lower in the walking task, since the robot was not relying on sensors (solely on

teleoperation) and could get closer to the elder. Hearing the robot was also easier for the walking task, as the speaker was placed in front of the robot (rather than inside the storage bin during the water task).

Post-Interaction Surveys with Elders

From the post interaction surveys (Figure 3.9), taken by the observer immediately after each interaction, low values of anxiety were observed which is different than observed in some studies [56]. Anxiety in this context is usually associated with the fear of the elder in breaking the robot or doing something wrong during the interaction, or also finding the robot scary or intimidating [55]. However, the nature of the tasks (requiring only touchscreen and water bottle retrieval from the bin) and robust appearance of the robot may have contributed for low anxiety.

Various parameters like perceived usefulness, perceived ease of use, perceived enjoyment and intention to repeat use were rated highly by the participants. This shows that the robot and the interactions with the robot were well received by the older adults. This high rating is also partly explained because the subject population had a considerably high rating for positive attitude towards technology. Regarding social presence, high rating values may be due to the fact that tasks were done at the PACE center with other people present. It was observed that the human-human interaction was enhanced by the presence of the robot, which may have changed the perception of the social presence of the robot itself. Particularly, sociability increased for the walking task, as it was observed elders would commonly greet their peers and smile on the hallway while walking with a robot.

Trust of the robot was much higher for the walking task, compared to water delivery task, which could be explained by the smaller number of errors that occurred when teleoperating the robot to encourage walking, compared to the errors during autonomous water delivery. These occurred mostly due to navigation errors during the robot motion along the narrow hallways, as well as dialog errors from the time delay between sending the commands and having the robot verbally saying them, leading to repetitions and cross sentences.

Design Guidelines

Considering the current design of the deployed robot and its considerations, improvements relating observations with possible design guidelines can be inferred. Table 3.4 presents some insights on possible design modifications for future robot deployments of the robot based on these observations from both deployments.

Table 3.4: Design Guidelines based on observations during both deployments

OBSERVATION	DESIGN GUIDELINE
Tendency to read instead of listen to instructions.	Use larger fonts for written text
Difficulty in touching on screen buttons for 0-10 scale for pain assessment	Bigger buttons on the screen, or physical buttons on the robot instead
Older adults requested the robot to repeat the instructions	Add "repeat" function or button
Tendency to answer YES/NO questions verbally instead of choosing on-screen options.	Implement "YES" / "NO" voice recognition
Low volume complaint (High pitch voices for older adults represents the most difficult hearing frequency in the vocal range [20])	Louder speakers, or change location to front of the robot.
Elders in walkers or wheelchairs could not easily reach the bin	Bin opening to the side (not the top) of the robot
Elders in walkers or wheelchairs could not touch buttons on the screen	External physical buttons and PAN/TILT tablet mount
Elders confused robot eyes with screen buttons	Better user interface design or physical buttons

3.2.2 Assessment of COVID-19 Symptoms and Exposure at an Elder Care Setting

The impact of COVID-19 on older adults has motivated an additional deployment of a SAR at a PACE center. Given the high contagiousness ratio of COVID-19, especially via community spread [51], extreme caution and use of personal protective equipment (PPE) is needed when assisting older adults with their Activities of Daily Living (ADLs) or Instrumental Activities of Daily Living (IADL) [146], as these activities require human contact. Long term care facilities implemented these steps to mitigate physical proximity between older adults and their clinicians and caregivers. Such preventive measures also limited the personnel and restricted visitors, directly affecting ongoing human subjects research at these locations. Specifically, the deployment of robots which interact with multiple people.

Endowing SARs with health screening capabilities can potentially benefit staff and older adults, allowing physical distancing (since multiple people are generally involved in the procedure), and permitting robots to be even more engaging at a personal level, rather than at a general, impersonal way. As a result, an investigation on the theme is needed, which can combine subjective and behavioural measures deemed essential to inform the stakeholder acceptance and usability of the system

Figure 3.10: COVID-19 symptoms and exposure screening of an older adult by Quori.

as well as the improvement of its functionalities. Therefore, a health screening interaction can provide information on which aspects of the interaction:

- Favors the healthcare worker assessment of the patient instead of the robot
- Favors the robot assessing a patient through a routine screening instead of a healthcare worker in close proximity with the patient
- Modifications to the robot such that the former can be improved, and the robot potentially favored over a healthcare worker.

We deployed an affordable SAR robot (Quori) at a Program of All-Inclusive Care (PACE) Center for older adults (Fig. 3.10). The robot screened PACE participants and employees (clinicians and caregivers) for symptoms and exposure of COVID-19 through dialogues and gestures. Every stakeholder (clinician, caregiver and older adult) who consented participated in the study. Data collection included observer and post-interaction surveys with every participant. Results inform aspects of human-robot-interaction (HRI) to consider when deploying robots amidst the COVID-19 pandemic. Despite the current relevance to the pandemic, this screening method will be useful also during the annual flu season, which also threatens the older adult population.

Deployment Methods: Adapted COVID-19 Screening Procedure

The current COVID-19 screening procedure at the PACE Center is illustrated in Fig. 3.11. A total of 3 people interact with the older adults from arrival to being granted access to the day center or sent home, depending on the assessment of their

symptoms, body temperature and blood oxygen level measurements (each repeated at maximum twice). The new proposed procedure performed by the robot (Fig. 3.12) summarizes the main screening routines (Symptom and Exposure), in addition to the temperature screening (not functionally done by the robot). A dialogue between the participant and the robot was coordinated by a finite state machine (described in Sec. 3.2.2). Voice recognition to switch between states (based on the participant's responses) was not utilized. Possible complications with muffling voices by mask usage or difficulty in having the robot near the participant due to COVID-19 preventive measures were the main contributing factors. Therefore, researcher's input (through a joystick) based on the observed response from the participants were the finite state machine guard conditions. A detailed description of the entire system's implementation follows.

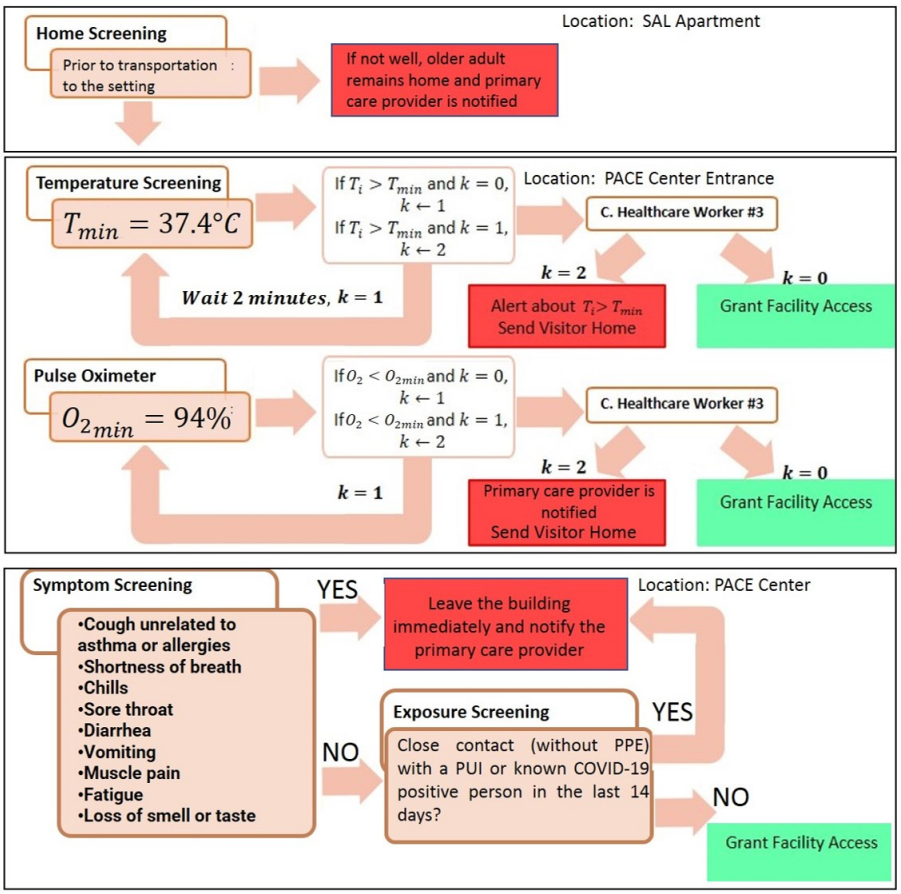

Figure 3.11: Screening Procedure at the PACE Center.

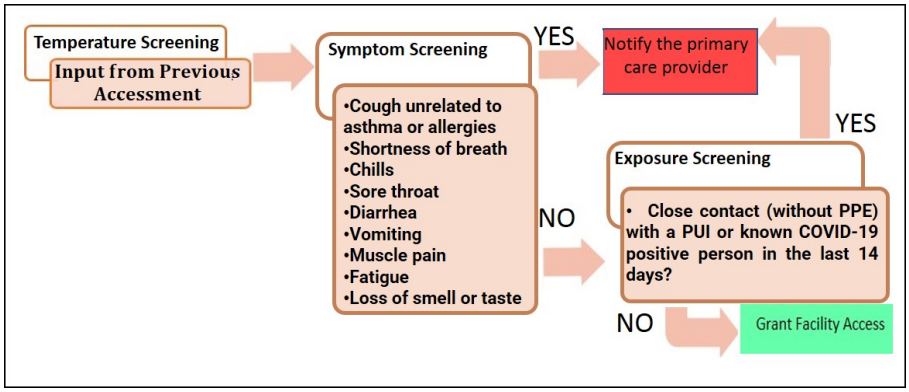

Figure 3.12: Screening Procedure performed by the robot.

Hardware and System Review

Previously, the thematic analysis completed for this study indicated all stakeholders expectancy for the robot to be polite and personable. In addition, the importance of design and programming to meet the individual needs of an older adult (either due to their physical or cognitive challenges) was found to be preferred over how the robot should look like. All participants were concerned about the safety of the robot. This is consistent with previous study findings [137, 109, 69], in which any device perceived by older adults, caregivers, or clinicians as unsafe would decrease the use of the technology. This original analysis informed the current SAR platform (Quori) hardware and software design.

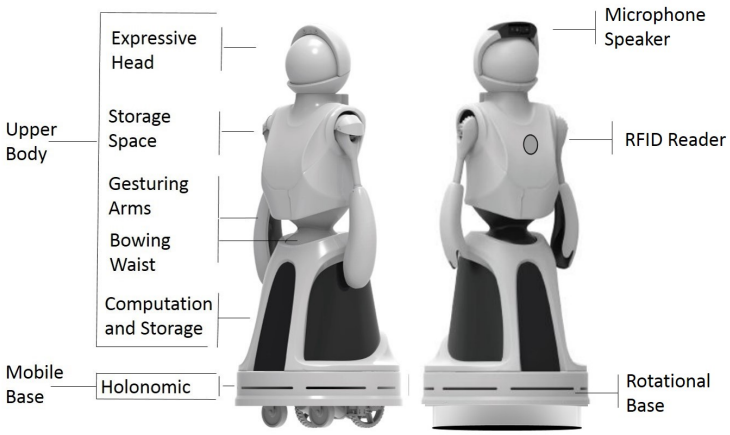

Figure 3.13: Quori (left) and hardware modifications for deployment in the proposed study (right)

Quori [150, 103] consists of a humanoid upper body attached to a omnidirectional mobile base. The original modular Hardware (shown in Fig. 3.13 left) is described

as a:

- Holonomic Mobile Base: Inspired by the design in [38] and mobility in [31], the base has three actuators for generating linear and angular velocities as well as orient the upper body of the robot, measuring 480 mm in diameter and 203 mm in height.

- Spherical Projection Head: To maximize flexibility and minimize cost, Quori's head consists of a retro-projected animated face (RAF) using a portable projector, a lens (or mirror), and a projection surface. Such technique is highly versatile since any face can be projected, and highly expressive, as previously shown in the literature [34, 107, 119]. Vibration noise is minimized by a rigid connection between the spherical surface and the projector.

- Gesturing Arms: As the purpose of Quori is human-robot interaction and expression, gesturing becomes an important and desired aspect on a social robot. The arms (not meant for manipulation) and two DOF shoulders are designed so that the arm can rotate continuously. Safety concerning proximity to humans was also considered by limiting the torque on the drive motors as well as using lightweight materials and low inertial, and stiffness arm.

- Spine In order to support the torso, a 1-DOF spine allows the robot to demonstrate different levels of engagement by leaning forward or backward. The spine can also minimize possible vibrations due to the robot's motion, resulting in natural and more appealing motion.

Hardware Modifications

Due to the nature of COVID-19 transmission, avoiding crowds and human contact is highly desired. Therefore, the robot would remain in one fixed location where the assessment would occur, and continuously navigating the environment was discarded. In addition, since the check-in procedures mostly required dialogue and indication of directions (for medical appointments for instance), the holonomic base was simplified to a purely rotational one. Another modification to the original hardware was the addition of the Radio Frequency Identification (RFID) reader to the robot. Relying on RFID for person identification is preferred as the subjects were wearing face masks, which imposed challenges to the implementation of facial recognition. The reader uses USB communication, has a 1m range and emulates a keyboard. To facilitate comprehension for hearing impaired older adults and promote physical distancing, external speakers were located near the participants. Lastly, since body temperature can vary depending on the location of the measurement on the body, and older adults and employees would only be admitted to the facility with body temperature under 37.4^{o}C, no temperature screening device was added to Quori.

Temperature screening dialogue, however, was included in the dialogue simply to provide more context and completion to the overall interaction.

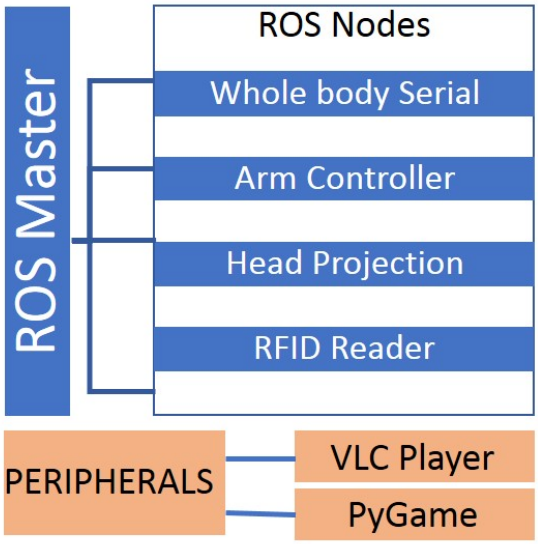

Figure 3.14: The software implementation framework. The ROS Master node controls the robot's movement and facial expression. The peripherals manage the finite state machine abstraction for the dialogue.

Software Implementation

An overview of the software framework is seen on Fig. 3.14. The robot architecture uses Robot Operation System (ROS)[1] for its main implementation. The core body motion of the robot runs on a *Whole body Serial* node, and the gesturing arms driven by anti-cogged brushless DC motors[2] running a PID controller (which considers torque and speed limits for the motion as safety precaution during interaction), implemented on an *Arm Controller* node. We have utilized a simple facial expression consisting on periodic blinking eyes with the intent to generate empathy and not overstate the robot's intelligence, implemented on the *Head Projection* node. Dialogues were input to a text-to-speech engine [3] and *mp*3 files were generated and played by the *VLC Player* peripheral. A low pitch and speed voice was preferred since those can impact the ability of the older adult to hear the interaction [79]. Finally, switching between states was done with a joystick using *PyGame* implementation.

[1] www.ros.org
[2] http://iq-control.com/
[3] www.kukarella.com

Table 3.5: Participants Demographics

Gender	Male 11	Female 28	Total 39
Age	25-50 10	51-60 12	61 or older 17
Race	African American 36	Other 3	Total 39
Status	Employee 22	Member 17	Total 39

State Machine Implementation

The interaction was implemented as a finite state machine (Fig. 3.15). To begin, the *RFID Reader* node utilized the USB reader device and RFID tags ($STATE$ 0). The robot greeted the participant by name and prompted them to remain steady while it (in a "Wizard of Oz" manner) checked their temperature ($STATE$ 1). After a 5 second delay, the robot engaged in a symptom check routine ($STATE$ 2), inquiring users' input on a list of symptoms (shown on Fig. 3.12). If the participant answered YES to any symptoms on the list, the robot referred (vocally and pointing) the user to a physician's room ($STATE$ 3) and the interaction ended. Otherwise, the robot engaged in an exposure check dialogue ($STATE$ 4), asking if the participant has had any close contact with a COVID-19 positive person in the last 14 days without a mask. Once again, a positive response referred the user to a physician ($STATE$ 3), otherwise to a caregiver ($STATE$ 5), finishing the interaction in sequence.

Table 3.6: Access to Technology

Experience with or use a
Computer 28
Tablet or e-reader 20
Cellphone 38
Exercise daily* 24

Deployment Results

The experimental set-up for the deployment is show in Fig. 3.17. The robot was placed at the dining hall of the PACE Center and participants instructed to interact with it (standing up or seated, depending on their mobility limitations) at

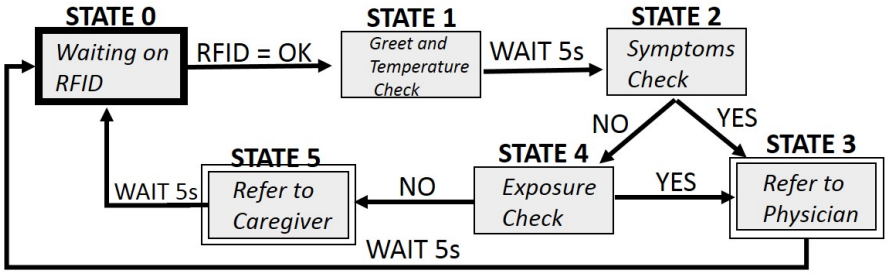

Figure 3.15: Finite State Machine abstraction for the dialogue and interaction implementations. The State Machine starts at $STATE$ 0 and finishes at $STATE$ 3 for any "YES" answer and $STATE$ 5 for "NO" answers. A detail description of the dialogues' content is shown in Fig. 3.12

a $1m$ distance. Third (Fig. 3.10) and first-person (Fig. 3.16) view cameras were used to record every interaction and an external bluetooth speaker placed near the participant as previously mentioned.

Figure 3.16: First-Person view camera installed on the robot.

A total of 39 participants interacted with the robot (see Table 3.5 for demographics). Almost all participants were African-Americans, 61 years and older and had cellphones (Table 3.6), with the majority having access to a computer and roughly half to tablets or e-readers on a daily basis. To analyze responses subjective and behaviorally, post-interaction and observer surveys were conducted by the research team. The subjective investigation considered two surveys: one based on the Almere [146] model for assessing technology acceptance for older adults, focusing on system usability (Fig. 3.20); a second (discussed in Sec. 3.2.2) with open-ended questions about positive and negative aspects of the robot, preference among human, robot or phone screening, and recommendation of use. The behavioral evaluation by an observer also considered a survey (Fig. 3.18), which informed the research team

additional reactions of the participants while interacting with the robot. The evaluation criteria included ability to see and hear the robot, facial expression of the participant (smiled, frown) during interaction, physical response, difficulty (or lack of) in understanding and following instructions and possible frustration. Robot errors were also monitored (Fig. 3.19). Initially, given the equivalent ratio of members (17) to employees (22), groups had their responses separately analyzed, and expressive differences in results (if any) reported as follows. Care was also taken to avoid the observer (or "Hawthorne") effect [136] during the interactions. All participants were consented prior to each interaction. The study was approved by the Institutional Review Board (IRB) of the University of Pennsylvania.

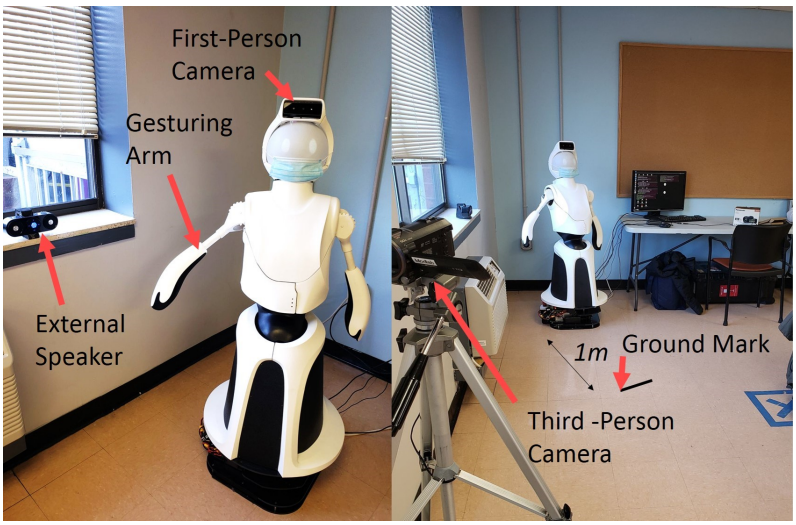

Figure 3.17: Experimental setup of the system in the common area. External speakers were mounted on different locations to facilitate comprehension depending on whether participants were standing up or seated. A ground mark distant 1m was set to standardize interactions.

Discussion

According to Fig. 3.18 almost no participant had trouble seeing the robot, was frustrated, upset or bored with it. No participant seemed scared or became unsteady during the interaction. Almost all participants talked back to the robot when questioned by it, smiled (heard as a laugh) and seemed comfortable with it. However, 44% of participants had trouble understanding the robot and 36% trouble hearing it. These were correlated, as participants often complained they could not adequately hear the robot, despite maximum volume of the external speaker. It was observed high background noise from the room's television and employees conversation. A surprising 77% of participants seemed uncomfortable during the

interaction. Although not pain related (as only one participant reported pain), a few factors could have contributed for this observation, specifically:

- The repetitiveness of a daily screening procedure (especially for the older adults, since most were screened twice before arriving to the center)
- The inability to hear the robot and not knowing what to answer at times, robot errors due to mispronunciation of names and words (Fig. 3.19).
- Possible embarrassment in answering to certain symptoms' screening questions (namely "vomiting" and "diarrhea").

With respect to the system's usability (Fig. 3.20), the great majority of participants strongly agree they would use the robot frequently, were confident using it, felt it was easy to use and its functions were well integrated. Participants also think little to no prior knowledge or assistance would be needed before using the robot, and found the system consistent and of low-complexity in general.

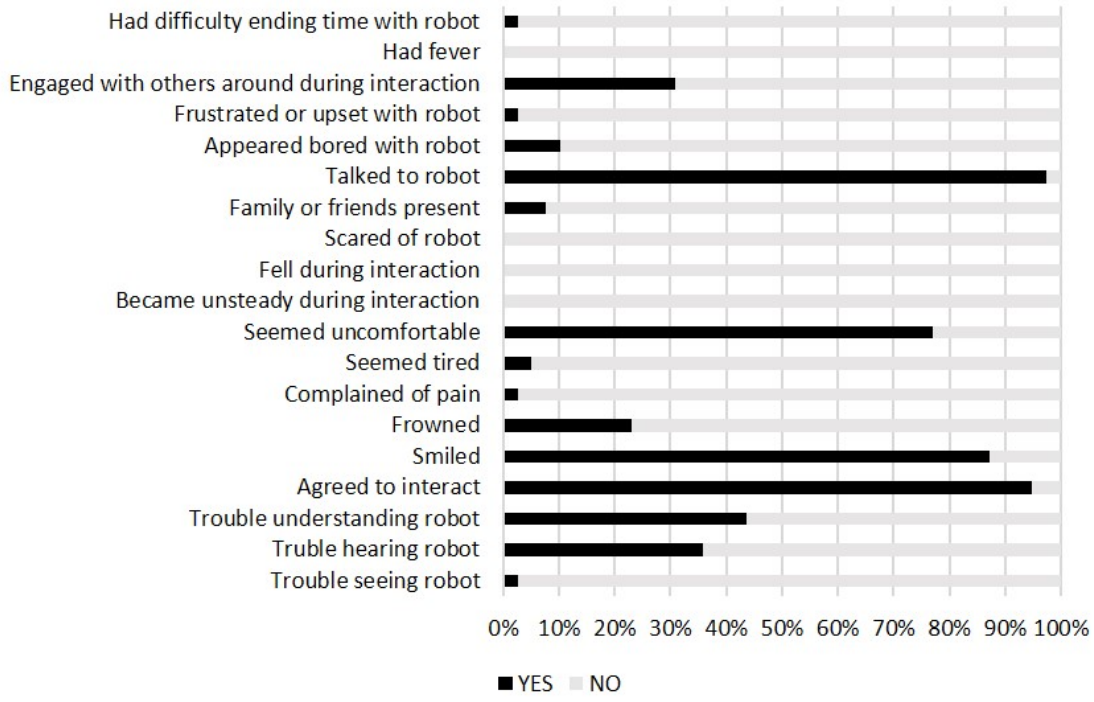

Figure 3.18: Observer survey results assessed by the research team during interactions.

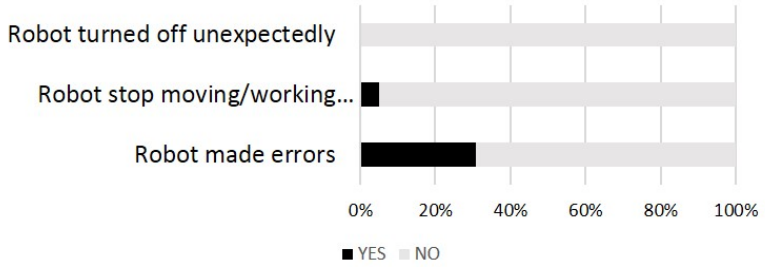

Figure 3.19: Observer survey results regarding the robot's observations.

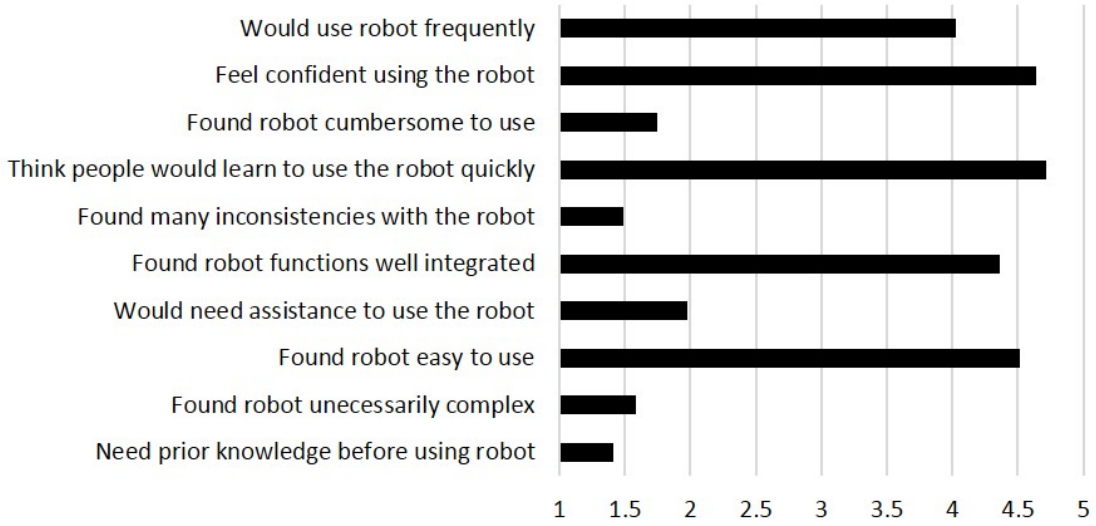

Figure 3.20: Agreement Scores for system usability, with 1 (strongly disagree) and 5 (strongly agree) scores.

General Observations

Participants were asked whether they would recommend the robot to a friend (Fig. 3.21 top). All employees answered positively and 94% of older adults would recommend the robot. When asked about their preference among different COVID-19 screening methods, employees preferred the robot over any other method, although almost 30% did not have a strong opinion. For older adults, more than half preferred human assessment over the robot, the latter in fact was rated the least screening method preferred (11.8%). This is an interesting finding, since despite most older adults recommended the robot, they would still prefer the human assessment over it. Preference towards person over robot screening included arguments such as "a person can handle the information", "computers make mistakes", "you can ask a person a question", "I can relate to a person" or "I am old-fashioned". Arguments

for robot screening were "it avoids physical contact", "responses can be kept confidential" and "it is easy to interact". A couple of participants would get closer to the robot (speaker) to hear it but all participants complied with the physical boundaries imposed by the interaction (e.g. staying behind the ground mark), useful indicator for systems with optimal distance for voice or facial recognition. We also asked subjects positive and negative aspects about the robot (Fig. 3.22). Being straight to the point, friendly, call participants by their names and having a clear voice were the most positive aspects. Most participants did not have any negative comments, but difficulty hearing the robot was widely noticed.

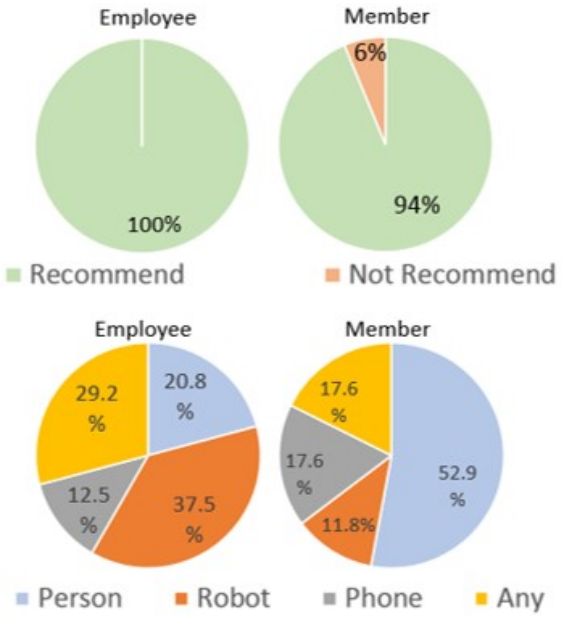

Figure 3.21: (Top) Members (older adults) and employee's response on recommending the robot and (bottom) preference towards different types of COVID-19 screening procedures.

Anecdotal Conclusions and Observations

- Getting older adult participants was difficult. The pandemic drastically limited the number of PACE members allowed inside the day center.
- The robot was not allowed in confined spaces (i.e. an office) and we had to set it up in a common area. This resulted in excessive background noise (such as television and employees' conversations) challenging comprehension for hearing impaired older adults.
- Placing the external speaker at different locations had an impact on the interaction. Specifically, when the device was placed to the right of one participant

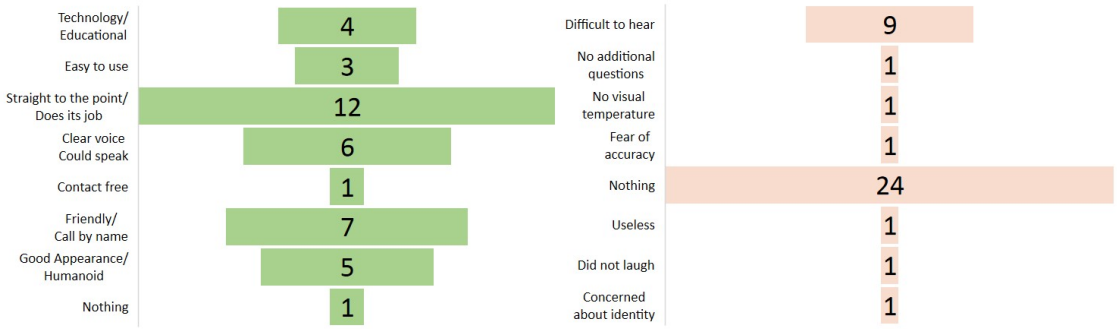

Figure 3.22: (Left) Positive and (Right) negative aspects of the robot interaction by the participants.

(and to the left of Quori), when prompted to "look at me for five seconds while I measure your temperature" by the robot, the participant turned towards the speaker instead of the robot.

- Quori's slow low pitch voice (to facilitate older adult's understanding) seemed to affect younger participants, as one commented "the robot talks too slow and made me a little impatient".
- Additional comments by participants considered the robot easy to speak with, quick to interact, pleasant, and suggestions included more interactive movements and sense of humor.

Overall results indicate acceptance of the robot as a screening method, in view of its easiness of use, direct and straight to the point behavior, as well as friendly aspect, although the older adult population still preferred a person assessment instead. Despite additional speakers' use, difficulty hearing the robot (especially among older adults) was still noticeable, emphasizing the challenges in designing social robots deployed at common areas and for different age groups.

3.2.3 Mobile Manipulation for an Interactive Physical Game

From our need finding and focus group study [137] a mobile manipulator robot that could be used for fetching objects or provide assistance in leisure activities emerged as important. The Savioke Relay mobile base was then modified by adding a low-cost two degree-of-freedom telescopic manipulator. This allowed the robot to have a greater reachable workspace over other conventional manipulators (Fig. 3.23), able to easily access objects in high cabinets or on the ground. The arm is also safe and able to be operated close to humans, as its lightweight (1.5Kg), does not have sharp edges, does not perform fast movements, without high torque manipulators.

Figure 3.23: Demonstration of the arm capability in reaching different heights with its telescopic feature.

System Description

The same mobile base deployed in [109] was adopted and modified in this present work. The manipulation task requirements were established based on our previous work [137, 69] and can be summarized as:

- Arm able to reach down to the ground, retrieve objects weighing up to 2 lbs, and hand them to a nearby human.
- Manipulate objects in limited workspaces in a PACE Center, such as common areas and kitchen.
- Safely be operated around elders and staff in a PACE Center and so avoid sharp edges, fast motions, or heavy high torque manipulators.

The Arm

Based on these requirements, we have chosen a two DOF manipulator that utilizes the spiral zipper extension technology [30] with a single rotational joint. This configuration is advantageous for its affordability and low-complexity. The spiral-zipper arm is light weight, retractable and human safe even if it comes in contact with a person. The arm can retract into a canister when not in use, improving the robot's ability to avoid collisions in dynamic or cluttered environments. Most of its components are laser-cut or 3D printed ABS plastic and there are only two actuators. The arm itself costs about $1000.

The arm's rotational joint is actuated via a single tether that runs to the top of the arm (Fig. 3.24). When the cable retracts, the arm is rotated upward. The effective workspace is about 120 degrees where resting position is straight down. The arm can extend up to 80 cm, and retract to 20 cm (Fig 3.26). To evenly distribute

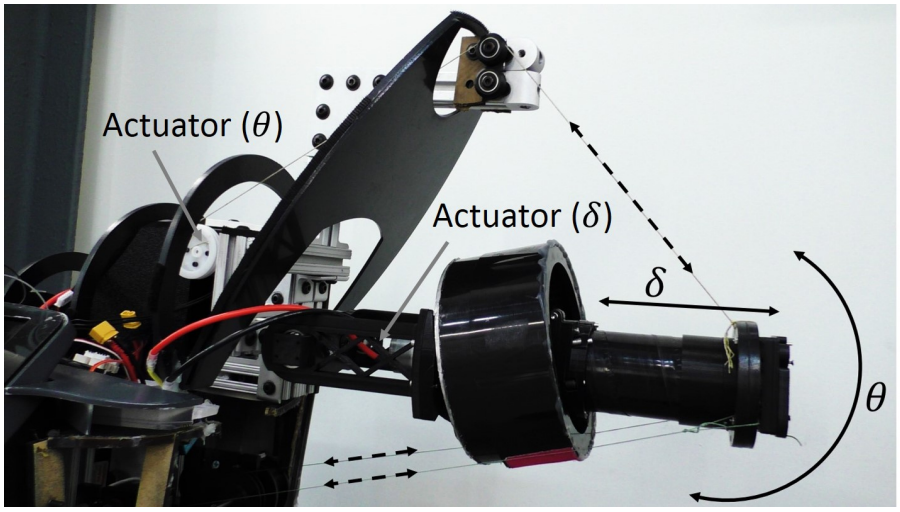

Figure 3.24: Degrees of Freedom of the arm (continuous arrows). The tethers attached to the arm are shown as dashed arrows.

the load along the arm column, additional cables were routed underneath to the end of the arm, as it can be seen on Fig. 3.24. The cables run directly to a pair of constant force springs (simulating a 2lb load) that balance the moment produced by the top cable on the column and makes the spiral zipper mechanism perform more robustly.

The mechanism (see Fig. 3.25) is driven upward by a motor embedded at the center of the meshing block, which we call the slider. The motor interfaces with the band via a rubberized omniwheel oriented along the axis of the helix. The omniwheel rollers grip the band as it rotates by, spinning it upward. The rollers on the omniwheel then passively counter-rotate downward in order to maintain vertical position relative to the motor. Because the system operates on the basis of friction, if the band is under a heavy load, the friction wheels will slip on the surface of the band and the band will not rotate upward acting as a clutch.

Consequently, we included the ability to adjust the normal force between band and wheel to guarantee that the transmissible torque through the wheel to the band is higher than the expected downward load on the arm itself. As seen on Fig. 3.25 (right), this can be expressed by:

$$\sum \tau_{\mathbf{i}} = \frac{1}{2} \sum \mathbf{T_i} l_i \sin 2\theta > \mathbf{F_n} R \tag{3.2.1}$$

The advantage of this particular style of manipulator is its simplicity and safety. The arm does not possess more DOF than necessary. Between the two DOF embedded in the design plus and two from the Savioke base itself, the arm can reach any object in its direct field of view (Fig. 3.27).

Finally, the arm is easy to retract into a low profile which is a useful attribute

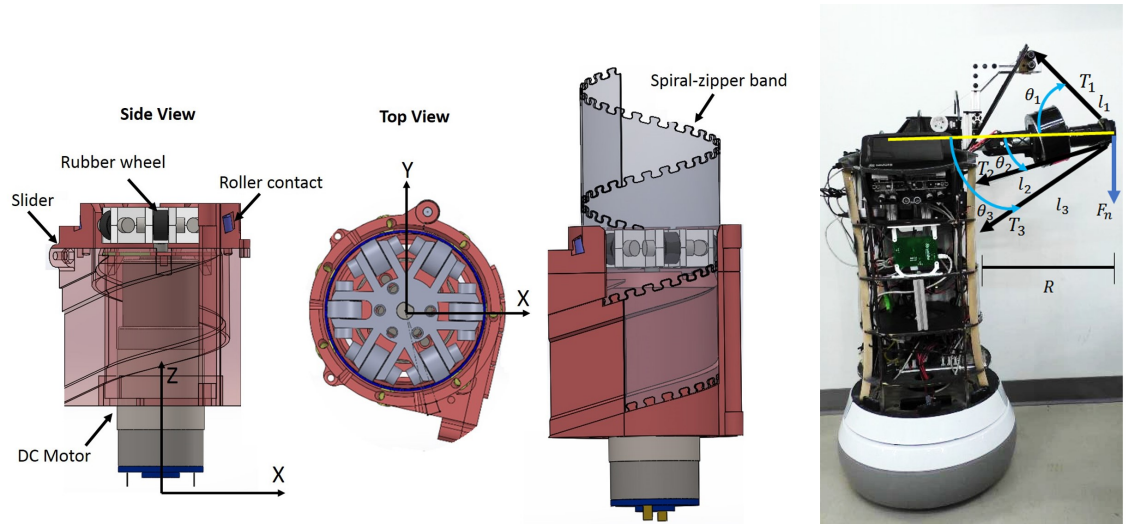

Figure 3.25: ((Left) Spiral zipper arm extension. The DC Motor spins a rubberized omniwheel, locked frictionally to the zipper band. Rollers on the omniwheel allow band to extend as the system rotates. (Right) Torque distribution on the arm.

in the cluttered living environments people often inhabit. The robot can travel in these environments more easily without increasing the chances of the system bumping into or getting caught on its surroundings. The extension is also useful since it can reach over cluttered spaces to pick up a desired object from far away without having to come up with a strategy to get closer without bumping into things.

The End-Effectors

With the purpose of facilitating robot interaction with older adults during manipulation, and investigate different designs for future deployments, we used two end-effectors. The first (Fig. 3.28 left and center) facilitates magnetically grasping items with embedded ferrous material using neodymium (Nd) magnets distributed as an array along the laser cut ABS shape, along with springs mounted for passive compliance. For tasks such as fetching single objects on the floor or on high cabinets and handing them off to the elders, we used a custom-made conventional 1 DOF two-fingered gripper with a 1 DOF wrist (Fig. 3.28 right). This 2 DOF prehensile end-effector is 3d-printed and uses Dynamixel Mx-106 motors as actuators.

Game set-up and Methods

The corn-toss game was modified to facilitate robot interactions. A ramp was added under the game board to keep bags from getting trapped underneath. Toss bags were filled with a ferrous material (380g total mass) to be magnetically grasped

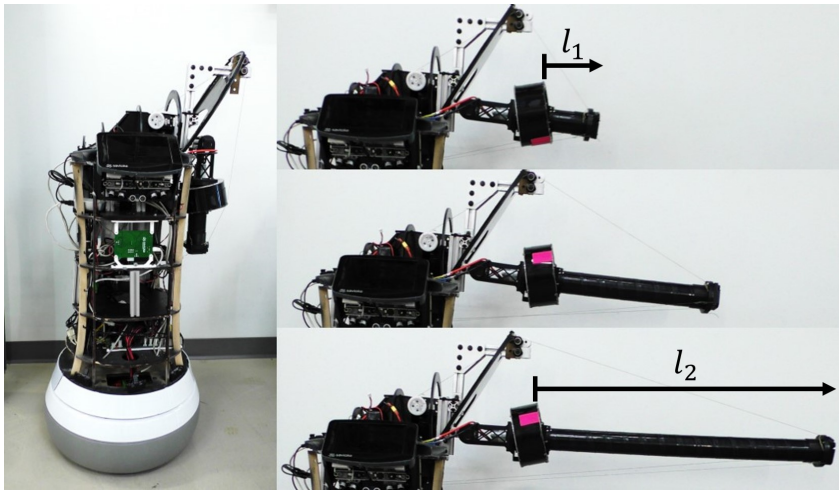

Figure 3.26: Spiral zipper arm extension, from $l_1 = 20$cm to $l_2 = 80$cm.

by the non-prehensile end-effector. Cameras were mounted on the robot and at the corner of the room to capture every aspect of the interactions. The robot was teleoperated to hand the bean bags to the older adult and each game was done in pairs, two older adults at a time, inducing competitiveness and increasing engagement.

To test the manipulator's ability to reach different heights, the bean bags were retrieved from high cabinets, brought to the elder, tossed by the older adult and retrieved from the ground. Four different interaction scenarios were proposed for comparison purposes and to avoid possible order effects (Fig. 3.30 and 3.31):

- First: No assistance during the game, the older adult would fetch the bean bag from the cabinet and the floor.
- Second: Caregiver assistance in fetching the bags before and after being tossed.
- Third: Robot assistance in fetching the bean bags before and after being tossed using Gripper 1 end-effector (non-prehensile grasp)
- Fourth: Robot assistance in fetching the bean bags before and after being tossed using Gripper 2 end-effector (two degrees of freedom)

The experimental setup is shown on Fig. 3.29. All deployments took place at a PACE center in Pennsylvania. As in our previous work, all subjects were consented and their confidentiality was maintained. The study was approved by the Institutional Review Board of the University of Pennsylvania.

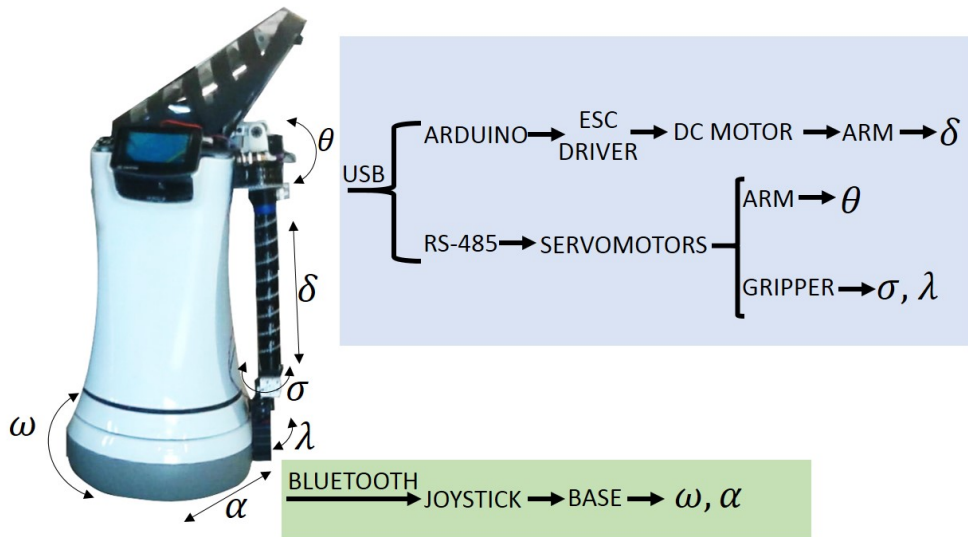

Figure 3.27: The controlled mechanism and respective DOF of the system.

Subjects

In total, 18 older adults participated in the corntoss game (see the demographics in Table 3.7). This PACE center includes more than 450 older adults eligible for Medicaid and Medicare whose education level ranged between an 8th-12th grade. Their access to technology was limited, though all older adults had a cellphone. Most older adults reported exercising daily (see Table 3.6). Every participant was consented, recorded by two different cameras and reactions evaluated by an observer in the scene. Observation criteria included facial expression, physical engagement and participation, task completion, robot errors, request for robot to return by the

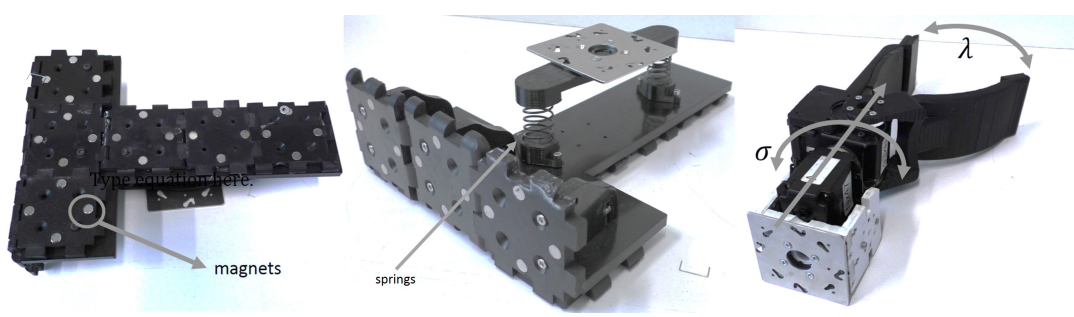

Figure 3.28: End-effectors used for the study: (left and center) a magnetic gripper with no actuators and springs for passive compliance, named "Gripper 1" and (right) a conventional 2 DOF angular gripper (λ aperture and σ the wrist joint), named "Gripper 2".

Figure 3.29: Study setup at the PACE center. The bean bags were initially placed in the cabinet and a ramp was added under the board to eject beanbags and facilitate its retrieval by the robot.

older adult and observer intervention.

Each older adult completed a Mini Mental Status Examination [46] and was capable of giving inform consent. The 18 participants were grouped into pairs for the game. The two end-effectors from Fig. 3.28 were separately used for retrieving the bean bags on the floor or on cabinets and to transfer them to the older adult.

Table 3.7: Fourth Deployment Demographics

Gender	Male 7	Female 11	Total 18
Age	55-65 5	66-75 9	75 or older 4
Race	African American 18	Other 0	Total 18

Results

In Fig. 3.32, general observer results are shown, with data collected by the observer during every interaction following the criteria described in the previous section. Despite robot errors occurring in more than half of the interactions, very few older adults seemed scared, tired or complained of pain when interacting with the robot.

(a) (b)

Figure 3.30: Different scenarios for retrieving the bean bag for the game (a) Solely by the elder and (b) With caregiver help.

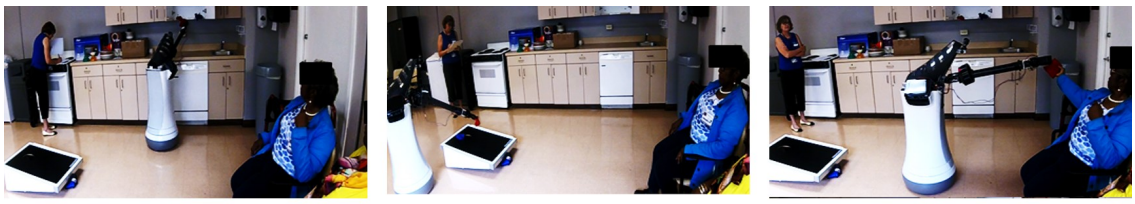

(a) (b) (c)

Figure 3.31: Robot assistance during the game for (a) retrieving the bean bags from the cabinet (b) from the ground after tossed by the elder (c) handing it off to the elder.

Four participants were unable to retrieve the bean bags either from the floor or cabinets, while others needed help stabilizing themselves when reaching. Many participants complained that the robot was too slow, but were patient and waited for the robot to release the bean bags to allow them to complete the game. High levels of competitiveness among the older adults were observed during every game. Most became upset if they did not score, others celebrated enthusiastically when they did score (Fig. 3.33). General observations about the corntoss game can be seen in Fig. 3.34. Despite considering 18 older adults for the study, one older adult did not meet the mini-mental status examination standards and was not included when analysing the following results.

Most elders agreed that the robot was simple and easy to interact with, feeling comfortable and satisfied with it. Even though the participants complained about the robot speed, a high score was attributed to completing the game quickly and efficiently with the robot (see Fig. 3.35). As shown in Fig. 3.36, different levels of assistance during the game were investigated and, as expected, the game was rated the easiest when assisted by a caregiver. For example, when users were asked how difficult was the process of retrieving the bean bags from the floor compared to themselves or with assistance they rated 1.70 for playing the game without as-

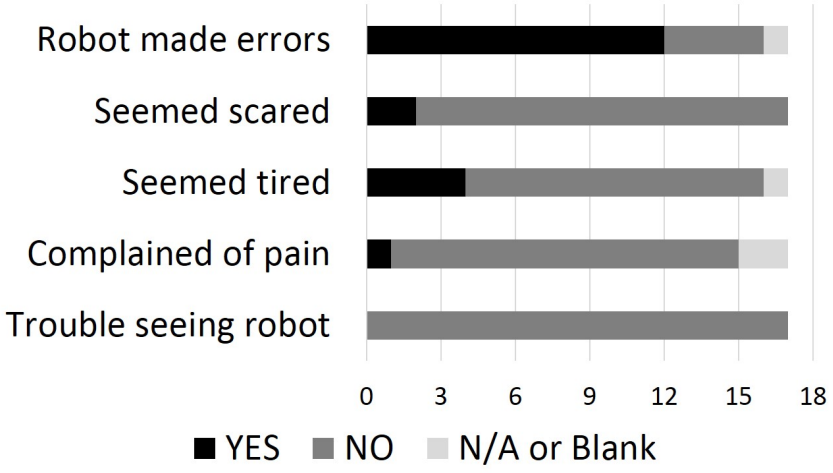

Figure 3.32: General observations of participants interacting with the robot from the point of view of the observer (percentages of from N = 17).

Figure 3.33: Older adults celebrating when scoring in the game

sistance, compared to 1.0 with human assistance, 1.67 with the robot assistance using Gripper 1 and 2.03 for assistance by the robot using Gripper 2. Retrieving and tossing the bean bags in the hole was the most difficult for the older adults to do independently, though this was improved when assisted by a caregiver or the robot using Gripper 1, possibly due to the non-prehensile grasp of Gripper 1, which allowed for a facile retrieval of the bean bags by the older adults. Gripper 2 had a higher difficulty score when retrieving the floor bean bags, likely due to the extended time needed for the arm to grasp the object. In this gripper two degrees of freedom had to be controlled, Unlike Gripper1, which had none. However, Gripper 1 was rated more difficult in retrieving the bean bags from the cabinet, likely due to the restricted degrees of freedom in achieving a desirable grasping configuration. Lastly, the older adults considered tossing the bean bags in the hole and competing with another person slightly easier when the game was assisted by the robot, compared to the caregiver assistance or no assistance at all. This can be an indicator on how to use robots in such physical game tasks.

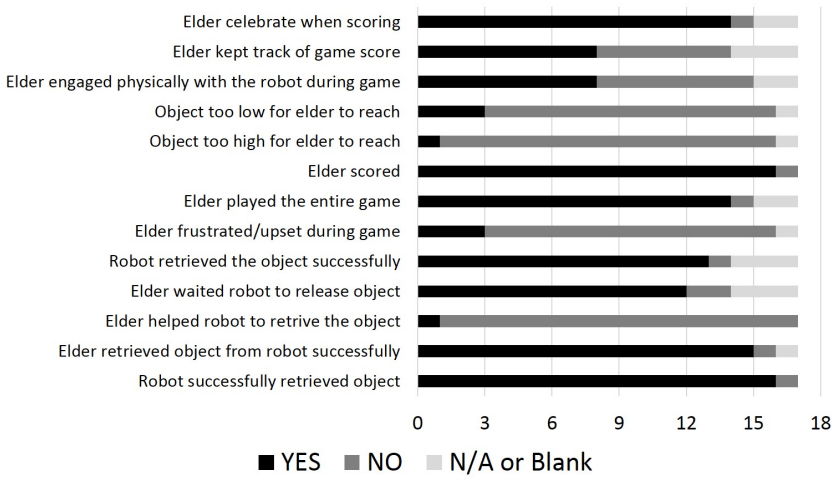

Figure 3.34: General observations of participants interacting with the robot while playing the corntoss game, from the point of view of the observer (Total participants N = 17).

Discussion

Numerous studies have explored robotic manipulation in assisting older adults with their ADLs, as in [126],[163] and [153] proposing different service robots to grasp and manipulate objects as well as different evaluation methods. The robot in [126] is capable of autonomous grasping and validation is done in an experimental set-up. In[153] the robot is teleoperated by a non-user and no evaluation studies were done. In [28] the user, with certain motor impairment, teleoperated the robot in a home setting using a head-tracker cursor as input device. Others studies explored virtual games as tools for cognitive stimulus in older adults [68], [85], [83], but little attention has been given to the system deployment at elder care facilities. To the authors'knowledge, this is the first study in which a mobile manipulation platform was used in a PACE setting with older adult participants, with a physical activity based of a game investigating older adult's interaction at different levels, including direct interaction with the robot. Different methods for handing off objects to older adults were also analyzed considering prehensile and non-prehensile grasping methods using two different end-effectors. The novel low-cost manipulation hardware was employed and also verified during the deployment and from observer's notes and post-interaction surveys with older adults overall scores indicated the best case application of the system in interacting with the participants.

As a result of the study, it was observed users enjoyed playing with the robot, as also demonstrated by the literature with companion robots [152, 1]. Users complained about speed of the robot, which was slow due to the manipulator speed, in particular with the configuration using Gripper 2. Previous work [144] discusses the importance of speed tracking for interaction with older adults. Another unex-

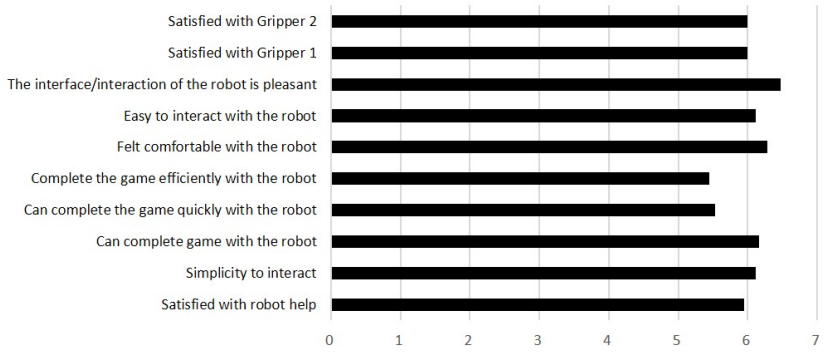

Figure 3.35: Average Agreement score, where the participant scored in a scale from 1 to 7 how much they agreed with different statements (1 meaning strongly disagree and 7 strongly agree). The number of participants that responded to each of the question varied and was taken into account when calculating the average (total participants was N = 17).

pected outcome was the type of gripper affecting speed and user perception, which was not discussed by the literature, It was expected that a gripper with a more intuitive, prehensile motion should be better accepted by the elders, but effectiveness was apparently a more valuable requisite. In addition, even though the robot was rated worse than a human for assistance in the game, users were able to see how the robot would be a game companion, since different scenarios for the game assistance were proposed, also not previously found in the literature. On one hand, as human assistance represented the best case in assisting the game, getting the robot as good as a human helper, or how good enough is enough not to trigger dissatisfaction is a theme that could be explored. On the other hand, the robot was better rated to accomplish a task, compared to no assistance, in most cases except in the cabinet retrieval task. This can be interpreted as an opportunity for improving the robot's ability and acceptance in precisely manipulating and handing off objects to the older adults even when considering the limitations of the platform (specifically the manipulator) such as the restrictive number of degrees of freedom (limiting the general motion and dexterity of the robot) as direct consequence of the expected affordability of the platform. An important question arises from these deployments: Can affordable systems using low-complexity methods be deployed in real world applications and successfully perform complex manipulation tasks? Two perspectives can be considered when attempting to answer this question: the task and the agent. For the task, this would represent whether the "instruments" (interpreted as objects of interest) can be modified to ease manipulation tasks, given the platform limitations. For the agent, whether novel hardware mechanisms and methods can be developed to account for various scenarios in addition to its own mobility and affordability constraints. We attempted to focus on the latter,

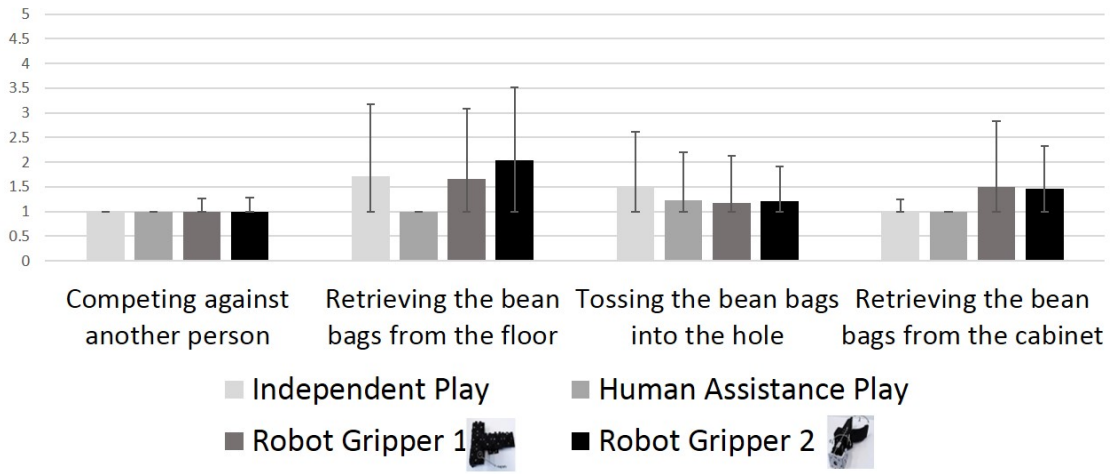

Figure 3.36: Average difficulty scores, where the participant scored in a scale from 1 (no difficulty) to 5 (high difficulty) how difficult each of the statements were. The number of participants that responded to each of the question varied and was taken into account when calculating the average. Total participants was N = 17.

while the former can be further explored as future work. As it follows, affordability and low-complexity will be investigated at the end-effector level, and methods and designs will be proposed aiming to address this emerging question.

Chapter 4

Affordable Low-Complexity Manipulation

The need assessment from Chapter 3 informed the necessity and efficacy of affordable, low complexity systems in performing complex tasks in real world applications, specifically aiding older adults in their ADLs and IADLs. As also observed, the type of end-effector has direct impact on the HRI for manipulations tasks. For older adults, the less complex the end-effector (and therefore more intuitive the interaction), the more acceptable it would be. To explore such findings, this Chapter investigates affordable end-effector designs with minimum complexity and how to combine these in manipulation tasks considered important by the need assessment with stakeholders.

Low-cost and low-complexity manipulation can be approached from a hardware and a task perspective. From a hardware level, low-cost manipulation would consider low-complexity end-effectors to achieve complicated tasks, such as throwing an object. This is an alternative to the conventional notions of grasp fixture (form and force closure). From a task perspective, low-cost manipulation can use the environment as means to achieve motions such as reorienting a part, or regrasping an object by in-hand manipulation. To investigate low-complexity applications, a conventional task of pick-in-place manipulation is chosen.

4.1 Pick-in-Place Manipulation (PnP)

A robotic object picking through in-hand manipulation using end-effectors with no internal mobility is proposed. Fig. 4.1 depicts this scenario in which the robot is picking the cylindrical object with the non-functioning parallel-jaw gripper (thus no internal mobility). This lack of mobility implies that generally it can be impossible to (1) control contact positions and contact wrenches and (2) guarantee desired grasp properties such as force- or form-closure. While objects have been shown to be stable with just two frictionless contacts [2], transitioning from grasps to release

such as picking up or placing an object can be complicated. The proposed scenario can be practically important for affordable low-complexity robotic manipulation. Costs of robotic grippers are often determined by the number of actuators. End-effectors with no internal mobility are simple and will use zero actuators (and thus no actuator cost). The scenario is also closely related to the important issue of robotic dexterity. For example, consider the parallel-jaw gripper, which may be by far the mostly used robotic end-effector. Although parallel-jaw gripping can be stable (it is well known that a grasp of two contacts that oppose each other can resist any external wrench applied to the object), it is necessary to impart sufficiently large internal forces to secure the object. The typical failure modes of parallel-jaw grippers thus include: object slippage due to insufficient internal forces, object damage from too large internal forces, and inability to make two contacts opposing each other (for example, due to limited range of joint motion). A more adaptive approach that depends less on frictional forces (and in turn, internal forces) and exact contact positioning will address those issues and render robotic manipulation more dexterous and practical.

A novel robotic in-hand manipulation technique for picking objects off a flat surface with an end-effector that can be abstracted as a collection of two point fingers with fixed separation distance is introduced. The end-effector thus lacks internal mobility and has to be controlled passively. The resulting operation incorporates tipping and regrasping as can be seen in Fig. 4.1. It will be shown how the object can be in static equilibrium with the two end-effector contacts that do not necessarily oppose each other. This technique can be applied to a wide range of scenarios, for example, it can complement the common parallel-jaw gripping by addressing the issues aforementioned. The picking technique can also be directly applied to placing objects back on a flat surface.

(a) (b) (c) (d) (e) (f)

Figure 4.1: (a)–(f) The robot is picking the snack carton through tipping and regrasping with the zero DOF end-effector – a parallel-jaw gripper that does not close.

4.1.1 Problem Description and Assumptions

The problem to be addressed concerns the planning and control for quasistatic object picking. The target object is assumed to be initially placed on a flat surface and the direction of gravity is normal to the surface. The objects of interest have

convex shape, long profile geometries with the longest dimension perpendicular to the contact surface. Therefore, for a conical object represented on the plane as an isosceles triangle for instance, the initial state has the base of the object in contact with the surface, as opposed to the legs. Other initial configurations of the object are proposed as future work. The end-effector is assumed to provide two contacts, as the common parallel-jaw gripper. Unlike parallel-jaw gripping, however, the problem entails more conservative scenarios in which it is not possible to control the distance between the two end-effector contacts, and thus to squeeze objects and attain force-closure grasps. The aim is to develop a method for picking objects through quasistatic in-hand manipulation with such simple end-effectors as depicted in Fig. 4.1. This can be practically important in case, for example, failing actuated grippers become frozen and it is impossible to exert sufficiently large internal forces (consider gripping a slippery, cone-shaped object with a parallel-jaw gripper).

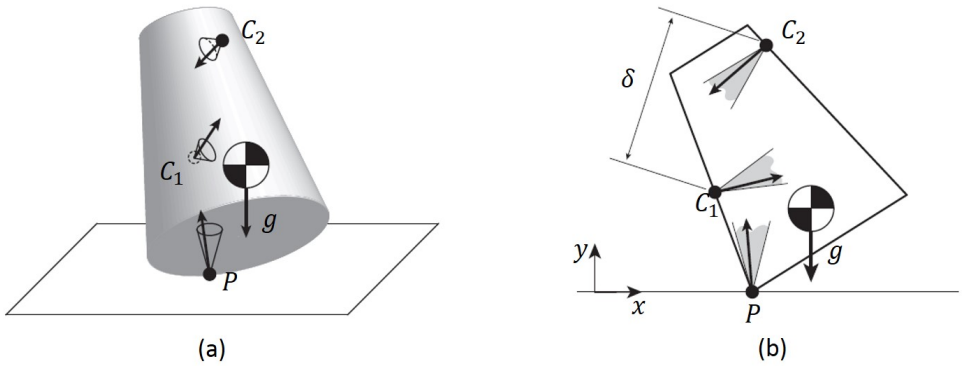

Figure 4.2: The 3D truncated cone and the 2D trapezoidal object are in contact with three external contacts at C_1, C_2, and P in (a) and (b), respectively. Our end-effector is abstracted as a collection of two contacts $\{C_1, C_2 | \delta \text{ is constant}\}$. The objects are supported by the ground at P. Each contact is shown with its friction cone.

The proposed scenario involves three contacts: two contacts with the end-effector plus one contact with the environment (Fig. 4.2(a)). According to *screw theory* [64], one approach to attaining static equilibrium with the three resultant contact wrenches and the wrench of gravity is to keep them necessarily co-planar. Motivated by this, the problem of object picking on the plane as described in Fig. 4.2(b) is to be investigated. The target *object* is a rigid polygon, moving on the plane, and placed stably on a flat surface, modeled as a sufficiently long line segment. An *end-effector* is then abstracted as a collection of two contact points whose distance is fixed; thus it is unable to squeeze an object by itself. Contacts on the object are modeled as *point contacts with friction* [111].The object desired state is to lie stable within the end-effector, that is, between the two contacts, during the picking operation, although some strong notions such as form-closure will not

be attainable due to the lack of mobility and sufficient number of contacts. The goal state features a stable grasp under the influence of gravity.The generalization of the resulting planar operation to three-dimensional picking problems will also be considered.

4.1.2 Tipping, Regrasping, and Picking with Two Contacts at Fixed Distance

This section presents the manipulation planning for the planar picking problem described in Sec. 4.1.1. The proposed approach features three types of atomic operations, arranged into a feasible manipulation plan for object picking. Properties of the manipulation planning are also discussed.

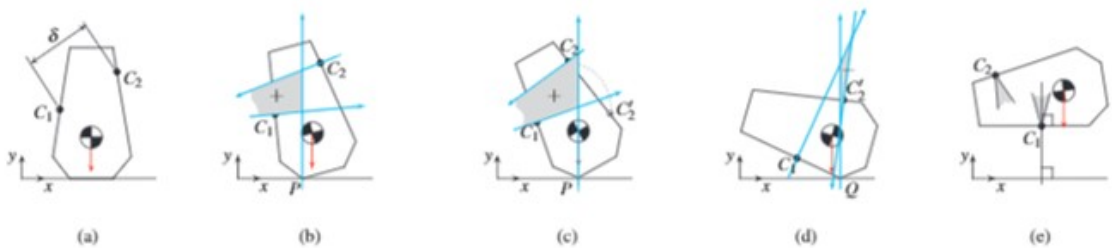

Figure 4.3: Picking the polygonal object with two point contacts at fixed distance (δ remains constant). The blue (red) arrows represent the frictionless contact wrenches (gravity). (a) Initially on the object, there are two point contacts, C_1 and C_2, with the end-effector and one line contact with the ground. (b) The object is tipping CCW. The object is in stable equilibrium even with frictionless contact wrenches: according to *moment labeling* [98], the composite wrench cone of the contact wrenches (the + labeled gray set) can resist gravity. (c) When the CoM is right above P, the object is marginally stable in that gravity can be balanced by a wrench on the boundary of the composite wrench cone. (d) The object is tipping CCW about the next pivot Q with the new grasp $\{C_1, C_2'\}$. This motion terminates when C_1 hits the ground. Static equilibrium is maintained. (e) The object can be lifted up with the frictional grasp $\{C_1, C_2\}$. In (b), (c), and (d), the object can be in static equilibrium even with the frictionless contact wrenches.

Atomic Operations

The three types of atomic operations for tipping polygonal objects over under the influence of gravity, with an end-effector making a non-antipodal contact pair at fixed distance can be defined. Without loss of generality, it is assumed the object's rotation is counterclockwise (CCW).

Type I Tipping With a nonantipodal contact pair, our end-effector can make two types of grasps in terms of the sign of the moments it can exert (see Lemma 1). For example, as can be seen in Fig. 4.3(b), the moment of the contact force couple at C_1 and C_2 can point in the positive (negative in Fig. 4.3(d)) z-direction. In *Type I Tipping*, the object is tipped CCW by the grasp that can impart positive z-directional moments (Fig. 4.3(b)).

Type II Tipping In *Type II Tipping*, the object is tipped CCW by the grasp that can impart negative z-directional moments (Fig. 4.3(d)).

Regrasping In *Regrasping*, the end-effector is rotated about one of the contact points. As a result of the regrasping, the sign of the moment of the contact forces switches.

These operations are exhaustive in terms of the relative position between the object's center of mass (CoM) and the vertex about which it rotates, as will be explained in the following subsection.

Planning for Picking

Given the contact location, the progress of the planning method shall be explained using Fig. 4.3 where the object rotates CCW monotonically, without loss of generality. The first step is to determine where to make contacts and how to acquire the contacts (Fig. 4.3(a)). As in parallel-jaw gripping, our end-effector is supposed to make two point contacts on an object's edge pair where it is possible to have an *antipodal* grasp, whose two contacts can "see each other by a line inside both friction cones" [92]. Such an edge pair (for example, a parallel edge pair) can be found by a combinatorial search in $O(n^2)$ time for an n-sided polygonal object [147]. Since antipodal frictional contacts determine planar force closure grasps [114]), what remains is to determine whether the non-antipodal type grasps lead to a static equilibrium state. Algorithm 1 takes as input the coordinates of n discretized points $\mathbf{q}_k$ and $\mathbf{r}_j$ of a pair of edges ($\overline{\mathbf{p}_i\mathbf{p}_{i+1}}$ and $\overline{\mathbf{p}_{n-1}\mathbf{p}_n}$) respectively on a convex two-dimensional polygon and its center of gravity, and returns a collection of grasps that can result in equilibrium, represented by the location of the frictional contacts and the object orientation $(\mathbf{q}_k, \mathbf{r}_j, \theta_i)$ respectively. It can also run in $O(n^2)$ time, with n number of discretized points on the pair of edges. The detailed description follows:

4.1.3 Algorithm for Grasp Synthesis

Lines 4-5: Force closure grasps between two edges can be determined by a set of constraints that assures the line connecting the contacts lies within their respective friction cones [7], or

Algorithm 1 GRASP-SYNTHESIS

Input: coordinates of n points, $\mathbf{p}_1, \cdots, \mathbf{p}_n$ (the end points of two edges, $\overline{\mathbf{p}_i\mathbf{p}_{i+1}}$ and $\overline{\mathbf{p}_{n-1}\mathbf{p}_n}$, and the center of gravity, $\mathbf{p}_g$).

Output: triples, $(\mathbf{q}_k, \mathbf{r}_j, \theta_i)$ - grasps that can be made equilibrium.

1: Discretize each pair of edges into a collection of m vertices: $\{\mathbf{q}_i | \mathbf{q}_i \in \overline{\mathbf{p}_i\mathbf{p}_{i+1}}\}$ and $\{\mathbf{r}_i | \mathbf{r}_i \in \overline{\mathbf{p}_{n-1}\mathbf{p}_n}\}$; discretize $[0, \pi)$ into a collection of angle vales, $\{\theta_i\}$. Place $(\mathbf{q}_k, \mathbf{r}_j)$ along edges $\overline{\mathbf{p}_i\mathbf{p}_{i+1}}$ and $\overline{\mathbf{p}_{n-1}\mathbf{p}_n}$ respectively
2: **for** each discretized vertices $\mathbf{q}_k$ **do**
3: **for** each discretized vertices $\mathbf{r}_j$ **do**
4: **if** $(\mathbf{q}_k, \mathbf{r}_j)$ is an antipodal grasp **then**
5: Label $(\mathbf{q}_k, \mathbf{r}_j)$ as FORCE-CLOSURE GRASP.
6: **else**
7: **for** each angle value θ_i **do**
8: **if** $(\mathbf{q}_k, \mathbf{r}_j, \theta_i)$ can be in equilibrium **then**
9: Label $(\mathbf{q}_k, \mathbf{r}_j, \theta_i)$ as NON-ANTIPODAL FEASIBLE GRASP.
10: **end if**
11: **end for**
12: **end if**
13: **end for**
14: **end for**

$$\begin{cases} (n_k - \mu n_k^{\perp}) \otimes (q_k - r_j) > 0 \\ (n_k - \mu n_k^{\perp}) \otimes (q_k - r_j) < 0 \\ (n_j - \mu n_j^{\perp}) \otimes (r_j - q_k) > 0 \\ (n_j - \mu n_j^{\perp}) \otimes (r_j - q_k) < 0 \end{cases} \quad j, k = 1 \cdots n \tag{4.1.1}$$

where $\otimes$ represents the 2D cross-product (or determinant in $\mathbf{R}^2$), n_k and n_j are the contact normals with respect to point fingers q_k and r_j respectively and $n^{\perp}$ is the unit vector perpendicular to n, with $n \otimes n^{\perp} = 1$.

Lines 8-9: If the triple $(\mathbf{q}_k, \mathbf{r}_j, \theta_i)$ is in equilibrium, label the grasp as a non-antipodal feasible grasp.

To determine the feasibility of non-antipodal grasps, denote the equality constraints $f_i(x)$, which include the net normal and friction forces and moments acting on the system, and inequality constraints $h_i(x)$ representing the friction cones at the point fingers. A uniform friction coefficient μ is assumed for all object edges. By considering the objective function identically zero, the optimal value will either be zero (for a non-empty feasible set) or ∞ for an empty feasible set. We can satisfy the system constraints by considering the following feasibility problem:

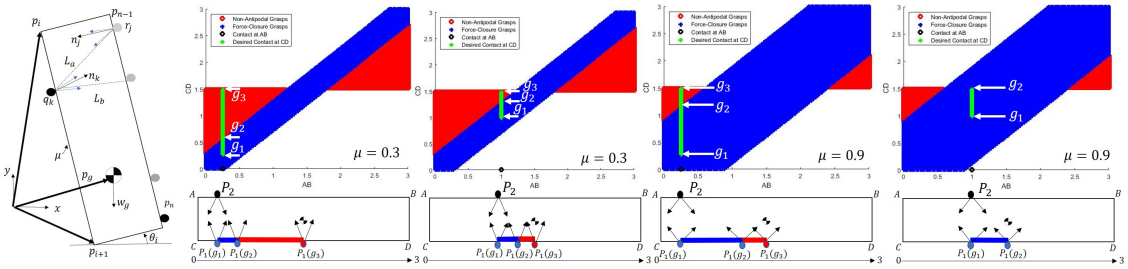

Figure 4.4: Mapping of force-closure and non-antipodal feasible regions for frictional coefficients of $\mu = 0.3$ and $\mu = 0.9$ respectively. The contact P_2 is fixed while analyzing the possible contact locations for contact $P_1(g_i)$. The graph indicates by vertical lines the desired location for placing a second contact given the first. For instance, g_1, g_2 are inside the force-closure region, and the pair $P_1(g_1)P_2$ or $P_1(g_2)P_2$ constitute a force-closure grasp, while g_2, g_3 represents a non-antipodal feasible region and $P_1(g_3)P_2$ a non-antipodal feasible grasp with the force of gravity. Therefore, the feasible grasp region is amplified from considering force-closure grasps only by adding the non-antipodal region, which does not translate in force closure but still allows the object to be manipulated.

$$\begin{aligned} \text{minimize} \quad & f^T x \\ \text{subject to} \quad & Ax \leq b \\ & A_{eq} x_{eq} = b_{eq} \end{aligned} \tag{4.1.2}$$

where we define:

$$f = \begin{bmatrix} 0_{1x4} \end{bmatrix}, x = \begin{bmatrix} n_k & \mu n_k & n_j & \mu n_j \end{bmatrix}^T$$

$$A = \begin{bmatrix} w(\mu) & 0_{3x2} \\ 0_{3x2} & w(\mu) \end{bmatrix}, w(\mu) = \begin{bmatrix} -1 & 0 \\ -\mu & 1 \\ -\mu & -1 \end{bmatrix}$$

$$A_{eq} = \begin{bmatrix} -\cos\theta & -\sin\theta & (\cos\theta q_{ky} - \sin\theta q_{kx}) \\ -\sin\theta & \cos\theta & (\sin\theta q_{ky} + \cos\theta q_{kx}) \\ \cos\theta & \sin\theta & (\sin\theta r_{jx} + \cos\theta r_{jy}) \\ -\sin\theta & \cos\theta & (-\sin\theta r_{jy} + \cos\theta r_{jx}) \end{bmatrix}^T$$

$$b = \begin{bmatrix} 0_{1x6} \end{bmatrix}^T, b_{eq} = \begin{bmatrix} 0 & w_g & w_g x_{cm} \end{bmatrix}^T$$

with 0_{ixj} non-square zero matrices ixj, w_g the weight of the object, $q_k = (q_{kx}, q_{ky})$, $r_j = (r_{jx}, r_{jy})$ and x_{cm} the moment arms of contacts q_k, r_j and of the center of mass respectively. By solving this feasibility problem, we can determine whether a given configuration satisfies or not the physical constraints for static equilibrium.

Considering the assumption that no motion between the end-effector and object occurs, the output of the algorithm can be used to determine the initial placement of the contact pair on the object. As seen in Fig. 4.4, for a fixed contact at edge AB, the second contact at edge CD could occur anywhere (shown as vertical lines in the graphs) between g_1 and g_2 (in blue, constituting a force-closure grasp region), or between g_2 and at the furthest right g_3 (in red, determining a non-antipodal feasible location). For this example, the regions are symmetric with respect to the perpendicular line thorough the center-of-mass, and as expected the larger the friction cone the larger the possibility for a force-closure grasp region, but there will still be possibility for non-antipodal feasible grasps. As a result, the end-effector capabilities can be extended and made more dexterous by allowing feasible grasps outside the force-closure grasping region, or contacts not necessarily opposing each other.

The two contact positions on each edge is selected so that their distance equals to δ, the distance between the two contact points of the end-effector. The end-effector is then position-controlled to follow a feasible path into the contact positions. Next, the atomic operations are performed sequentially to roll the object CCW until the inward pointing contact normal at the contact C_1 is anti-parallel to the force of gravity (Fig. 4.3(e)). The position of the object's CoM relative to the contact normal at the ground contact determines which action to take. If the CoM is on the right (left) half plane delimited by the contact normal, as illustrated in Fig. 4.3(b) (Fig. 4.3(d)), the end-effector is controlled to perform *Type I Tipping* (*Type II Tipping*). If the CoM is on the line of the contact normal (Fig. 4.3(c)), the end-effector is controlled to perform *Regrasping* from grasp $\{C_1, C_2\}$ to $\{C_1, C_2'\}$. If other edge of the object hits the ground in the meantime, the motion proceeds with the new pivot (see the pivot changes from P to Q between Fig. 4.3(c) and (d)). Thus, during the whole manipulation process the pivot can switch at most n times for an n-sided polygonal object. Finally, at most one *Regrasping* may be needed in order to properly counteract the moment of gravity before lifting the object: for example, between Fig. 4.3(d) and (e), the grasp has changed from $\{C_1, C_2'\}$ to $\{C_1, C_2\}$ before the lifting-up happens. During the tipping and regrasping operations and upon the termination of the process, the contact forces can properly counteract gravity; thus the object remains in static equilibrium (see Lemma 1). The manipulation process should terminate and can be applied to any polygonal shape that admits antipodal grasps (see Lemma 2). Furthermore, because two distinct poles of rotation (one for the tipping, the other for the regrasping) suffice for the operations, it is possible to implement the picking process using a position-controlled robot arm with two DOF. Two types of implementation can be considered: reactive control based on force feedback and deliberative control by planning in advance (see Sec. 4.2).

Discussion

The following lemma shows that the object remains in static equilibrium during the manipulation; thus it is possible to execute the picking operation in a quasistatic manner.

Lemma 4.1.1. *During the manipulation process stated in Sec. 4.1.2, an object can be in static equilibrium with two point contacts on an edge pair that can accommodate antipodal grasps.*

Proof. First, static equilibrium during the tipping operation can be checked. If the two end-effector contacts are antipodal, they form a *force-closure* [111] grasp that can be in static equilibrium. Otherwise (with two nonantipodal contacts), the two contacts alone cannot be in force-closure because they fail to be in *torque-closure* [112], that is, the moments of the two contact forces are necessarily unilateral and the sign is determined by their relative position. Still, the two contacts are in *force-direction closure* [112], where the contact wrenches span the space of all forces. No matter where the contacts are located on the edges, the condition of force-direction closure is invariant. According to the description of *Type I/II Tipping*, the signs of (1) the moment of gravity with respect to the pivot and (2) the moment of the contact force couple are always opposite. Therefore, the system of all wrenches can be in torque-closure and this in turn implies force-closure and possibility of static equilibrium.

Second, during the regrasping, the ground contact and one of the two end-effector contacts are able to exert wrenches counteracting the wrench of gravity. In Fig. 4.5(a), the friction cones define a band (see the orange set) between the two supporting hyperplanes (parallel to the direction of gravity) of the two convex regions that are the composite wrench cone. As long as the line of the force of gravity remains in the band, the object can be in static equilibrium. The finite size of the band implies the regrasping operation can be performed with some robustness in the actual orientation of the object. Third, at the terminating condition, the line of the contact normal at C_1 is supporting the composite wrench cone because it is delimited by the edges of the friction cone at C_1 (Fig. 4.5(b)). At the same time, the contact normal is parallel to the wrench of gravity. Therefore the wrench of gravity can be spanned by the composite wrench cone. □

By taking advantage of frictional contact forces, the whole process can actually be terminated before the terminating condition is satisfied exactly. This is because the composite wrench cone is pointed at C_1 as can be seen in Fig. 4.5(b). Therefore the contact normal at C_1 does not have to be necessarily parallel to the force of gravity. During the tipping operations, if the center of rotation of the end-effector is on the pivot (P or Q in Fig. 4.3), then it is possible to tip over the object with no sliding. If the pole is off the pivot, the object will slide both on the ground and the end-effector while tipping over; contact mode analysis shows that it is feasible

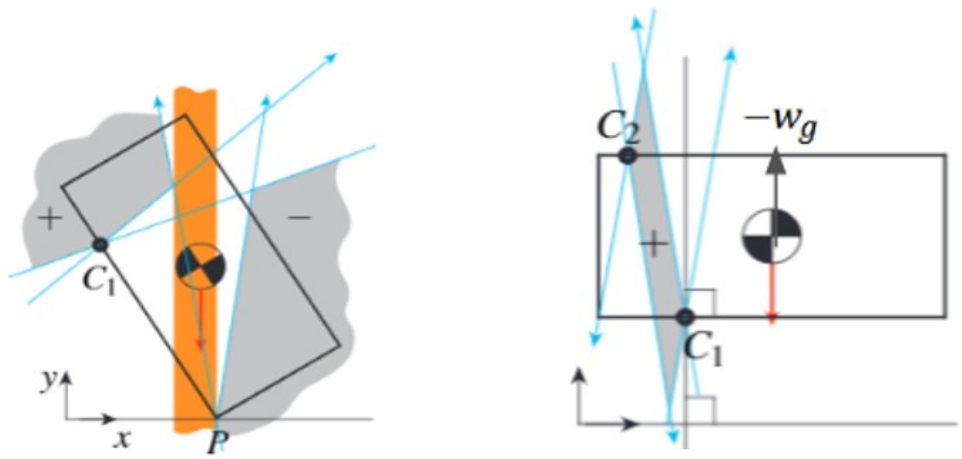

(a) (b)

Figure 4.5: The +/− labeled gray sets represent the composite wrench cone of the contact wrenches with Coulomb friction according to the moment labeling technique when (a) there is one contact with the ground at P and one contact with the end-effector at C_1; and (b) the tipping operation terminates.

without losing static equilibrium. While it is possible to tip over an object with only one point contact, with two contacts it is possible to rely less on frictional forces and exact contact positioning as discussed in the proof of Lemma 1. In contrast, in one-contact object tipping, friction and contact positioning is critical [88]. In our two-contact manipulation, it is also possible to retain the object within the end-effector, which is impossible with only one contact.

The following lemma shows that the picking operation can be applied to a wide range of shapes.

Lemma 4.1.2. *The manipulation process stated in Sec. 4.1.2 terminates for any polygonal shape that admits antipodal grasps.*

Proof. A polygonal object is in contact with a sufficiently large flat surface only at the vertices on its convex hull. Therefore the object keeps turning CCW by the manipulation process of Sec. 4.1.2 because it is impossible for concave vertices to make contact with the surface (Fig. 4.6). The angle between the contact normal at C_1 and the force of gravity changes monotonically and thus the motion terminates. □

Departing from the two-dimensional polygonal object model, our technique can be applied to three-dimensional objects by effectively suppressing the motions off the plane, for example, using curved fingers as investigated in our previous work [138]. This point shall be demonstrated in the next section with experiments performed with essentially prisms and objects with rotational symmetry, a class of object

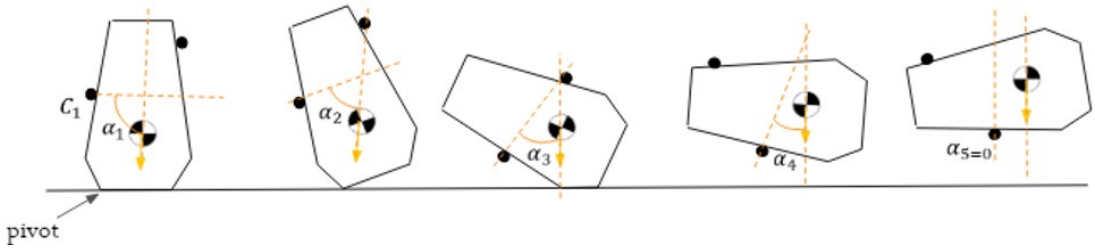

Figure 4.6: Demonstration of how the angle α_i changes monotonically for polygonal objects that admit antipodal grasps until the process terminates, according to Lemma 4.1.2

shapes which may be found in various human-robot interaction scenarios, as well as industrial applications. The picking technique can also be applied to object placing, by reversing the picking motion in a quasistatic manner. Experiments will demonstrate both applications.

The lemmas above imply that our object picking technique with the passive, zero DOF end-effector model can be as complete as two-dimensional parallel-jaw gripping in the sense that it can be executed by two contacts on an edge pair accommodating parallel-jaw grasps (that is, antipodal grasps). This method can also generalize the way common parallel-jaw grippers are used by (1) not depending on antipodal contacts (thus no need to search for feasible antipodal grasps and less sensitive to sensing/positioning accuracy), (2) not squeezing the objects (thus no need to control contact/friction forces), and (3) adapting the shape of the gripper fingers. This approach can thus be applied even to a failing parallel-jaw gripper, which is not able to squeeze objects, to do successful object picking. But, the object may roll on its convex hull until the tipping operation terminates and the regrasping actions will need sufficiently large free space, which can render end-effector accessibility and reachability check harder than parallel-jaw gripping.

4.2 Implementation and Experimentation

For experimentation, we propose a custom-made direct-drive arm capable of joint torque sensing and a state machine software built upon the model of mechanics discussed in Sec. 4.1.2. Sec. 4.2.1 introduces the hardware and software system and Sec. 4.2.2 presents experiments for object picking and placing performed with the direct-drive arm. The state machine software enabled the arm to transition between Type I/II Tipping and Regrasping actions in an autonomous manner through joint torque feedback. Experiments with a conventional 7 DOF manipulator are also presented in Sec. 4.2.3. See Fig. 4.14 for the objects used here.

4.2.1 Direct-Drive Arm: Hardware and Software

(a) (b) (c)

Figure 4.7: (a) CAD exploded view showing two motors, a parallelogram linkage (the black links), and two white rigid body fingers constituting a zero DOF end-effector. The motor axes are collinear. (b) Set-up implementation. (c) Two different types of end-effector configuration adopted.

Object Picking

A two DOF arm using a parallelogram five-bar linkage with a closed-loop kinematic chain (Fig. 4.7) was developed; similar approaches can be seen in [8]. Its two DOF motions are composed of one DOF internal deformation and the rigid body rotation of the parallelogram itself. The links are laser-cut ABS plastic. 3D-printed, single rigid body fingers can be attached to the arm linkage using mechanical adapters. We employ direct-drive actuation. Two iPower GBM6212H-150T brushless DC motors (torque limit: 0.5Nm) are directly coupled to two links of the parallelogram linkage, with no gearbox. If the two motors, denoted M_1 and M_2 (Fig. 4.7(a)), spin with the same angular velocity, the parallelogram linkage performs rigid body rotation. If M_2 spins solely, the parallelogram is deformed. The motors are controlled by IQinetics IQ-MC-17-15-24C-H motor controllers[1] running a PID controler at 2 kHz and commutation frequency at 22 kHz, with a high resolution position sensing capability (12 bits or 4096 counts per revolution). The direct-drive arm is capable of reliable joint torque sensing with no explicit torque sensor [118], and thus enables low-cost, autonomous manipulation in a reactive manner. The torque on the motors is calculated from their current readings, with $\pm 20\%$ estimated errors due to noise and friction at the joints. Serial communication with the motors is realized using FTDI USB to serial UART. MATLAB software was used for communicating with the motors and implementing functions for not only low-level torque calculation

[1] http://iqinetics.com/

but also in-hand manipulation capabilities. The operation can be explained using the abstraction of a finite state machine, also can be seen in [74, 86, 45], with the following four states:

Regrasp CCW The arm rotates the end-effector CCW about one of the two fingers.

Regrasp CW The arm rotates the end-effector CW about one of the two fingers.

Tip The arm itself rotates CCW.

Lift The arm translates the end-effector upward by deforming the parallelogram linkage.

The organization of these states can be customized to suit the purpose of experiments (that is, object picking or placing), as will be elaborated as follows.

4.2.2 Experiments with the Direct-Drive Arm

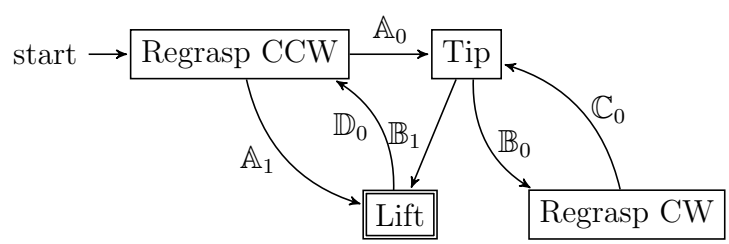

Figure 4.8: Finite state machine for object picking. Its operation terminates in "Lift" state.

$$\mathbb{A}_0 : \tau_{M_2} > 0.12, \text{ and } \theta_{M_1} = 0 \tag{4.2.1}$$
$$\mathbb{A}_1 : \tau_{M_2} > 0.12, \text{ and } \theta_{M_1} > 0 \tag{4.2.2}$$
$$\mathbb{B}_0 : \tau_{M_1} + \tau_{M_2} - \tau_{\overline{M}} < 0.04 \tag{4.2.3}$$
$$\mathbb{B}_1 : \tau_{M_1} + \tau_{M_2} - \tau_{\overline{M}} > 0.35, \text{ and } \theta_{M_1} < \pi/2 \tag{4.2.4}$$
$$\mathbb{C}_0 : \tau_{M_2} > 0.085 \tag{4.2.5}$$
$$\mathbb{D}_0 : \tau_{M_2} < 0.06 \tag{4.2.6}$$

Fig. 4.8 represents the software for object picking mode, implementing the planning in Sec. 4.1.2. A precondition regarding the initial placement of the fingers is necessary: one of the two fingers is already in contact with the object. This

is because the 2 DOF arm lacks sufficient mobility to address general path planning/trajectory following scenarios. This can be relaxed by using, for example, a conventional 6 DOF industrial arm. Given the precondition, the finite state machine of Fig. 4.8 is executed. First, in Regrasp CCW state the end-effector is rotated until the condition of edge label $\mathbb{A}_0$ is satisfied (this is the moment when the other finger also makes contact with the object). Then in Tip state the arm rotates CCW until $\mathbb{B}_0$ is satisfied (at this moment the CoM is on the line of the contact normal at the ground contact). Next, after the regrasping is done ($\mathbb{C}_0$) in Regrasp CW state, the arm rotates CCW again in Tip state. If $\mathbb{B}_1$ is satisfied, we enter Lift state. If the lifting operation is unsuccessful ($\mathbb{D}_0$), the state is transitioned to Regrasp CCW before attempting to lift again.

Those edge labels ($\mathbb{A}_0$, $\mathbb{B}_0$, and so on), called the *state guard conditions*, are formulated using (1) τ_{M_1} (τ_{M_2}), the torque sensed on motor M_1 (M_2) in Nm; (2) $\tau_{\overline{M}}$, the sum of no load torques on both motors; and (3) θ_{M_1} (θ_{M_2}), the absolute angle of motor M_1 (M_2) in radians. Each condition was obtained empirically. For example, $\mathbb{B}_0$ (Eq. 4.2.3) concerns the moment when the center of mass is right above the pivot. At the instant when the event happens, in principle $\tau_{M_1}+\tau_{M_2}=\tau_{\overline{M}}$. But, in practice a small positive margin is needed to make the condition more robust. We chose 0.04 Nm in Eq. 4.2.3, which resulted in a local maximum in terms of the experiment success rates. Other conditions were determined in a similar manner and are as follows:
Fig. 4.9 represents two of the experiments done with the direct-drive arm running the state machine in Fig. 4.8. Due to its reactive nature, the picking operation is performed autonomously with no information on object mass properties and frictional characteristics of the object, fingers, and table top. For planning purposes, the shapes of the objects in Fig. 4.9 can be projected into a trapezoid and a triangle, respectively. When it comes to executing the resulting manipulation plan, the combination of the semicircular and straight fingers help stabilize the three-dimensional object by suppressing the motions off the plane (Fig. 4.7 c).

Such experiments were repeated with a range of objects and surface conditions. See Table 4.1. Two experiments with objects #8, #12 and #13 are shown in Fig. 4.10. In total, 165 out of 210 trials (78%) were successful. Recall that objects are allowed to slide on the ground and on the end-effector (discussion in Sec. 4.1.3). To check the effect of the sliding on stable picking, the distance between the pivot of tipping and the motor axis was varied from 5 to 35mm for object #7. Here 27 out of 30 trials (90%) were successful. In unsuccessful trials, the empirically determined guard conditions did not seem to work, as in some cases the contact torque detection was too high and the object would start rotating with the end-effector motion. The possible ±20% errors in torque estimation inherit from the motor controller may also have accounted for the failed trials. Specifically, the direct-drive arm made a wrong estimate of the position of the CoM in case of thin, lightweight objects. Since the alignment of the center of mass with respect to the ground contact is essential

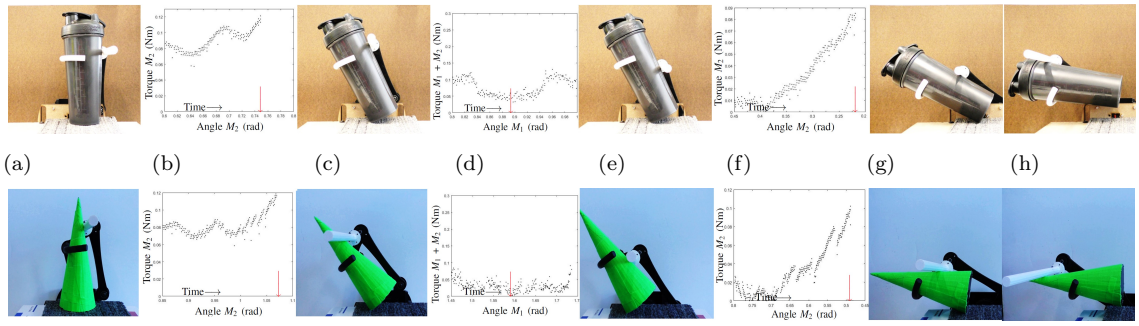

Figure 4.9: Two picking experiments with the beverage container (upper) and the cone-shaped object (lower). In (a), the two fingers (one curved, one straight) are in contact with the objects at the instant guard condition $\mathbb{A}_0$ (Eq. 5.3.1) is satisfied, or the contact generated by the rotation of motor M_2 occurs. The instant is marked with the red arrow in (b) where M_2 angle is increasing with time. In (c), the CoM is right above the pivot at the instant guard condition $\mathbb{B}_0$ (Eq. 5.3.3) is satisfied. The instant is marked with the red arrow in (d) where M_1 angle is increasing with time, and the sum of motor torques $\tau_{M1} + \tau_{M2}$ indicates a minima. (e) show the configurations after regrasping at the instant guard condition $\mathbb{C}_0$ (Eq. 4.2.5) is satisfied. The instant is marked with the red arrow in (f) where M_2 angle is decreasing with time, indicating a contact has been made with the object. After further rotation (g), the objects are lifted up (h).

during the regrasping operation, this caused unwanted sliding of the objects. The shifting COM position for object #7 accounted for some failure cases. Despite using the curved finger, the same could only accommodate a set of object dimensions and for objects #4 and #5 it did not suppress off plane motions, resulting on object slipping for several trials. The dimension of the objects also impacted the results, where objects were either too bit (#13) or too small (#11) for the end-effector dimensions.

Object Placing

Picked objects can be placed again by reversing the picking motion in a quasistatic manner. See Fig. 4.11 for the state machine in the placing mode. A new guard condition for detecting the event of object touchdown is required: $\overline{\mathbb{D}_0} : \tau_{M_1} + \tau_{M_2} - \tau_{\overline{M}} < 0.57$. Starting from Touchdown state, the operation of the state machine can be explained similarly to the picking mode. Experiments with objects #6 and #7 were performed and out of 30 trials, 20 (67%) were successful (Table 4.1). The considerable rate of unsuccessful trials for placing can be attributed to the the wrong estimate of the object state during the Touchdown. Specifically, as initial conditions varied (such as contact location with respect to the object's COM), some objects

Figure 4.10: Picking experiments with objects #13 #8 and #12.

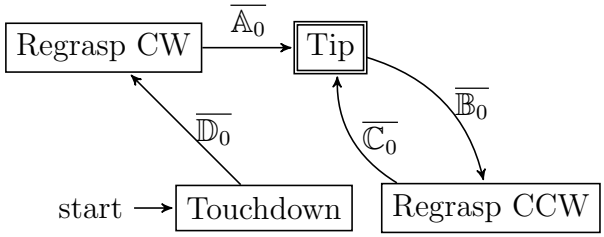

Figure 4.11: Finite state machine for object placing.

would rotate more to achieve ground contact and would slip. This was often verified with objects shifting their COM when containing liquid inside. Heavy objects (such as #6) were also noticeably difficult to place, since the limited torque of the motors would not be able to maintain the object stable prior to the Touchdown, causing it to fall.

4.2.3 Experiments with a Conventional Manipulator

Object picking and placing was also investigated using a conventional manipulator, the Rethink Robotics' Sawyer arm (Fig. 4.12(a)). The robot has a parallel-jaw gripper (Fig. 4.12(b)) equipped on the wrist of a 7 DOF arm. For the experiments here, the robot's parallel-jaw gripper is not actuated. Our 3D printed, curved finger can be used with the default, straight finger when handling curved objects (Fig. 4.12(c)).

Given an object of interest, the gripper trajectory for picking is obtained using the direct-drive arm and the Sawyer robot is then position controlled to follow the trajectory in a feed-forward, open-loop manner due to its lack of torque sensing capability. Object placing is done in a similar manner, with the placing trajectory

(a) (b) (c)

Figure 4.12: (a) Rethink Robotics's Sawyer. (b) Original end-effector. (c) Adapted end-effector with a curved finger.

prescribed again by the direct-drive arm. A set of experiments with six different objects resulted in overall success rate of 73% (see Table 4.1). Initial positioning errors and external disturbances (such as the vibration of the manipulator) may account for the unsuccessful trials. Since the method was implemented in an open-loop manner, placing the object at different initial positions would lead to incorrect amount of rotation of the object, often too much and causing it to fall. Fig. 4.13 presents picking and placing experiments with the cone-shaped object.

4.2.4 Discussion

A few remarks on this method can be made:

- The necessity for a larger free space for the atomic operations, compared to pick-in-place with conventional end-effectors (such as the PJG) can difficult manipulation in constrained or cluttered spaces (such as the common areas in nursing homes). However, symmetrical objects may require less free space since the object can pivot on a single vertex until termination condition.

- As discussed in Sec. 3.2.3, the preference was towards a non-prehensile end-effector that allows for easy object retrieval. Retrieving objects from this zero DOF end-effectors is straight forward since no internal forces are applied nor need to be controlled by the gripper for releasing the object.

- The design of the end-effector is directly linked to the object's dimensions. This is in part true for any end-effector (even human hands) since objects with large dimensions may not be "grasped" but carried in a non-prehensile manner. Therefore, although a single design may accommodate grasps of objects with or without parallel edges (such as objects $\#10, \#15, \#16$), the dimension of the contact edges along with the position of the center of mass determine the unique end-effector design parameter δ .

(a)

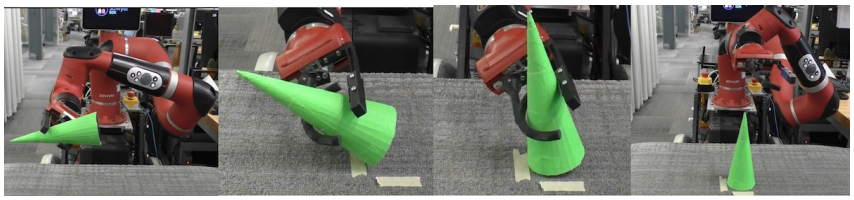

(b)

Figure 4.13: Implementation on the Sawyer robot showing (a) object picking (clockwise from the top leftmost panel) and (b) placing (left to right).

- Since the atomic operations rely on torque estimation of the motors, specifically for the center of mass detection, over or underestimations would slide or misplace the object respectively. Therefore more accurate torque readings would mitigate grasping failures.

Table 4.1: Experimental results for object picking and placing

Object						
Description	**Mass (g)**	**Task**	**Platform**	**Surface**	**Trials**	**Successes**
Cylinder (#1, Fig. 4.14)	140	Picking	DD Arm	Rubber	5	5
Aluminium 8020 (#2)	180	Picking	DD Arm	Rubber	5	5
Metal bar (#3)	265	Picking	DD Arm	Rubber	5	5
Bottle brush (#4)	125	Picking	DD Arm	Rubber	5	2
Oil can (#5)	205	Picking	DD Arm	Rubber	5	1
Potato chip carton (#6)	185	Picking	DD Arm	Rubber	5	3
Potato chip carton (#6)	185	Picking	Sawyer	Carpet	5	3
Potato chip carton (#6)	185	Placing	DD Arm	Rubber	5	3
Potato chip carton (#6)	185	Placing	DD Arm	MDF	5	2
Beverage container (#7)	190	Picking	DD Arm	Rubber	30	27
Beverage container (#7)	215 (25ml water)	Picking	DD Arm	Rubber	10	10
Beverage container (#7)	240 (50ml water)	Picking	DD Arm	Rubber	10	8
Beverage container (#7)	190	Picking	DD Arm	ABS plastic	10	7
Beverage container (#7)	190	Picking	DD Arm	MDF	10	8
Beverage container (#7)	190	Picking	DD Arm	Paper	10	8
Beverage container (#7)	190	Picking	DD Arm	Carpet	50	41
Beverage container (#7)	190	Picking	DD Arm	Masking Tape	10	10
Beverage container (#7)	190	Placing	DD Arm	Rubber	5	5
Beverage container (#7)	190	Placing	DD Arm	MDF	5	4
Beverage container (#7)	215 (25ml water)	Placing	DD Arm	MDF	5	3
Beverage container (#7)	240 (50ml water)	Placing	DD Arm	MDF	5	3
DVD (#8)	75	Picking	DD Arm	Rubber	5	3
Pencil case (#9)	90	Picking	DD Arm	Rubber	5	2
Sip cup (#10)	120	Picking	DD Arm	Rubber	5	3
Index cards (#11)	120	Picking	DD Arm	Rubber	5	2
Wool spool (#12)	74	Picking	DD Arm	Rubber	5	5
Milk carton (#13)	80	Picking	DD Arm	Rubber	5	1
Water bottle (#14)	190	Picking	Sawyer	Carpet	5	4
Conic glass container (#15)	275	Picking	Sawyer	Carpet	5	4
ABS cone (#16)	100	Picking	DD Arm	Carpet	5	3
ABS cone (#16)	100	Picking	Sawyer	Carpet	5	4
Pasta carton (#17)	125	Picking	Sawyer	Carpet	5	4
Soap container (#18)	125	Picking	Sawyer	Carpet	5	4
Aluminum foil carton (#19)	125	Picking	Sawyer	Carpet	5	2

Figure 4.14: Objects used for the experiments in Table 5.1.

Chapter 5

Dynamic Grasping for Object Picking Using Passive Zero-DOF End-Effectors

The technique proposed in the previous Chapter successfully demonstrated grasps of a variety of daily use objects, however the quasi-static assumptions makes the motions slow and also dependent on torque sensing feedback at the in-hand re-grasping operation. To achieve a faster and more dexterous manipulation for picking objects with zero DOF end-effectors, inertia forces have to be considered. To satisfy the equilibrium requirements of the system, an external acceleration force and torque are imposed to the object by the manipulator up to a desired position of stability, and so the grasp occurs dynamically. A closed form solution (e.g. a trajectory) for the dynamic picking of the object can be derived.

5.1 Problem Description

Our problem extends the earlier zero DOF end-effector work [108] regarding its initial configuration. The same assumptions from Sec. 4.1.1 are valid here, aside from the quasi-static motion. Given a target object placed on a flat surface with gravity normal to it (Fig. 5.2), and an end-effector that provides two frictional point contacts P_1, P_2, at a fixed (non-controllable) distance $r_{P_1P_2}$ at opposing edges, such that the contacts can tilt the object and accelerate it away from the contact surface, the problem can be summarized by finding a trajectory $p(t)$ in the world frame $[X, Y]$ such that the object can be accelerated to a final horizontal configuration while satisfying dynamic constraints that keep the object from moving relative to the contacts (attainable according to *screw theory* [64] if the resultant contact wrenches and the wrench of gravity are co-planar). The problem of dynamic object picking considers the following assumptions:

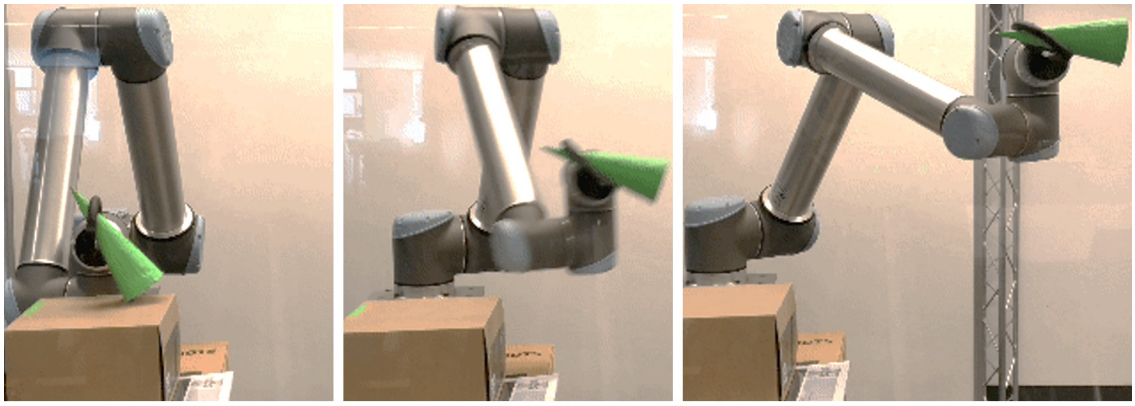

(a) (b) (c)

Figure 5.1: Dynamic grasping of an object with a zero DOF end-effector. The initial tilting angle (a) depends on the frictional contacts of the end-effector and the ground surface, (b) a trajectory considering the system dynamics and acceleration force constraints is imposed to the object by the manipulator, until a termination condition (c) is reached.

- The target object is modeled as a rigid polygon that moves on the plane.
- The object is stably placed on a flat surface with the gravity vector perpendicular to it.
- The end-effector provides two contacts at a fixed distance, modeled as Coulomb *point contacts with friction* [111] and one frictional contact is provided by the surface.
- The two contacts provided by the end-effector can be non-antipodal.

Although notions of force or form-closure cannot be obtained by the fixed-shape end-effector, dynamic closure [99] is desirable in order to guarantee contact constraints. The goal for the dynamic motion is to maintain object stability between the two end-effector contacts and under the influence of gravity in a planar analysis. Similar to [108], extensions towards the three-dimensional problem can be considered by suppressing out of plane motions.

5.2 Grasp Planning

As stated in Sec. 5.1, the dynamic grasp planning problem seeks to determine a trajectory $p(t)$ for which two frictional point contacts can dynamically pick the object off a surface and move it to a final stable configuration that is held by the robot. Since non-antipodal grasps can be admitted, determining the contact locations for

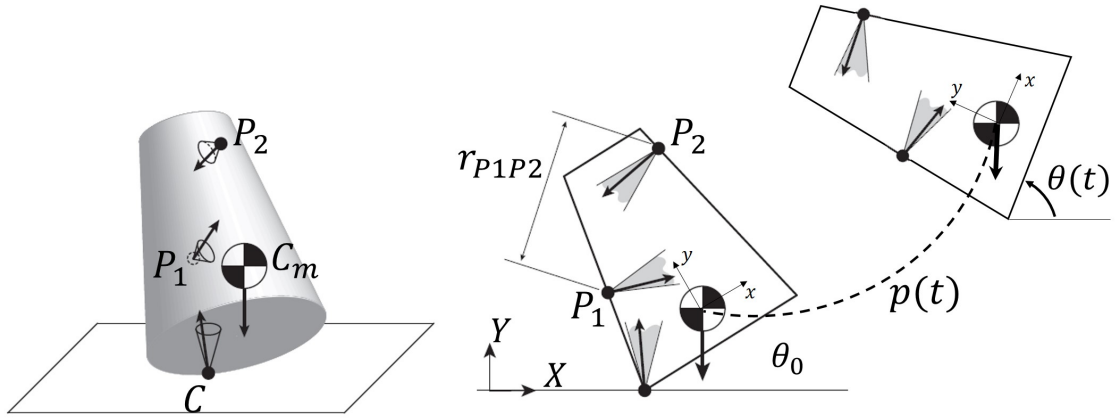

Figure 5.2: Given an end-effector that provides two frictional point contacts P_1P_2, center-of-mass location (perpendicular the surface) and a ground contact C (left) our problem consists on finding the contact locations that are not necessarily antipodal but can result in a feasible grasp and a trajectory $p(t)$ that leads to this feasible state. The distance between the contacts r_{P1P2} is fixed throughout the motion, since the end-effector has no mobility, therefore no internal forces can be applied to the object.

feasible grasps can be achieved by the grasp synthesis algorithm presented on Sec. 4.1.3. The dimensions of the end-effector can also be derived from the algorithm, since it relies on the contact locations, which are fixed with respect to each other. Furthermore, the dynamic analysis of the system and the constraints imposed to the problem will inform admissible acceleration values for which constraints will determine feasible trajectories.

5.2.1 Planning for Picking

Initially it is assumed that the contacts are at a feasible location (according to Algorithm 1 presented on Sec. 4.1.3). about the object's opposite edges. A graphical method such as the moment labeling technique [92] can inform us how the wrenches can contribute to the stability of the system from the initial to the final state of the motion.

Initial Maximum Tipping Angle

The motivation for this initial motion is to facilitate the separation of the object from the contact surface and also allow for shorter trajectories, which could be a problem given that manipulators have limited workspace. With the object placed on a flat surface, we can rotate the object counterclockwise (CCW) about C (Fig. 5.3). A maximum angle $\theta_{0_{MAX}}$ can be derived as a function of the angle ν and angle $\epsilon_s = \tan^{-1}\mu_s$ as indicated in Fig. 5.3. As long as the object's gravity wrench

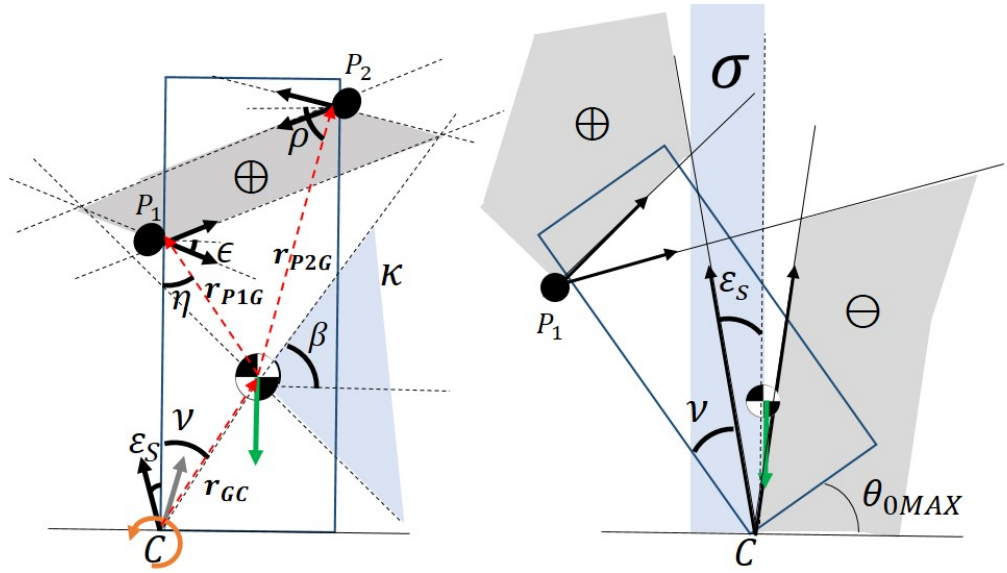

Figure 5.3: The moment labeling of the composite wrench cone by the two frictional contacts. The κ region (left) indicates the range of acceleration that can be exerted by the contacts P_1 and P_2 when considering the positive labeled region.Angle β is the range of possible directions for the acceleration applied on the object by the contacts. The tipping operation (right) is limited by an angle $\theta_{0_{MAX}}$ which is function of the contact friction cones.

rests within region σ, a single contact can balance the object [108]. The maximum tipping angle $\theta_{0_{MAX}}$ is:

$$\theta_{0_{MAX}} = \nu + \epsilon_s \tag{5.2.1}$$

The angle β of interest determines the range of possible directions for the acceleration applied on the object by the contacts, and can also be calculated by:

$$\begin{aligned} \beta &= \tan^{-1} \tfrac{y_p - y_{cm}}{x_p - x_{cm}}, \\ x_p &= \tfrac{1}{2}\left(\tfrac{y_{P2} - y_{P1}}{\mu} + x_{P1} + x_{P2}\right), \\ y_p &= \tfrac{1}{2}\left(\tfrac{x_{P2}}{\mu} + y_{P1} + y_{P2}\right) \end{aligned} \tag{5.2.2}$$

System Dynamics

The rigid body dynamics subjected to frictional contact [92] can be formalized as:

$$F_{ext} + \sum k_{ij} F_{ij} = M\dot{T_w} - [ad_{T_w}]^T M T_w, \quad k_{ij} \geq 0, \quad F_i \in W_{ij} \quad i = 1,2 \quad j = l, r \tag{5.2.3}$$

with F_{ext} the gravity wrench imposed on the object, M the spatial inertia matrix, T_w the object's twist, $\sum k_{ij}F_{ij}$ the contact wrenches on the object, $[ad_{T_w}]$ the *adjoint representation* of the twist T_w and W_{ij} the possible wrenches able to act on the object through contact i. The center of rotation of the object is chosen to be at contact P_1. This facilitates tracking the rotational motion of the trajectory, since contact P_1 can be aligned with the joint axis of the manipulator (by design). The rotation angle θ will be given by the rotation of the manipulator's wrist joint attaching the end-effector. In this case, the moment from gravity will introduce an additional term to the rotational motion, and no moment on the object will be generated by contact P_1.

Considering Fig. 5.3, these values are defined as:

$$F_{ext} = \begin{bmatrix}0 & 0 & mgr_{P1G}\sin(\eta+\theta) & 0 & -mg & 0\end{bmatrix}^T$$
$$, T_w = \begin{bmatrix}0 & 0 & \dot{\theta} & \dot{X} & \dot{Y} & 0\end{bmatrix}^T$$
$$\dot{T_w} = \begin{bmatrix}0 & 0 & \ddot{\theta} & \ddot{X} & \ddot{Y} & 0\end{bmatrix}^T, ad_{T_w} = \begin{bmatrix}[\omega] & 0 \\ [v] & [\omega]\end{bmatrix}$$
$$[\omega] = \begin{bmatrix}0 & -\dot{\theta} & 0 \\ \dot{\theta} & 0 & 0 \\ 0 & 0 & 0\end{bmatrix}, [v] = \begin{bmatrix}0 & 0 & \dot{Y} \\ 0 & 0 & \dot{X} \\ -\dot{X} & \dot{Y} & 0\end{bmatrix}$$
$$M = \begin{bmatrix}I_{P1} & 0 \\ 0 & mI_{3x3}\end{bmatrix}^T, I_{P1} = \begin{bmatrix}0 & 0 & 0 \\ 0 & 0 & 0 \\ 0 & 0 & I_{cm}+mr_{P1G}^2\end{bmatrix}$$
$$F_{1l} = \begin{bmatrix}0 & 0 & 0 & \cos(\epsilon+\theta) & \sin(\epsilon+\theta) & 0\end{bmatrix}^T$$
$$F_{1r} = \begin{bmatrix}0 & 0 & 0 & \cos(\epsilon-\theta) & -\sin(\epsilon-\theta) & 0\end{bmatrix}^T$$
$$F_{2l} = \begin{bmatrix}0 & 0 & r_{P2P1}\sin(\phi-\epsilon) & -\cos(\theta+\epsilon) & -\sin(\theta+\epsilon) & 0\end{bmatrix}^T$$
$$F_{2r} = \begin{bmatrix}0 & 0 & r_{P2P1}\sin(\phi+\epsilon) & -\cos(\theta-\epsilon) & -\sin(\theta-\epsilon) & 0\end{bmatrix}^T$$

with I_{P1} the moment of inertia of the object about contact P_1, $\dot{X}, \dot{Y}.\ddot{X}, \ddot{Y}, \dot{\theta}, \ddot{\theta}$ are the components of the linear velocity and acceleration ($\mathbf{a_d} = \ddot{X}\mathbf{i} + \ddot{Y}\mathbf{j}$) and angular velocity and acceleration ($\ddot{\theta} = \ddot{\theta}\mathbf{k}$) imposed to the object respectively.

In general terms, it is desired for applied linear and angular accelerations $\mathbf{a_d}$, $\ddot{\theta}$ to overcome the gravitational and rotational (i.e. centrifugal) ones. We apply a graphical method such as moment labeling to analyze the instant t_0 immediately after the object loses contact with the surface (Fig. 5.4 a). The left and right edges of the friction cone at contact P_1 are F_{1l} and F_{1r} respectively and contact at P_2 is assumed to be frictionless to facilitate visualization of feasible solutions without loss of generality ($\epsilon = 0$ at the contact and so $F_{2r} = F_{2l} = F_{2n}$ becomes the contact normal). The moment labeling of the composite wrench cone of the contacts generate a positive labeled region about which the contacts can only exert

positive torque (according to the right hand rule). By definition, no wrench can pass through the region and therefore the scenario in Fig. 5.4 (a) is not stable (since the actuation line of the gravity wrench L_w passes through the positive labeled region) and the object will fall. However, considering Fig. 5.4 (b), if an inertial acceleration $\mathbf{a_d}$ is imposed to the object, the contacts will be able to apply a vector sum $\mathbf{a_N} = \mathbf{a_d} - \mathbf{f_c}$ (with $\mathbf{f_c} = \mathbf{w_g} + \mathbf{a_c}$) to match the wrench of gravity and the applied acceleration. The vector sum can be translated along its line of actuation L'_w without modifying its value, and be generated by a linear combination of the friction cone at P_1 ($k_{1l}F_{1l} + k_{1r}F_{1r}$) and normal at P_2 (k_2F_{2n}). Since this resultant wrench respects the labeled region by generating a positive moment with respect to the positive labeled regions, the system is instantaneously stable. Equation 5.2.3 becomes:

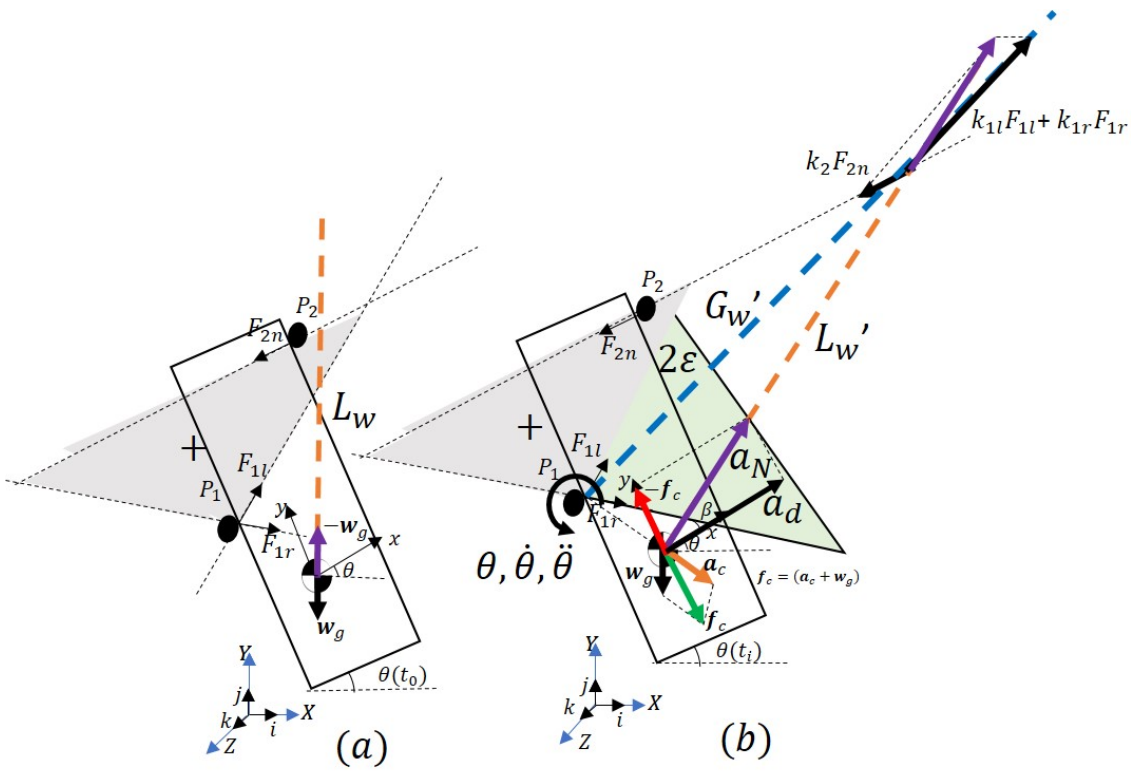

Figure 5.4: When losing contact with the ground (without loss of generality considering contact P_2 as frictionless), if the object was to become static, the moment labeling of the system indicates the contacts cannot generate a wrench to balance gravity. However, for an acceleration $\mathbf{a_d}$ the resulting acceleration $\mathbf{a_N}$ can balance $\mathbf{f_c} = \mathbf{w_g} + \mathbf{a_c}$ (which comprises gravity and centrifugal acceleration) and be generated by the contacts. The segment G'_w has to lie inside the friction cone at contact P_1 (2ϵ, with $\epsilon = atan\mu$).

$$\begin{bmatrix} 0 & 0 & r_{P2P1}sin\phi \\ cos(\epsilon+\theta) & cos(\theta-\epsilon) & -cos\theta \\ sin(\epsilon+\theta) & sin(\theta-\epsilon) & -sin\theta \end{bmatrix} \begin{bmatrix} k_{1l} \\ k_{1r} \\ k_{2n} \end{bmatrix} = \begin{bmatrix} I_{P1}\ddot{\theta} + mgr_{P1G}sin(\eta+\theta) \\ m(\ddot{X} - \dot{\theta}\dot{Y}) \\ m(\ddot{Y} + \dot{\theta}\dot{X} + g) \end{bmatrix} \tag{5.2.4}$$

$$k_{1l}, k_{1r}, k_{2n} \geq 0 \tag{5.2.5}$$

with $\mathbf{a_c} = \dot{\theta}\dot{Y}\hat{\mathbf{X}} - \dot{\theta}\dot{X}\hat{\mathbf{Y}}$ the "centrifugal" acceleration resulting from the angular motion on the object. As the assumption of a frictionless contact is included in the frictional space of solutions, a solution found to Eq. 5.2.4 will also satisfy the frictional case. To validate a solution, according to Eq. 5.2.5, the constants k_{ij} have to be non-negative. Consequently, to guarantee the system stability throughout the motion, a candidate trajectory can be evaluated by its linear and angular accelerations, and if these will satisfy Eq. 5.2.4 with Eq. 5.2.5 constraints. A candidate acceleration $\mathbf{a_d}$ and applied torque $I_n\ddot{\theta}$ that result in non-negative k_{ij} values can therefore be proposed.

Trajectory Generation

The acceleration will change at every time step (according to the rotation angle θ), and an infinite number of trajectories can satisfy the constraints. We can, however, integrate the limits of the minimum and maximum $\mathbf{a_d}$ that satisfy the constraints to determine the boundary trajectories. Therefore, any trajectory within these boundaries is a feasible trajectory. The termination condition can also be determined (Fig. 5.4), since for $\theta(t_n) \geq \pi/2 - \beta$ the contact wrenches will be able to span the gravity wrench with no imposed acceleration needed. However, as a result of the dynamic motion, the system will still be accelerated and has to be slowed down. From Eq. 5.2.3, the acceleration $\mathbf{a_d}$ and torque $I\ddot{\theta}$ can be chosen to stop rotation and linearly decelerate the object. Although there are infinite choices for the acceleration, by coupling $\mathbf{a_d}$ and θ while $t \leq t_n$ (Fig. 5.4 b) it is possible to constrain the system's trajectory at the termination condition for no rotation of the object, just translation while decelerating. This is expressed by:

$$\begin{aligned} &\mathbf{a_d(t)} = \ddot{X}\hat{\mathbf{X}} + \ddot{Y}\hat{\mathbf{Y}} = h_0(\cos\theta(t)\hat{\mathbf{X}} + \sin\theta(t)\hat{\mathbf{Y}}), \\ &h_0 \geq 0, \quad 0 \leq \theta(t) \leq \pi/2 \end{aligned} \tag{5.2.6}$$

with $\hat{\mathbf{X}}, \hat{\mathbf{Y}}$ the unit vectors in the world frame axis $[X, Y]$ respectively. To determine the acceleration magnitude h_0, for every $0 \leq \theta \leq \pi/2$, we consider the constraint on the non-negative k_{ij} which will determine a lower bound for h_0 and therefore to the acceleration $\mathbf{a_d}$. Eq. 5.2.4 assumes the angular motion $(\theta, \dot{\theta}, \ddot{\theta})$ is imposed by the manipulator's wrist joint (which is able to rotate the end-effector). This single joint motion trajectory can be planned as a quintic polynomial (Fig. 5.5), considering the following boundary constraints:

$$\begin{aligned} &\theta(0) = \theta_0 \quad \dot{\theta}(0) = 0 \quad \ddot{\theta}(0) = 0 \\ &\theta(t_n) = \pi/2 \quad \dot{\theta}(t_n) = 0 \quad \ddot{\theta}(t_n) = 0 \end{aligned} \tag{5.2.7}$$

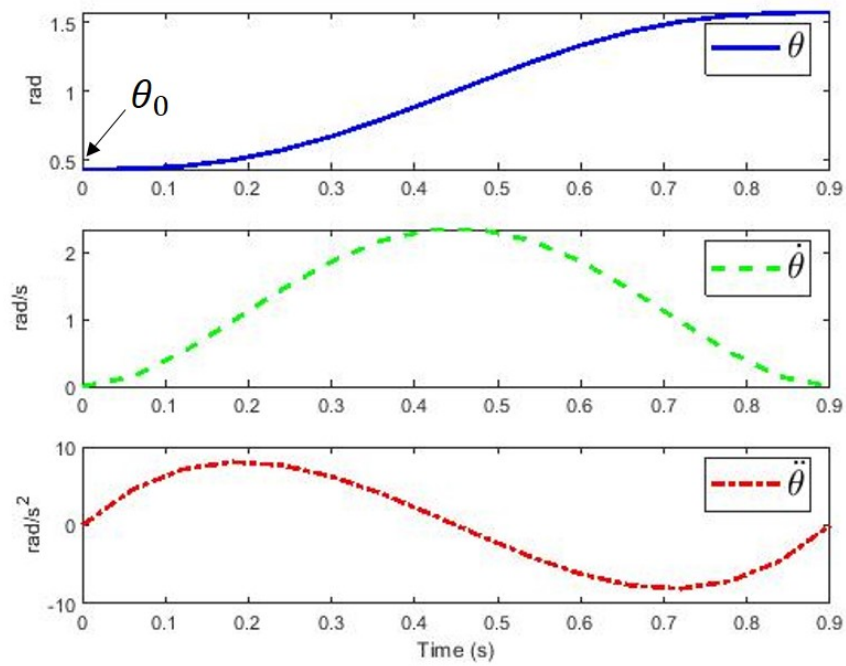

Figure 5.5: Example of the quintic polynomial trajectory for the $\theta(t)$ angular motion.

Finally, a trajectory can be generated by integrating the acceleration profile for finite timesteps. The integration can be done using conventional mathematical software such as the *ode*45 integration function in *Matlab*. Fig. 5.11 shows an example of the output of these values for different frictional contact coefficients.

5.3 Implementation

To implement the dynamic grasping of various objects and geometries, a 6 DOF conventional manipulator was programmed to follow the generated trajectories. A simulator determined the feasibility of the trajectories and discovery of singularities, if any. We assumed the following:

- The end-effector is in contact with the object at the start (t_0).
- The initial contact locations are known and can lead to a feasible grasp according to Algorithm 1.

- The end-effector and object dimensions, center of mass location and friction coefficients are known.
- Objects are symmetric about the Y axis
- While stability is known when $\theta + \beta \geq \pi/2$, β depends on the friction values which are hard to model and measure. So, a more conservative value of $\theta = \pi/2$ is considered as an upper bound value for the trajectory.

5.3.1 Software

An overview of the experimental procedure is shown in Fig. 5.6. We used $MATLAB$ to generate the trajectories abstracted as a Finite State Machine (Fig. 5.8). We used $CoppeliaSim$[1] to check for singularities and simulate the motion dynamics. Finally, $LoggerPro$ was used to analyze the motion kinematics.

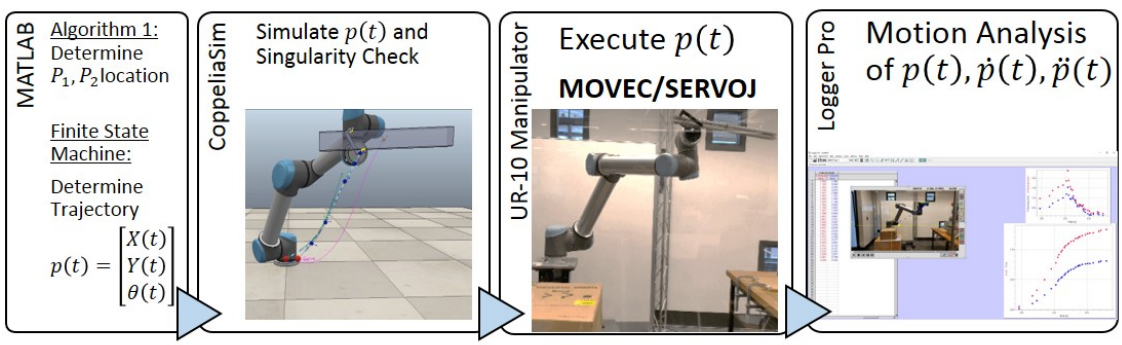

Figure 5.6: Overview of the experimental procedure pipeline. Trajectories for dynamic grasps are generated according to the discussion on Sec.5.2. The CoppeliaSim software is used to validate the trajectory and check for singularities. The trajectory is input to the UR-10 manipulator and lastly analyzed with $LoggerPro$ software for position, velocity and acceleration of the end-effector and of the object.

5.3.2 Hardware

A Universal Robots[2] $UR-10$ model robot arm demonstrated the applicability of the method. The arm has 6 DOF and a 10 kg payload capability, joint speed limits of 2.09 rad/s for the base and shoulder joints and π rad/s for the remaining joints. The maximum Tool Center Point (TCP) speed is 3000 mm/s. The general constraints for the trajectories are shown in Fig. 5.7. The trajectory was commanded to the UR-10 using the waypoints at the timesteps shown, with functions such as $MOVEJ$

[1] https://www.coppeliarobotics.com/
[2] https://www.universal-robots.com/

and $MOVEC$ to rotate joints independently or command the TCP to move in a Cartesian circular path, respectively. These commands, although readily accessible through the robot's pendant, constrain the motion in terms of planning and path geometry. Therefore, trajectory generation using the $SERVOJ$ command (which allows the user to determine the acceleration profile) were also implemented. These were sent to the manipulator via Real-Time Data Exchange (RTDE) interface in Python, where a set of desired Cartesian poses for the end-effector (representing the desired path) were translated to joint angles to be reached at specified times, depending on the minimum acceleration value as discussed on Sec. 5.2.

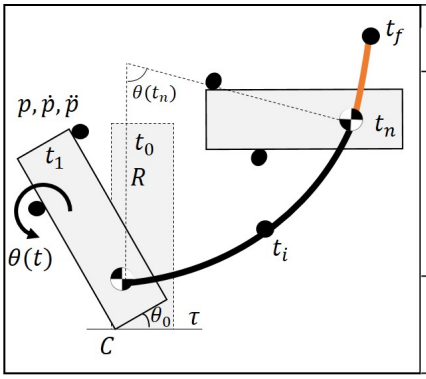

$\boldsymbol{t_0}$	$\boldsymbol{p(t_0) = \begin{bmatrix} 0 \\ 0 \\ \theta_0 \end{bmatrix}, \dot{p}(t_0) = \begin{bmatrix} 0 \\ 0 \\ 0 \end{bmatrix}, \ddot{p}(t_0) = \begin{bmatrix} 0 \\ 0 \\ 0 \end{bmatrix}}$
$\boldsymbol{t = t_1 \rightarrow t = t_n}$	$\boldsymbol{p(t_i) = \begin{bmatrix} X(t_i) \\ Y(t_i) \\ \theta(t_i) = \frac{\pi}{2} - \beta \end{bmatrix}, \ddot{p}(t_i) = \begin{bmatrix} h_0 cos\theta(t_i) \\ h_0 sin\theta(t_i) \\ \ddot{\theta}(t_i) \end{bmatrix}}$ $\boldsymbol{p(t_n) = \begin{bmatrix} X(t_n) \\ Y(t_n) \\ \theta(t_n) = \frac{\pi}{2} \end{bmatrix}, \ddot{p}(t_n) = \begin{bmatrix} 0 \\ h_0 \\ 0 \end{bmatrix}}$
$\boldsymbol{t = t_n \rightarrow t = t_f}$	$\boldsymbol{p(t_f) = \begin{bmatrix} X(t_f) \\ Y(t_f) \\ \theta(f) = \frac{\pi}{2} \end{bmatrix}, \dot{p}(t_f) = \begin{bmatrix} 0 \\ 0 \\ 0 \end{bmatrix}, \ddot{p}(t_f) = \begin{bmatrix} 0 \\ 0 \\ 0 \end{bmatrix}}$

Figure 5.7: General constraints imposed to the trajectory. As described by the state machine (Fig. 5.8), the initial tilting of the object θ_0 occurs at $t = t_0$, the "Lift" from $t = t_1 \rightarrow t_{t_n}$. Finally, the "Slowdown" stage from $t = t_n \rightarrow t_f$ brings the object to rest.

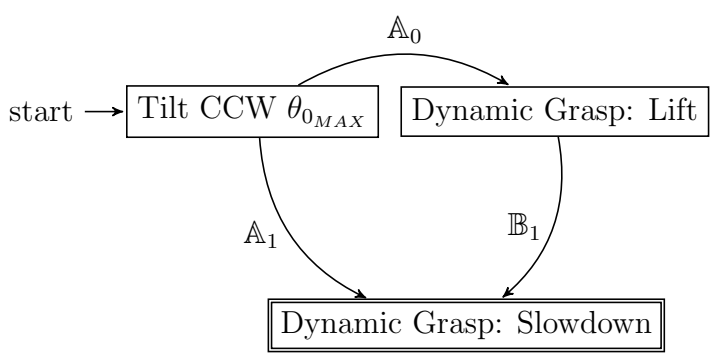

Figure 5.8: Finite state machine for the dynamic object picking, with the terminal operation at the "Slowdown" state.

$$\mathbb{A}_0 : \theta_{0_{MAX}} < \pi/2 \tag{5.3.1}$$
$$\mathbb{A}_1 : \theta_{0_{MAX}} \geq \pi/2 \tag{5.3.2}$$
$$\mathbb{B}_1 : \theta_{0_{MAX}} + \theta(t_n) \geq \pi/2 \tag{5.3.3}$$
$$\tag{5.3.4}$$

5.3.3 Results

Three different types of end-effector were tested (Fig. 5.9) with a variety of object shapes and geometries (Fig. 5.10), many of them clearly not following the assumed characteristics for our approach to help us determine the robustness to our model assumptions. A total of 152 out of 160 trials were successful (95%). Experimental results are shown on Table 5.1. Unsuccessful trials occurred when objects with liquid inside shifted their center-of-mass (Objects #7 and #10), which is not taken into account in this formulation. Additionally, air resistance seemed to have caused Object #9 (which is lightweight) to fall during the accelerated motion. Air drag was not modeled. Finally, even though in a desirable grasp the object remains static with respect to the end-effector throughout the motion $p(t)$ (no slipping or sliding occurs), relative motion was observed, but in most cases not enough to cause the object to leave the end-effector. This can be attributed to indeterminacy in friction coefficient estimations and the long profile geometry of the testing objects, enough so they would not escape the end-effector even when sliding occurred.

Successful versus unsuccessful dynamic grasps for object #3 is shown in Fig. 5.12. As can be seen, a successful grasp would satisfy the minimum calculated value for the acceleration value h_0 according to the corresponding angle of rotation θ. If the h_0 value is below (or close to) the minimum calculated value (shown as a dark line) in Fig. 5.12 (B), the more likely the object is to slide along the end-effector due to the uncertainty in our friction model. An unsuccessful grasp (fail) does not attain the desired forces and the object slips from the end-effector.

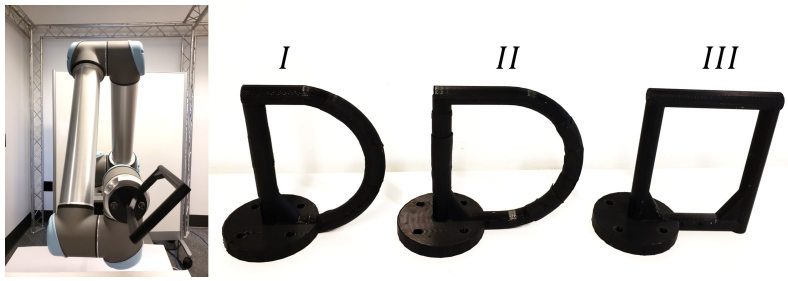

Figure 5.9: On the left, the Universal Robot UR-10 manipulator with the end-effector. On the right the, different types of end-effector designs to account for the different dimensions and geometries of the testing objects.

Table 5.1: Experimental results for Dynamic Picking. See Fig. 5.10 for the objects used here.

Object Description	Mass (g)	E.E. type	Trials	Successes
Cylinder (#1)	150	II	10	10
Aluminium Bottle (#2)	322	II	10	10
Aluminum 8020 (#3)	327	III	30	30
Tennis Balls (#4)	211	II	10	10
Spray (#5)	141	I	10	10
Cleaner (with liquid) (#6)	681	III	20	20
Cone (with liquid) (#7)	99	I	20	19
Water bottle (with liquid) (#8)	441	II	10	10
Bottle Brush (#9)	69	III	20	15
Oil Can (with liquid) (#10)	136	II	10	8
Graduated Cylinder(#11)	45	I	10	10

Figure 5.10: Objects used for the experiments in Table 5.1.

5.3.4 Discussion

The manipulation method presented in this chapter was intended to extend Ch. 4 approach in terms of dexterity and applicability to real world manipulation, envisioning fetching applications in elder-care settings. As previously observed, quasi-static assumption for manipulation may impose challenges when physically implemented in robotic systems, since the conditions guaranteeing the quasi-static regime are often strict. These conditions can easily fail as a result of disturbances or imprecise sensorial measurements, and a grasp not be attained. The motion speed also matters and quasi-static systems tend to be very slow. In this chapter, the fixed shape end-effector with no actuation ability from Ch. 4 is used to grasp objects still in a non-fixture, non-prehensile manner. However, the system dynamics is considered and analyzed, which allows for faster, more dexterous and applicable

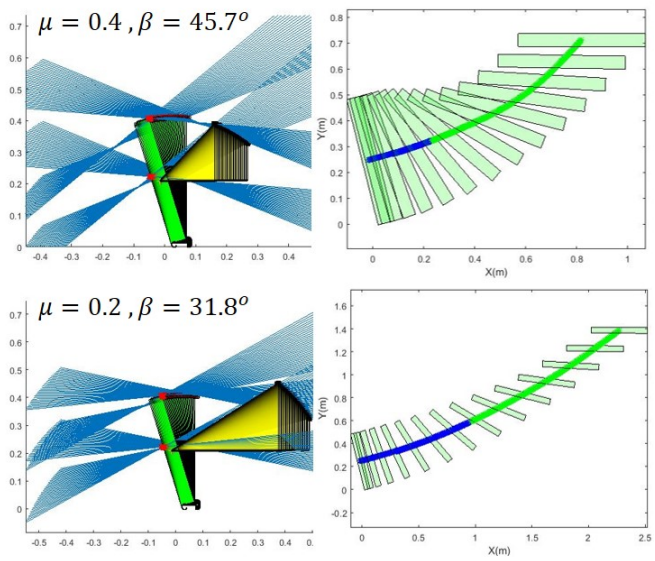

Figure 5.11: Example considering $\mu = 0.4$ (top) and $\mu = 0.2$ (bottom). On the left, angle β is calculated based on the friction cones of the contacts. On the right, the pointwise integration of the resulting acceleration leading to a feasible trajectory for dynamically grasping the object. The color change indicates when the condition for $\theta(t) + \beta \geq \pi/2$ is satisfied (or when the contacts can balance the gravity wrench).

scenarios for manipulating the object, with many different geometries and object shapes successfully grasped. A few remarks may be considered for improving the proposed approach:

- Planar analysis: the planar assumption, although convenient and feasible, does require some adaptation and limits the set of trajectories leading to a successful grasp. The former is done by designing round end-effectors that suppress off plane motions (mainly for circular profile objects), and the latter by constraining the manipulator TCP to a planar motion. The disadvantage is that more shapes of grippers are needed for a set of cylindrical like objects, and the workspace of the manipulator is limited to be on the same plane throughout the motion, possibly leading to more singularity resulting trajectories. By extending the analysis to three-dimensions, not only off plane motions will be compensated by the trajectory itself (therefore not requiring especial designs), but the larger workspace will facilitate grasps in places such as in cluttered environments, or limited, narrow spaces as are the common areas of elder-care facilities.

- Friction indeterminacy: A closed form solution is not necessarily "closed" as the assumptions on friction are not often precise. Embedding frictional and slipping sensing capabilities [27] can lead to better estimations and motion

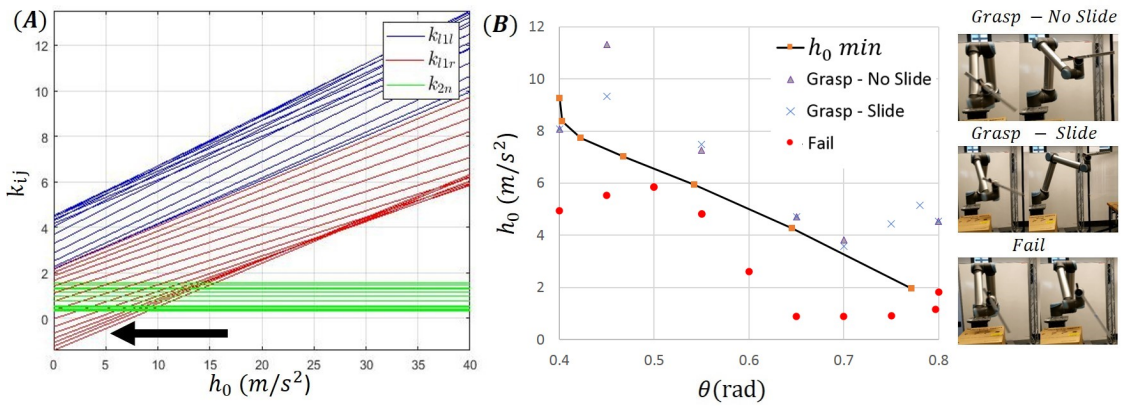

Figure 5.12: (A) Plot values for h_0 vs the k_{ij} multiplicative coefficients of the contact wrenches F_{1l}, F_{1r}, F_{2n} for object #3. The arrow indicates the direction of increasing θ. A minimum h_0 that leads to positive k_{ij} coefficients is desired. Since we assume frictionless contact at P_2, approximate values for minimum h_0 can be a solution. (B) shows two cases where the trajectory was planned to satisfy the minimum values of h_0 (shown as dashed lines) with different acceleration profiles, whereas in the fail case it was not.

compensation in case of slippage.

- End-effector shape: For the set of experimented objects, three different end-effectors were necessary. The critical point, besides the off-plane motion previously discussed, is the distance between the contacts with respect to the object dimension and position of the center of mass. Since this distance is not directly controllable and fixed, perhaps modifying the end-effector mechanical structure (using a combination of soft, deformable materials for instance) with passive compliance may increase the compatibility of objects per end-effector design.

- Perception: The initial assumption had the object and end-effector already in contact and at a feasible configuration. In practical scenarios, computer vision algorithm are needed to determine the object contours and combined with the algorithm in Sec. 4.1.2 determine where to place the end-effector along the object.

Finally, dynamic grasping is relatively an unexplored area. Its adoption can facilitate more affordable and dexterous manipulation as simple end-effectors will be capable of achieving complex grasps, and more tasks in spaces such as in manipulation for helping older adults more effectively be addressed.

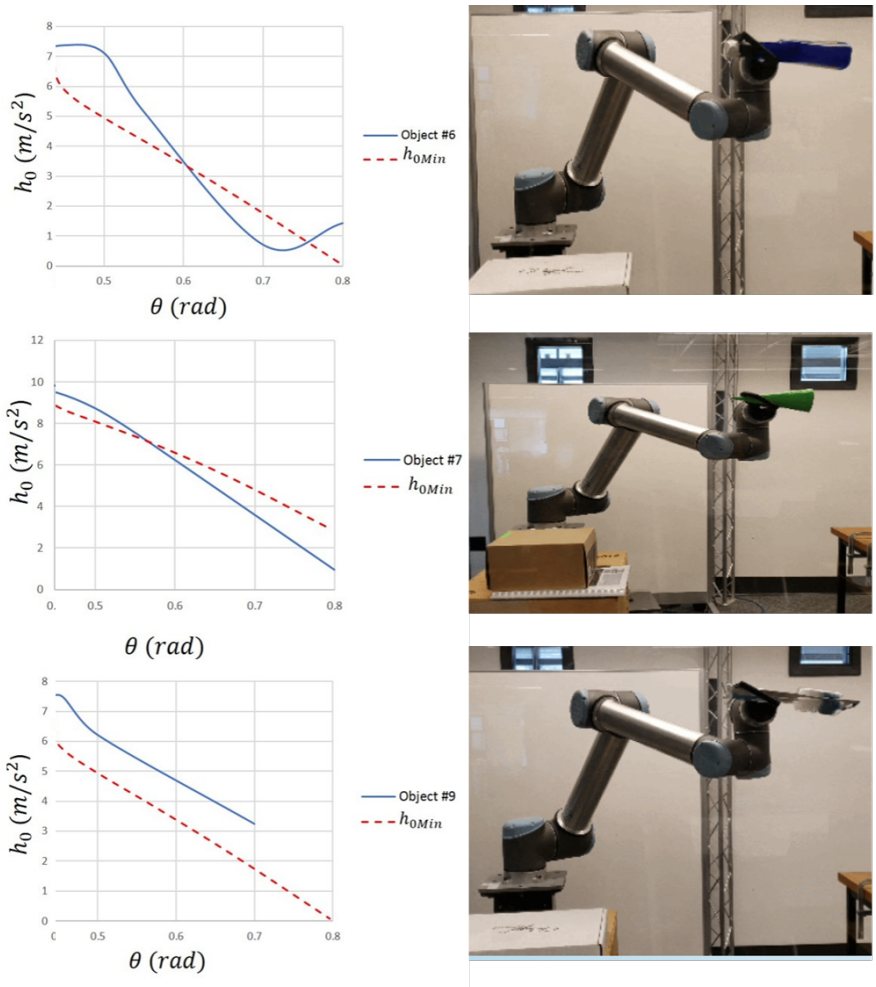

Figure 5.13: Successful experiments with objects #6, 7, 9 from top to bottom respectively.

Chapter 6

Planar Sequential Grasping of Multiple Objects

The tasks ranked by the study on Chapter 3 included manipulation such as fetching dropped items on the floor, or retrieve items from different heights. Current robot end-effectors have been shown to be able to precisely manipulate a variety of objects with high dexterity, but mostly focusing on a single object at the time. Although in some cases grasping multiple objects may be easier than a single one, such as picking a deck of cards, or a pile of coins, in elder care facilities the initial configuration of the objects in space might be sufficiently far (e.g. a pill container and a water bottle) that a conventional gripper will not be able to retrieve multiple objects in sequence due to hardware constraints, and therefore travel multiple times to fetch each item. To allow for sequential grasps of objects using a single end-effector a specialized design becomes necessary.

A low-cost underactuated serpentine-like end-effector is therefore proposed. It combines the capabilities of locking constraints [4] and conformation to the object shape and estimate cylindrical objects radii, or grasp multiple objects in sequence without the need to consider the contact interaction forces between the objects (see Fig. 6.1). Various industrial applications such as picking and placing multiple items can be made easier and not need customized grippers. Other robotic applications include service robots for cleaning, sorting tasks. This work is specifically looking to be applied to elder care by manipulating household objects in areas difficult to reach for elders such as the floor or cabinets. The compliant design facilitates grasps of a large range of shapes, as later demonstrated by experiments.

6.1 End-Effector Design Parameters

The gripper is composed of a series of identical links that form a chain that can be used to encircle and conform to objects using a single tether for actuation. Autonomous deployment of the gripper for arbitrary objects relies on a passive

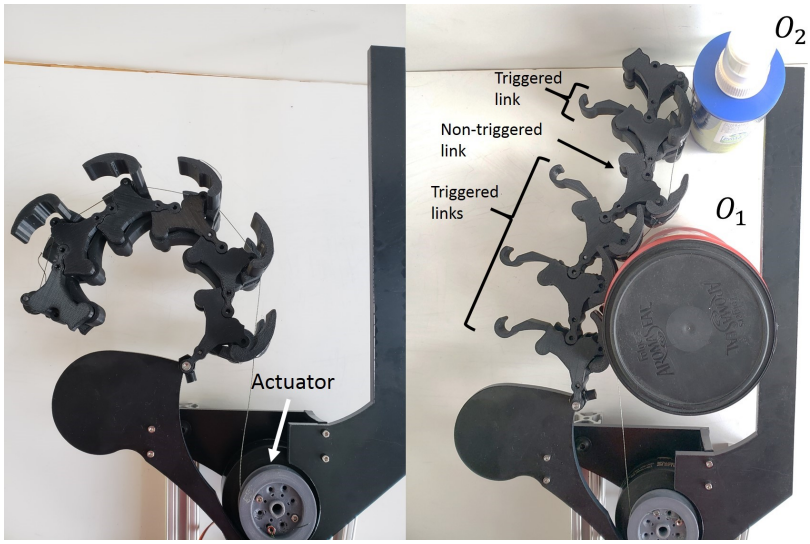

Figure 6.1: Example of a grasp of two objects with links triggered upon contact with the objects. The end-effector actuator pulls the tether driven chain of links. In this case, the non-triggered link did not make any contact with the objects and so it remains locked. As a result, object O_1 can be securely grasped while also grasping object O_2.

locking/unlocking mechanism. The end-effector motions occurs in stages depending on whether contact is made with a link or not. Each link i represents a frictional point contact on the object, capable of applying internal force f_i to it and rotate about a pulley at hinge point O_i. Upon contact with the object at the $i-1_{th}$ link (which rotates about another pulley at hinge point O_{i-1}), link i becomes unlocked by the contact force so that the new rotation axis becomes hinge point O_i and link i can apply internal force f_i to the object (Fig. 6.2). Therefore, while the links contacting the objects are static, the pulleys will still rotate, until either all links have contacted the object or a limit torque has been achieved and no further contact with the object is possible. A similar mechanism focused on a two DOF finger clutching mechanism has been proposed in [161]. It can be shown that if all n links are designed to have equal dimensions, for symmetric type objects (e.g. with circular profile), values for the design parameters of the end-effector can be correlated to those of the object, as well as the minimum number of contacts necessary to achieve force closure.

The relationship between a circular object (of radius R_O) and the end-effector is shown in Fig. 6.3. The contact point and hinge point between links form a radial line to the center of the circular object with successive links forming the angle α_i. Thus, triangle ΔADB is isosceles, and the radial distance of the design parameters R_G and d, for an object with radius R_O and the law of cosines leads to:

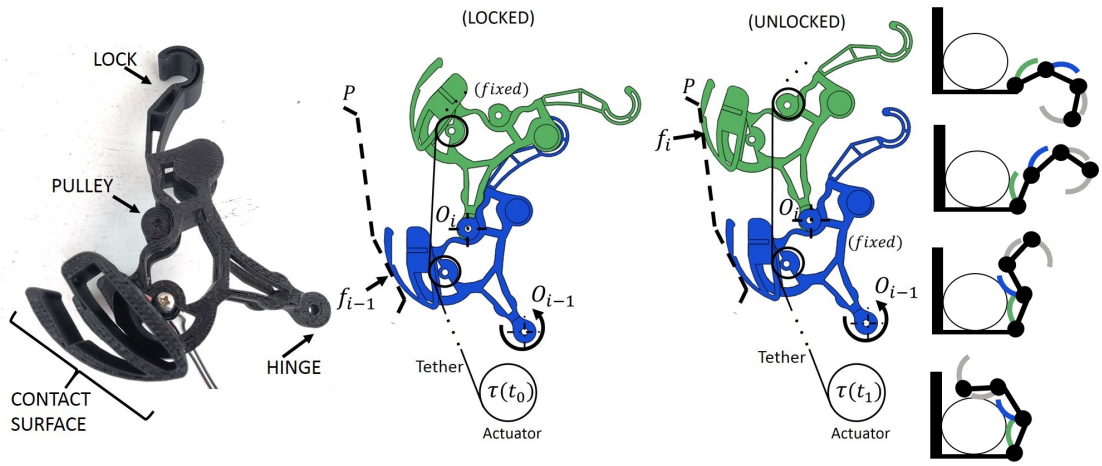

Figure 6.2: The end-effector link and locking mechanism. For a counterclockwise rotation of link $i-1$ (in blue) about a pulley at hinge point O_{i-1}, upon contact with the object P (shown as dashed lines) and a sufficient applied normal force f_{i-1}, link i (in green) will be unlocked and freely rotate counterclockwise about a pulley at hinge point O_i. Link $i-1$ will remain fixed with respect to the object. The unlocking is sensed as the torque difference $\Delta\tau(t_1 - t_0)$ empirically determined. The motion sequence for a single object is shown on the right hand-side (top to bottom order).

$$\alpha_i = cos^{-1}\left[1 - \frac{d^2}{2(R_O + R_G)^2}\right] \tag{6.1.1}$$

with the total angle containing all contacts given by

$$\alpha_{n_c} = \sum_{i=1}^{n} \alpha_i = n_c \alpha_i \tag{6.1.2}$$

and n_c the total number of links in contact with the object.

In this case, we can determine the minimum angle α_{n_c} such that, for two frictional point contacts c_i and c_n with applied normal forces f_i and f_n respectively, and friction coefficient μ_o, the force closure condition is satisfied. As can be seen in Fig. 6.4 (a), force closure will occur if the line between the contacts lies within their respective friction cones [110], or:

$$\alpha_{nf} > \pi - 2\,tan^{-1}\mu_o \tag{6.1.3}$$

$$n_f = \frac{\alpha_{nf}}{\alpha_i} \tag{6.1.4}$$

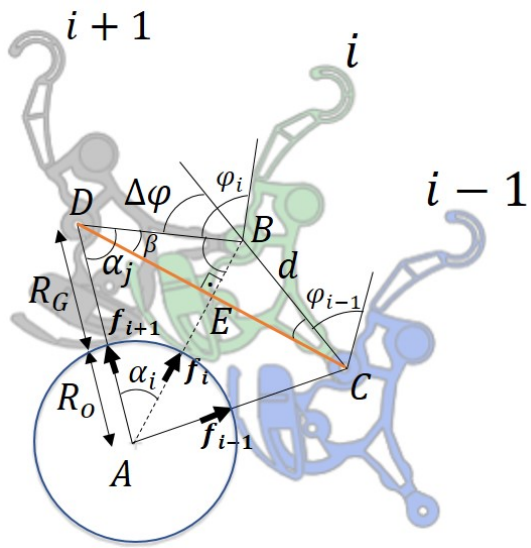

Figure 6.3: The geometric relationship between the object radius and design parameters R_G and d is shown. The radius can be estimated from the displacement of the links $\Delta\phi$.

where α_{nf} and n_f represent the minimum angle and number of links required for a force closure grasp respectively. If $\alpha_{min} > \alpha_{nf}$, object O will be ejected from the end-effector (Fig. 6.4 (b)). Furthermore, since each link is of equal dimension, triangles $\Delta ABC, \Delta ADB, \Delta DBC$ are all isosceles, and the radius of the object R_O can be estimated using the following relations:

$$R_O = \frac{d}{2cos\alpha_j} - R_G \ , \ \alpha_j = \frac{\pi - \Delta\phi}{2} \tag{6.1.5}$$

where $\Delta\phi = \phi_i - \phi_{i-1}$ and angle ϕ_{i-1} (or ϕ_i) is the rotation angle between link i (or $i+1$) making contact with the object and the locking position, as indicated on Fig. 6.3. Since no information is known about where the contact between the object and the link surface is made, at least three contacting links are needed for the estimation knowing that the object is cylindrical.

6.2 Implementation and Experimentation

A low-cost end-effector and test set-up using 3d-printed and laser-cut parts was custom built (Fig. 6.5). Two types of experiments were performed to investigate the capabilities of autonomous grasping of cylindrical shaped objects using estimated torque and force sensing and grasping multiple objects of various shapes. To test for robustness in position, experiments were also done varying the initial position

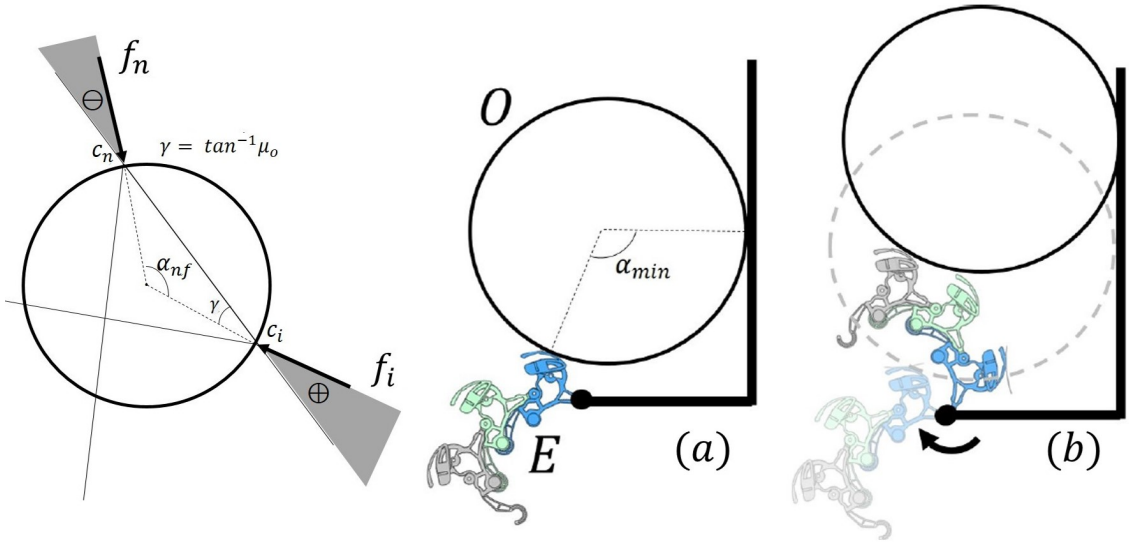

Figure 6.4: (Left) Two frictional point contacts determine force closure grasps. The $\pm$ regions indicate the moment labelling [97]. (Right) (a) Object in force closure if $\alpha_{min} \leq \alpha_{nf}$ or (b) ejected from the end-effector if not.

of the objects against the palm β, as shown in Fig. 6.7. The palm acted as an opposing contact to facilitate the unlocking of the series of links while maintaining the object within the boundaries of the end-effector. A successful grasp was defined in case the object was not loosen or did not escape the end-effector. A total of 165 grasps were attempted with 19 different objects, and 143 were successful grasps (86%).

6.2.1 End-effector Design

The 3D-printed end-effector prototype with $n = 5$ links (Fig. 6.5) was designed to be cable driven and actuated by an iPower GBM6212H-150T brushless DC motor with no gearbox (torque limit: $0.5\,Nm$). The motor is controlled using an IQinetics IQ-MC-17-15-24C-H motor controller[1] with estimated joint torque sensing [118], enabling low-cost, autonomous manipulation in a reactive manner. Serial communication with the motor is done through an FTDI USB to serial UART and Matlab for low-level torque calculation and implementation. Each link is capable of locking and triggering upon contact, as seen on Fig. 6.2. Design parameters for experiments were chosen to facilitate grasping of common household objects ($17mm < R_O < 60mm$, $R_G = 33\,mm$ and $d = 43\,mm$). Link 1 is defined as the most proximal link to the actuator, as shown in the figure.

[1]http://iqinetics.com/

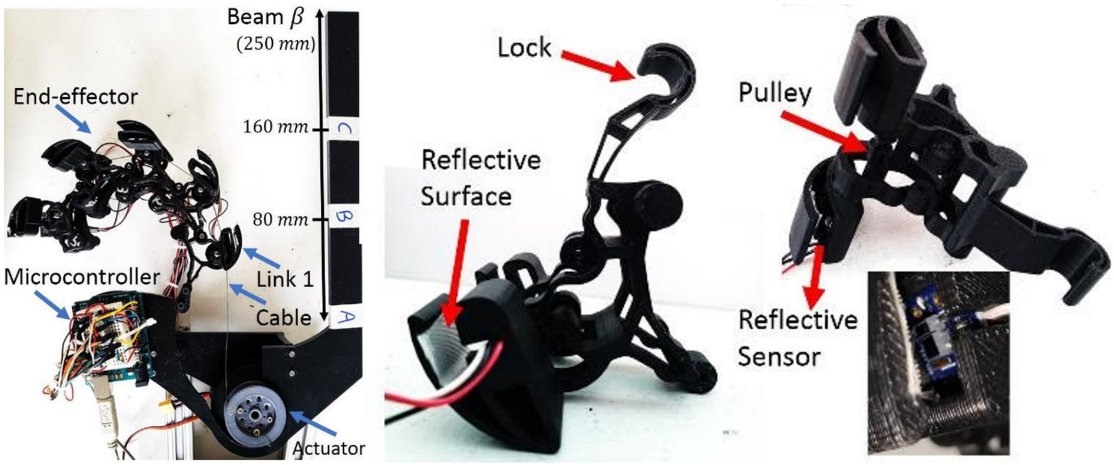

Figure 6.5: Experimental setup with the end-effector system (left) which includes the end-effector mounted to a beam β that acts like a palm (to hold objects against it) and sensor mount (right).

6.2.2 Applied Force Estimation

In order to estimate the applied normal force, f_i, to the object by the end-effector, an IR reflective sensor (SFH 9206, sensing range $0-5mm$) was added to each link as shown on Fig. 6.5. Each sensor signal is read by a microcontroller (*Arduino Uno)*. Forces were mapped and calibrated to a piece-wise quadratic function as shown on Fig. 6.6. The upper limit sensed for each link was $3N$. This limited the range of mass sensed from the objects, and the precision for estimating large applied internal forces.

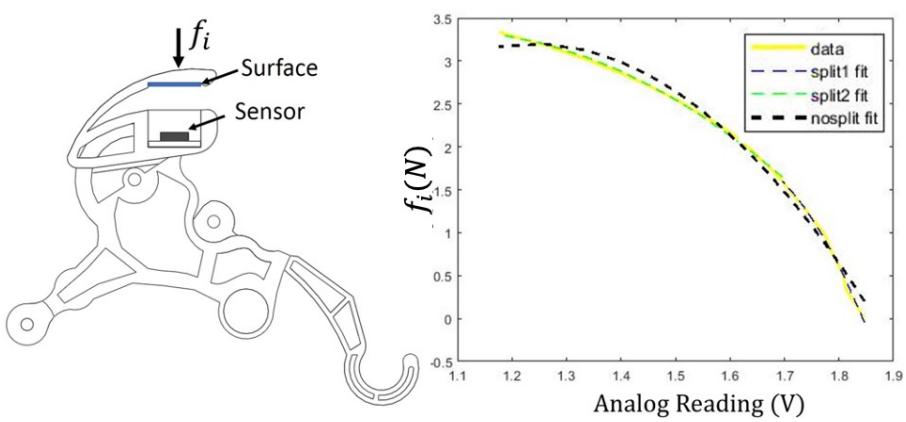

Figure 6.6: Photo-reflective sensor placement and calibration data fit, where the resulting data was fit with piece-wise quadratic lines.

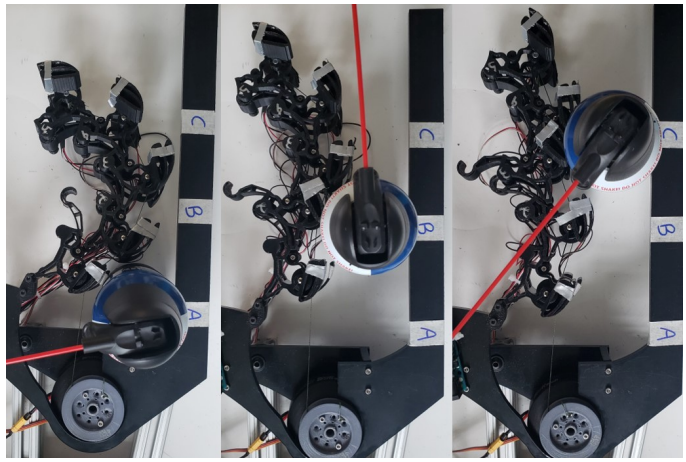

Figure 6.7: Objects were placed at different positions (A, B, C each distant $80mm$) along the end-effector palm β.

6.2.3 Experiments with Cylindrical Objects: Autonomous Grasping

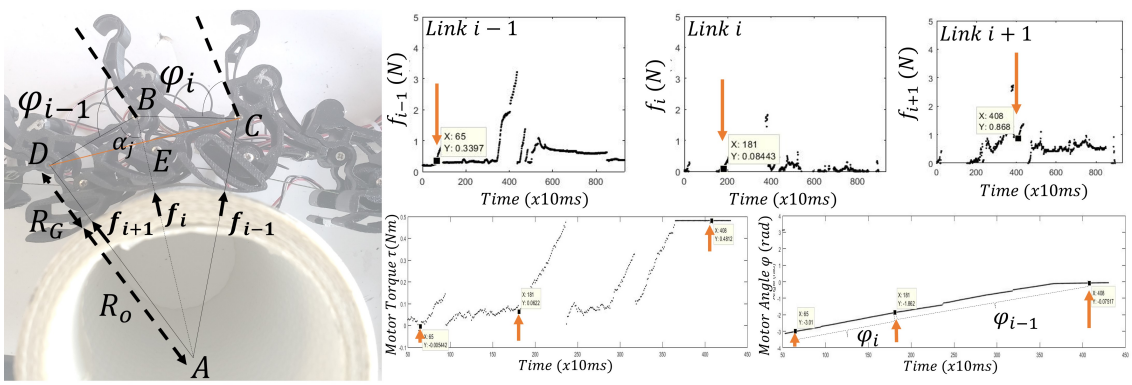

Figure 6.8: To estimate the radius of the object R_O, at least three contacts are needed. The force sensed from each link is used to determine instant of contact with the object and the motor angle graph used to retrieve the value of $\Delta\phi = \phi_i - \phi_{i-1}$ to calculate angle α_j used in eq. 6.1.5.

The end-effector design can facilitate the grasp of single objects, considering the passive compliance due to the numerous links and mechanical enveloping resultant from contacting the object. In addition, circular profile objects' geometry (radius R_o) can be estimated considering the end-effector design parameters and angular displacement of the actuator. Thus, the minimum number of links for a force closure grasp can be calculated using Eqs.6.1.1-6.1.4 and an autonomous grasp mode considering torque sensing from the actuator implemented.

Object Radius Estimation

Objects with cylindrical geometry had their radii estimated according to eq. 6.1.5. To determine the time of contact between links and object, the force applied by the links and motor angle readings were used, as show in Fig. 6.8. All objects were placed at the same position B along β for more uniform sensed force readings. Since three contacts are needed to the estimation, only objects #1, #2, #3, #6 (Fig. 6.10) had their radius estimated (end-effector is too big for objects #5 and #7; object #4 is too fragile and deformable for a three contact grasp). The remaining objects had their radii manually input for the autonomous grasp implementation. In such cases, smaller links and more sensitive force sensors could allow for detection of smaller and more fragile objects. For each object, five trials were averaged and results summarized on Table 6.1.

Table 6.1: Objects Radii Estimation $\overline{R_O}$

Object Description (Fig. 6.10)	$\overline{R_O}(mm)$	$R_O(mm)$	Trials
Coffee Package (#1)	48.64	50	5
Metal Spool (#2)	32.45	32.5	5
Paper Towel (#3)	58.83	60	5
Tape Roll (#6)	34.21	39	5

Reading errors occurred due to lightweight and low friction of the objects (especially object #6) causing it to move during the grasp process. The snapping action during unlocking of links combined with the tether stiffness also affected the accuracy of the motor angle readings. The end-effector would sometimes loose contact with the object.

Autonomous implementation

Autonomous grasping by estimating the minimum number of contacts is advantageous when grasping multiple objects, since more available links allow more objects to be grasped. With the objects dimension known or estimated previously, the minimum number of links for a force closure grasp can be calculated using eqs. 6.1.1-6.1.4, with a caveat that the palm works as an opposing contact, and so eq. 6.1.3 is reduced by $\pi/2$. Detection of each grasping stage was done as shown on Fig. 6.11. The chosen objects for the experiments are presented on Fig. 6.10 and results shown on Table 6.2, where the friction coefficients are approximated. The software implementation can be abstracted as a finite state machine (Fig. 6.9). States were defined as:

Close $n - n_c$ The end-effector closes the chain of $n - n_c$ links which are not in contact with the object (n_c).

Update Depending on the sensed motor torque, update the number of links in contact with the object n_c.

Halt A minimum required number of links are in contact with the object with minimum required sensed torque, so the grasp terminates.

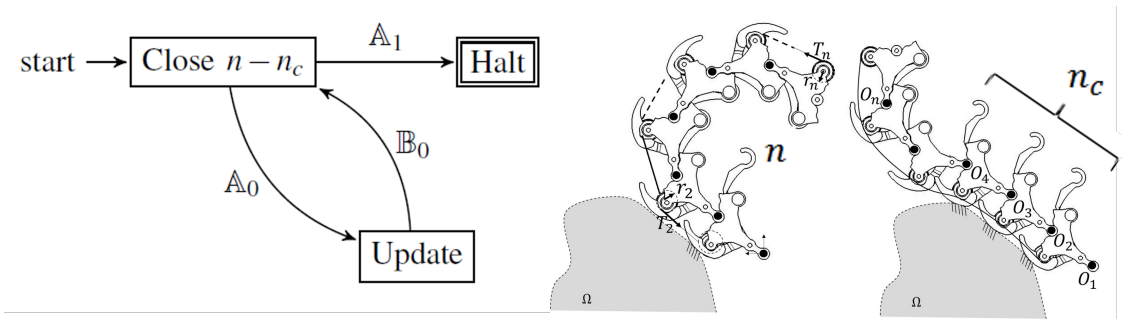

Figure 6.9: Finite state machine for autonomous grasp of circular objects. The operation terminates in the "Halt" state.

The edge labels ($\mathbb{A}_0, \mathbb{A}_1$, $\mathbb{B}_0$) are the *state guard conditions*, and formulated according to (1) the torque τ sensed on the motor (in Nm); (2) The total number of links in contact with the object n_c and (3) the minimum number of contacts required for force closure n_f. The autonomous implementation considers actuator torque and link force profiles such as depicted on Fig. 6.11. When the link unlocks there is a sudden drop in torque $\Delta\tau(t_i)$ which can be observed at time t_i. This indicates the unlocking of a link upon contact with the object. A minimum detectable value was obtained empirically. For a desired known angle α_{nf} given by eq.6.1.3, using eq. 6.1.4 the minimum number of links n_f necessary for a force closure grasp can be determined. The state guard conditions were determined as follows:

$$\mathbb{A}_0 : \Delta\tau > 0.1, \text{ and } \tau < 0.35 \tag{6.2.1}$$

$$\mathbb{A}_1 : n_c > n_f, \text{ and } \tau >= 0.35 \tag{6.2.2}$$

$$\mathbb{B}_0 : n_c <= n_f \tag{6.2.3}$$

Objects were also placed at different locations along the end-effector palm β as seen on Fig. 6.7. From 105 attempts, 97 (92%) were successful. Unsuccessful grasps can be attributed to torque reading errors while attempting to match motor angle readings and therefore determine the value for $\Delta\phi$ and sliding of the object due to low friction. The initial placement of the object often caused it to be ejected, and small objects (such as object #5) were caught in between the links, and in times were not detected by the force sensors.

Table 6.2: Experimental results for autonomous grasping of round objects

Object Description (Fig. 6.10)	Position	$R_o(mm)$	μ	$\alpha_i(rad)$	$\alpha_{nf}(rad)$	n_f	Trials	Successes
Coffee Package (#1)	A	50	0.4	0.54	0.8	2	5	5
Coffee Package (#1)	B	50	0.4	0.54	0.8	2	5	5
Coffee Package (#1)	C	50	0.4	0.54	0.8	2	5	4
Metal Spool (#2)	A	32.5	0.4	0.70	0.8	2	5	5
Metal Spool (#2)	B	32.5	0.4	0.70	0.8	2	5	5
Metal Spool (#2)	C	32.5	0.4	0.70	0.8	2	5	5
Paper Towel (#3)	A	60	0.3	0.48	1	3	5	5
Paper Towel (#3)	B	60	0.3	0.48	1	3	5	5
Paper Towel (#3)	C	60	0.3	0.48	1	3	5	4
Paper Cup (#4)	A	35	0.3	0.67	1	2	5	5
Paper Cup (#4)	B	35	0.3	0.67	1	2	5	5
Paper Cup (#4)	C	35	0.3	0.67	1	2	5	5
Graduated Cylinder (#5)	A	17	0.4	0.95	0.8	1	5	4
Graduated Cylinder (#5)	B	17	0.4	0.95	0.8	1	5	5
Graduated Cylinder (#5)	C	17	0.4	0.95	0.8	1	5	2
Tape Roll (#6)	A	39	0.4	0.63	0.8	2	5	5
Tape Roll (#6)	B	39	0.4	0.63	0.8	2	5	5
Tape Roll (#6)	C	39	0.4	0.63	0.8	2	5	4
Oil Canister (#7)	A	28.5	0.5	0.75	0.6	1	5	5
Oil Canister (#7)	B	28.5	0.5	0.75	0.6	1	5	5
Oil Canister (#7)	C	28.5	0.5	0.75	0.6	1	5	4

6.2.4 Experiments with Multiple Objects

To demonstrate the end-effector capability of grasping multiple objects sequentially, objects used daily were chosen (Fig. 6.10) and attempted to be grasped in pairs (see Fig. 6.1). Although some objects are cylindrical and could be grasped similarly as previously discussed, different shapes were considered. Each grasp terminated when the end-effector reached its peak torque value, as show in Fig. 6.12. The torque variations were monitored for benchmark among other grasps and the sensed force values f_i used as indicators of how much force could be applied on a second object while a first one was already grasped. Experimental results are shown on Table 6.3. From 60 attempts, 46 (76%) were successful. Most unsuccessful grasps occurred

Table 6.3: Experimental results for grasping multiple objects

Object Description (Fig. 6.10)	Trials	Successes
Cylinder (#19) and Spray (#8)	10	5
Plastic Bottle(#18) and Spool (#10)	10	10
Prism Package (#11) and Brush (#13)	10	7
Cone (#17) and Glass Bottle (#14)	10	5
Cleaner(#16) and Glue (#12)	10	9
Water bottle (#9) and Book (#15)	10	10

Figure 6.10: Test objects for autonomous grasps of cylindrical geometry (left) and grasps of multiple objects (right).

due to insufficient maximum torque from the actuator ($0.5\,Nm$), not enough force to grasp objects at the most distal links (similar to pinch grasping) while having another object grasped in the proximal ones. Friction (objects #8 and #19, Fig. 6.10) and nonparallel edges (object #17, Fig. 6.10) were also factors that contributed to grasping failures.

6.2.5 Discussion

Although successfully demonstrating the grasp and dimension estimation of single objects, along with the sequential grasp of multiple objects, the end-effector design can benefit with some improvements, mainly:

- Better force sensing capability at the links: the photo-reflective sensors at each link not only could be disturbed by light, but also made readings which depended on the deflection of the reflective surface at each link (Fig. 6.5). Since the calibration procedure considered forces applied at the same position on this surface, contact forces further away from this position would be underestimated. A better calibration model or different sensing method is required for improvement.

- Object dimensions often impacted the success or failure of a grasp. Since there is a spacing in between links, smaller objects can be caught in between and not be detected by the force sensors, nor make enough contacts to be grasped. A redesign able to account for that will allow grasping of more object shapes and sizes.

- The opposing beam β if replaced by another finger (or series of links) can render the end-effector more robust to initial placement of the objects (due to a

larger free space), or facilitate force sensing (with more sensing links available). In addition, more geometries and dimensions will be accommodated by the pair, since more links lead to more passive compliance.

- The end-effector design was limited to make contacts in the plane. This can difficult grasping of certain geometries which are inherently non-symmetric, causing for instance the object to topple. By off-centering the plane of action to a three-dimensional design (where the links can be arranged in a spiral geometry for instance), more contact points in different locations along the object can certainly facilitate more robust and secure grasps.

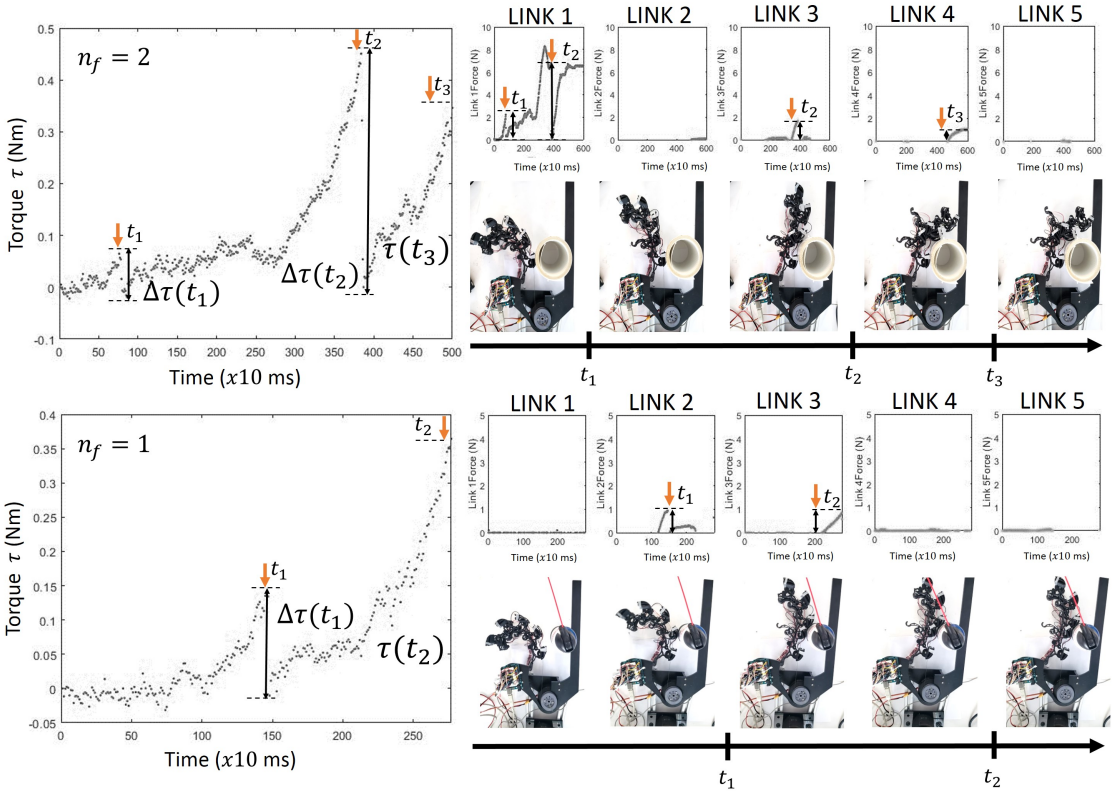

Figure 6.11: Example of grasp detection for object #6 (top) and #7 (bottom). The number of links in contact with the object is measured from each $\Delta\tau(t_i)$ on the motor torque graph, which indicates a subtle change in torque caused by the unlocking motion. This number is compared with the value of n_f, the minimum number of links necessary for force closure, and in case torque applied by the motor $\tau(t3)$ achieves a maximum defined limit (close to $0.35Nm$) on the end-effector, the grasp can terminate. In the top case, a minimum of two links ($n_f = 2$) is needed for force closure, so after the two drops in $\Delta\tau$ are detected (from links one and three) and the torque increases to the defined maximum, the grasp terminates at instant t_3. Similarly, for the bottom case at least one link ($n_f = 1$) is required for a force closure grasp, so a single drop in $\Delta\tau$ indicating link two unlocked link three, followed by a maximum torque $\tau(t2)$ which terminates the grasp.

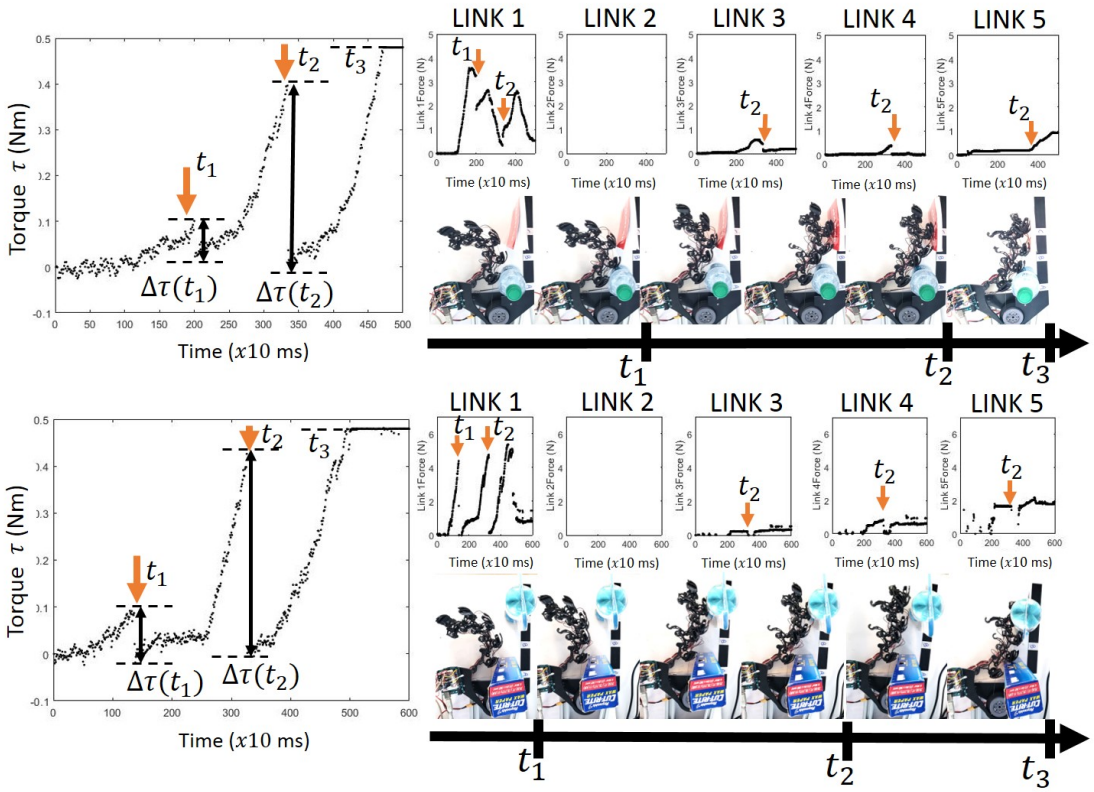

Figure 6.12: Example of two successful grasps of two objects. In the upper case (object #9 and #15), two end-effector links were unlocked, as seen by the torque plot and applied forces. Link two has not made contact with the objects. The bottom case (objects #11 and #13) has also two links unlocked and link two did not make contact with the objects. For all cases, the grasp terminates once the actuator reaches its maximum torque (at instance t_3).

Chapter 7

Contributions and Future Work

7.1 Contributions

This thesis contributes to the field of service and assistive robots for older adults proposing task validations for robot deployments, specifically at low-income elder care facilities, considering all stakeholders (clinicians, caregivers and older adults). A behavioral investigation of human-robot interaction through qualitative and quantitative analysis of these deployments was considered and insights on robot and interaction improvements proposed. Service-robot manipulation was proposed by the development of a novel low-cost hardware platform and its subsequent validation in assisting older adults with different manipulation tasks. The deployment led to a technical investigation with main contributions to the field of robotic grasping and manipulation, specifically the theory, design and experimentation of low-cost low-complexity end-effectors with zero mobility suitable for pick-and-place applications. The method applies mostly to convex objects and is an alternative to grasping fixture notions of force or form-closure in a planar analysis by considering the force of gravity as an extra contact. Both quasi-static and dynamic approaches were proposed, along with experimentation with various object shapes and geometries. The method also extends dexterity for commonly used end-effectors such as the parallel-jaw gripper, since it has the same shape, yet allows the end-effector to pick or place objects even if its actuators become non-functional, or if contacts on the object cannot be directly antipodal. An algorithm for grasping synthesis under the planar assumption was also presented. Lastly, extending end-effector capabilities for grasping multiple objects in a sequential manner and dimension estimation of circular profile objects was proposed with the design and experimentation of single-actuated serpentine type end-effectors.

7.2 Future Work

Despite older adults acceptance of different robot embodiments presented on Chapter 3, the screening deployment for COVID-19 symptoms and exposure did not meet our expectations in terms of their preferences (having the robot rated the least preferred method). Future studies aiming towards increasing acceptance of robots as screening agents should consider restricted and less social environments (as opposed to the common areas). Additionally, the ability to tailor the interaction to user needs (such as slow low-pitch voice and increased volume for the hearing impaired or fast pace for younger participants) may result in broader adoption of a single platform, given those were sources of frustration and discomfort during the interactions.

Future deployments of manipulation tasks at the elder care facilities can consider adding the end-effectors and methods proposed in this thesis. Improvements for these can also be listed. For the quasi-static and dynamic approaches to minimalist manipulation, the former reliance on torque sensing feedback for switching atomic operations could be improved by introducing better estimation at the actuator level (to account for the 20% error in motor driver estimation) or adding a complementary external sensor at the fixed shape grippers. As for the dynamic approach, since the location of the objects was known a priori and limited to a planar analysis, natural extensions would include planning the entire motion, considering the manipulator arm's reachable workspace, along with the extension to the three dimensions. The assumption of having the object perpendicular to the surface could be relaxed by investigating possible designs, additional atomic operations or dynamic motions considering any initial configuration. Furthermore, addressing failing issues during experiments such as shifting center of mass for liquids, air resistance and also placing an object on a surface (proposed on the quasi-static method [108]) dynamically are left as future work. Enhancements to the end-effector and method of grasping multiple objects sequentially include exploring scaling for attempting grasps on a wider range of objects. Pulley design also assumed to have no friction. As no bearings or lubrication were used, the presence of friction caused a non-uniform applied force distribution. The force sensing method applied, although low-cost and responsive, had limited sensing range and also depended on the contact location. This often led to inconsistent readings, despite a valid calibration procedure. A longer range distance sensor could provide more accurate force readings and can be explored, along with different locking designs.

Finally, as expressed on the Discussion on Sec. 3.2.3, this thesis approach towards affordable systems to accomplish manipulation tasks focused on the agent (the robot) rather than the "instrument" (or the object of interest). It is an open and promising field exploring solutions addressing the design of the environment in order to improve robotic performance, especially when deploying robots for HRI tasks and at elder care facilities.

7.3 Concluding Remarks

This thesis investigated robot interactions with older adults in low-income elder care facilities, presenting guidelines, designs and novel manipulation techniques for the robot hardware and software based on human-robot interactions using tasks determined to be important from previous stakeholder focus groups and surveys. Initially, a need assessment using a qualitative descriptive study with all stakeholders in elderly care settings was conducted to determine how a robot could facilitate older adults' independence. Two highly rated tasks (hydration reminder with water bottle delivery and walking assistance) requiring a mobile-only robotic base were chosen for study and the robot was adapted to perform both. A third deployment consisted on using a SAR for assessing symptoms and exposure of COVID-19 among older adults and healthcare workers. Data was collected on the robot's performance including aspects of human-robot interaction. Tasks such as fetching objects on the floor and in cabinets or opening doors emerged on the focus groups and surveys, as in other studies [5, 61, 146] leading to novel hardware modifications to the mobile base. Thus, mobile manipulation in the context of elder care was addressed by a fourth deployment with a low-cost custom made manipulator in a PACE center. The arm has two degrees-of-freedom and was proven effective in reaching different heights (floor and ceiling), grasping and handing off the bean bags to the older adults by using both prehensile and non-prehensile end-effectors. A physical game of "corntoss" was played by the participants with three different levels of assistance: no assistance, assistance by a caregiver or by the robot. Results indicated the older adults found it simple and easy to interact with the robot, feeling comfortable around it and also patient when the robot was slow to retrieve bean bags. Competitiveness and engagement in the game were observed and tossing the bean bags or competing with another person were considered easier when the game was assisted by the robot, compared to independent play. A non-prehensile end-effector was better perceived during the cabinet retrieving task when compared to a conventional end-effector, and different alternatives to conventional grasping and manipulation techniques were investigated. A robotic in-hand manipulation technique for picking and placing objects was presented. It takes advantage of two non-antipodal contacts at fixed distance and gravity and can be applied to a wide range of objects and robot platforms, being less dependent on exact contact positioning and sufficiently large internal forces. An algorithm for grasp synthesis was proposed. Experiments with a custom-made autonomous manipulator and a conventional manipulator had high success rates for picking and placing several objects on different surface conditions. In sequence, the in-hand manipulation approach under a quasi-static assumption was relaxed, and achieving grasps of convex planar objects dynamically was proposed. A technique for choosing acceleration profiles considering the system dynamics was investigated. By considering inertial and acceleration forces, the dynamic grasp can be advantageous for real world applications

since it can occur at greater speeds than the previous work which assumed quasi-static motions. The method also extends the conventional notions of grasp stability as no internal forces can be applied to the object, yet results in a stable grasp. Experiments with various object sizes and geometries demonstrated the method's robustness to some unmodelled conditions such as non-convex shapes and objects with shifting center-of-mass.

Finally, the design of a novel, low-cost serpentine type underactuated end-effector capable of autonomously grasping cylindrical type objects and estimating their radii and sequentially grasping multiple objects was also proposed. Design parameter calculation based on the objects geometry was presented and a prototype capable of force and torque sensing was built to demonstrate the gripper versatility on grasping various object shapes and geometries, either single or paired with a second object not necessarily in the vicinity of the first, therefore grasping objects in a sequential manner.

List of Figures

List of Tables

Table 1: Top 14 Tasks from Confidential Surveys and Member Checks identified for Elders

ELDERS	**CONFIDENTIAL SURVEY (N=42)**			**MEMBER CHECK (N=4)**		
	Rank	X_i	F_i	Rank	X_i	F_i
Having additional assistance when pain flares up	1	2.89	0.52	5	2.5	1
Outings (casino, theater, shopping)	2	2.42	0.42	1	3	1
Having your food preferences known	3	2.41	0.44	9	2.33	0.67
Getting a drink	4	2.27	0.18	1	3	1
Being asked about your preferences	5	2.26	0.47	6	2.5	0.75
Having assistance with being in bed (changing position, putting on blankets)	6	2.26	0.26	5	2.5	1
Having caretakers help keep your spirits up	7	2.26	0.206	5	2.5	1
Reaching things on high shelves	8	2.24	0.48	6	2.5	0.75
Getting around in a wheelchair	9	2.21	0.29	1	3	1
Walking	10	2.12	0.4	7	2.5	0.5
Games, including bingo	11	2.08	0.208	8	2.5	0.25
Caretakers working to increase your socialization opportunities	12	2.07	0.25	3	2.75	0.75
Having clothing taken out	13	2.04	0.36	9	2.33	0.67
Having assistance finding items in the closet	14	2	0.44	4	2.67	0.67

Table 2: Top 11 Tasks from Confidential Surveys and Member Checks identified for Clinicians

CLINICIANS	**CONFIDENTIAL SURVEY (N=14)**			**MEMBER CHECK (N=8)**		
	Rank	X_i	F_i	Rank	X_i	F_i
Providing Input	1	3.0	0.3	21	2.75	0.13
Evaluating Homes for Safety	2	3.0	0.25	2	3.0	0.43
Coming up with ways to keep someone safe at home	3	2.93	0.62	2	3.0	0.43
Toileting	4	2.92	0.25	15	2.8	0.60
Matching cognitive ability to tasks	5	2.92	0.36	6	2.88	0.38
Confirming that members have taken medications	6	2.91	0.6	4	3.0	0.33
Reminding members to drink (water, health drink)	7	2.91	0.36	8	2.86	0.33
Checking weights	8	2.90	0.56	11	2.86	0.14
Providing a listening ear	9	2.85	0.25	21	2.75	0.13
Providing companionship to members when they are upset	9	2.85	0.25	16	2.88	0.13
Having small conversations with members	10	2.85	0.17	21	2.75	0.13

Table 3: Top 14 Tasks from Confidential Surveys and Member Checks identified for Caregivers

CAREGIVERS	**CONFIDENTIAL SURVEY (N=15)**			**MEMBER CHECK (N=4)**		
	Rank	X_i	F_i	Rank	X_i	F_i
Making sure members ate and are not missing meals	1	3.0	1.0	5	3.0	0
Providing a listening ear	2	3.0	0.11	4	3.0	0.25
Assisting members with taking medications	3	3.0	0	5	3.0	0
Helping members get ready for the doctors /providers apt.	3	3.0	0	4	3.0	0.25
Preparing meals	3	3.0	0	4	3.0	0.25
Working with members with physical challenges and need extensive assistance	3	3.0	0	4	3.0	0.25
Assisting with morning routines	3	3.0	0	3	3.0	0.33
Helping members comply with care plans	3	3.0	0	2	3.0	0.5
Encouraging members to see nurses when not feeling well	3	3.0	0	1	3.0	0.67
Providing companionship to members when they are upset, depressed or lonely	3	3.0	0	4	3.0	0.25
Matching cognitive ability to task	3	3.0	0	5	3.0	0
Providing comfort measures to members	3	3.0	0	5	3.0	0
Reminding members to use their walkers	3	3.0	0	5	3.0	0
Helping members reach things on high shelves	3	3.0	0	5	3.0	0

Table 4: Fourth Deployment Access to Technology

Experience with or use a
Computer 6
Tablet or e-reader 5
Cellphone 18
Exercise daily* 12

Bibliography

[1] Hojjat Abdollahi, Ali Mollahosseini, Josh T Lane, and Mohammad H Mahoor, *A pilot study on using an intelligent life-like robot as a companion for elderly individuals with dementia and depression*, 2017 IEEE-RAS 17th International Conference on Humanoid Robotics (Humanoids), IEEE, 2017, pp. 541–546.

[2] Tamara Abell and Michael Erdmann, *Stably supported rotations of a planar polygon with two frictionless contacts*, Intelligent Robots and Systems 95.'Human Robot Interaction and Cooperative Robots', Proceedings. 1995 IEEE/RSJ International Conference on, vol. 3, IEEE, 1995, pp. 411–418.

[3] Eric W Aboaf, Christopher G Atkeson, and David J Reinkensmeyer, *Task-level robot learning: Ball throwing*, (1987).

[4] Soroush Abyaneh, Omid Saber, and Hassan Zohoor, *A cable-driven grasping mechanism with lock/unlock constraints*, ASME 2013 International Design Engineering Technical Conferences and Computers and Information in Engineering Conference, American Society of Mechanical Engineers, 2013, pp. V06AT07A059–V06AT07A059.

[5] Eileen P Ahearn, *The use of visual analog scales in mood disorders: a critical review*, Journal of psychiatric research **31** (1997), no. 5, 569–579.

[6] Yasumichi Aiyama, Masayuki Inaba, and Hirochika Inoue, *Pivoting: A new method of graspless manipulation of object by robot fingers*, Intelligent Robots and Systems' 93, IROS'93. Proceedings of the 1993 IEEE/RSJ International Conference on, vol. 1, IEEE, 1993, pp. 136–143.

[7] John R Amend, Eric Brown, Nicholas Rodenberg, Heinrich M Jaeger, and Hod Lipson, *A positive pressure universal gripper based on the jamming of granular material*, IEEE Transactions on Robotics **28** (2012), no. 2, 341–350.

[8] Haruhiko Asada and Kamal Youcef-Toumi, *Direct-drive robots: theory and practice*, MIT press, 1987.

[9] Marian R Banks, Lisa M Willoughby, and William A Banks, *Animal-assisted therapy and loneliness in nursing homes: use of robotic versus living dogs*,

Journal of the American Medical Directors Association **9** (2008), no. 3, 173–177.

[10] Momotaz Begum, Rosalie Wang, Rajibul Huq, and Alex Mihailidis, *Performance of daily activities by older adults with dementia: The role of an assistive robot*, Rehabilitation Robotics (ICORR), 2013 IEEE International Conference on, IEEE, 2013, pp. 1–8.

[11] Roger Bemelmans, Gert Jan Gelderblom, Pieter Jonker, and Luc de Witte, *Socially assistive robots in elderly care: a systematic review into effects and effectiveness.*, Journal of the American Medical Directors Association **13** (2012), no. 2, 114–120.e1.

[12] Hugh Bethell, *The health benefits of exercise for older people*, GM: Midlife & Beyond (2010).

[13] Antonio Bicchi and Alessia Marigo, *Dexterous grippers: Putting nonholonomy to work for fine manipulation*, The International Journal of Robotics Research **21** (2002), no. 5-6, 427–442.

[14] Karl-Friedrich Böhringer, Russell Brown, Bruce Donald, Jim Jennings, and Daniela Rus, *Distributed robotic manipulation: Experiments in minimalism*, The 4th International Symposium on Experimental Robotics IV (Berlin, Heidelberg), Springer-Verlag, 1997, pp. 11–25.

[15] Elizabeth Broadbent, Rie Tamagawa, Anna Patience, Brett Knock, Ngaire Kerse, Karen Day, and Bruce A MacDonald, *Attitudes towards health-care robots in a retirement village*, Australasian Journal on Ageing **31** (2012), no. 2, 115–120.

[16] Joost Broekens, Marcel Heerink, Henk Rosendal, et al., *Assistive social robots in elderly care: a review*, Gerontechnology **8** (2009), no. 2, 94–103.

[17] Jeremy D Brown, Andrew Paek, Mashaal Syed, Marcia K O'Malley, Patricia A Shewokis, Jose L Contreras-Vidal, Alicia J Davis, and R Brent Gillespie, *An exploration of grip force regulation with a low-impedance myoelectric prosthesis featuring referred haptic feedback*, Journal of neuroengineering and rehabilitation **12** (2015), no. 1, 104.

[18] M Buhler and Daniel E Koditschek, *From stable to chaotic juggling: Theory, simulation, and experiments*, Proceedings., IEEE International Conference on Robotics and Automation, IEEE, 1990, pp. 1976–1981.

[19] Robert M Byers, *Control of a serpentine manipulator with collision avoidance*, (1993).

[20] Michelle M Byrne, *Evaluating the findings of qualitative research*, AORN journal **73** (2001), no. 3, 703–706.

[21] Gerard Canal, Guillem Alenya, and Carme Torras, *A taxonomy of preferences for physically assistive robots.*

[22] Jeanie Chan and Goldie Nejat, *Promoting engagement in cognitively stimulating activities using an intelligent socially assistive robot*, Advanced Intelligent Mechatronics (AIM), 2010 IEEE/ASME International Conference on, IEEE, 2010, pp. 533–538.

[23] Jo-Ana D Chase, *Physical activity interventions among older adults: a literature review.*, Research and theory for nursing practice **27** (2013), no. 1, 53–80.

[24] Nikhil Chavan-Dafle and Alberto Rodriguez, *Prehensile pushing: In-hand manipulation with push-primitives*, Intelligent Robots and Systems (IROS), 2015 IEEE/RSJ International Conference on, IEEE, 2015, pp. 6215–6222.

[25] ———, *Stable prehensile pushing: In-hand manipulation with alternating sticking contacts*, 2018 IEEE International Conference on Robotics and Automation (ICRA), IEEE, 2018, pp. 254–261.

[26] Bei Chen, Simon Marvin, and Aidan While, *Containing covid-19 in china: Ai and the robotic restructuring of future cities*, Dialogues in Human Geography **10** (2020), no. 2, 238–241.

[27] Wei Chen, Heba Khamis, Ingvars Birznieks, Nathan F Lepora, and Stephen J Redmond, *Tactile sensors for friction estimation and incipient slip detection—toward dexterous robotic manipulation: A review*, IEEE Sensors Journal **18** (2018), no. 22, 9049–9064.

[28] Matei Ciocarlie, Kaijen Hsiao, Adam Leeper, and David Gossow, *Mobile manipulation through an assistive home robot*, Intelligent Robots and Systems (IROS), 2012 IEEE/RSJ International Conference on, IEEE, 2012, pp. 5313–5320.

[29] Richard Colbaugh, Homayoun Seraji, and Kristin Glass, *Decentralized adaptive control of manipulators*, Journal of Robotic Systems **11** (1994), no. 5, 425–440.

[30] Foster Collins and Mark Yim, *Design of a spherical robot arm with the spiral zipper prismatic joint*, Robotics and Automation (ICRA), 2016 IEEE International Conference on, IEEE, 2016, pp. 2137–2143.

[31] John Tighe Costa and Mark Yim, *Designing for uniform mobility using holonomicity*, 2017 IEEE International Conference on Robotics and Automation (ICRA), IEEE, 2017, pp. 2448–2453.

[32] Kathrin Cresswell, Sandeep Ramalingam, and Aziz Sheikh, *Can robots improve testing capacity for sars-cov-2?*, Journal of medical Internet research **22** (2020), no. 8, e20169.

[33] Nikhil Chavan Dafle, Alberto Rodriguez, Robert Paolini, Bowei Tang, Siddhartha S Srinivasa, Michael Erdmann, Matthew T Mason, Ivan Lundberg, Harald Staab, and Thomas Fuhlbrigge, *Extrinsic dexterity: In-hand manipulation with external forces*, Robotics and Automation (ICRA), 2014 IEEE International Conference on, IEEE, 2014, pp. 1578–1585.

[34] Frédéric Delaunay, Joachim De Greeff, and Tony Belpaeme, *Towards retro-projected robot faces: an alternative to mechatronic and android faces*, RO-MAN 2009-The 18th IEEE International Symposium on Robot and Human Interactive Communication, Ieee, 2009, pp. 306–311.

[35] Mehmet Dogar and Siddhartha Srinivasa, *A framework for push-grasping in clutter*, Robotics: Science and Systems VII (2011), 65–72.

[36] Bruce Donald, Larry Gariepy, and Daniela Rus, *Distributed manipulation of multiple objects using ropes*, Robotics and Automation, 2000. Proceedings. ICRA'00. IEEE International Conference on, vol. 1, IEEE, 2000, pp. 450–457.

[37] H. Durrant-Whyte and T. Bailey, *Simultaneous localization and mapping: part i*, IEEE Robotics Automation Magazine **13** (2006), no. 2, 99 –110.

[38] Ahmed El-Shenawy, Andrea Wellenreuther, Andre S Baumgart, and Essam Badreddin, *Comparing different holonomic mobile robots*, 2007 IEEE International Conference on Systems, Man and Cybernetics, IEEE, 2007, pp. 1584–1589.

[39] Satu Elo and Helvi Kyngäs, *The qualitative content analysis process*, Journal of advanced nursing **62** (2008), no. 1, 107–115.

[40] Michael A Erdmann and Matthew T Mason, *An exploration of sensorless manipulation*, IEEE Journal on Robotics and Automation **4** (1988), no. 4, 369–379.

[41] Connor Esterwood and Lionel Robert, *Robots and covid-19: Re-imagining human–robot collaborative work in terms of reducing risks to essential workers*, Available at SSRN 3767609 (2021).

[42] Juan Fasola and Maja J Mataric, *Robot exercise instructor: A socially assistive robot system to monitor and encourage physical exercise for the elderly*, RO-MAN, 2010 IEEE, IEEE, 2010, pp. 416–421.

[43] D. Feil-Seifer and M. J. Mataric, *Defining socially assistive robotics*, 9th International Conference on Rehabilitation Robotics, 2005. ICORR 2005., June 2005, pp. 465–468.

[44] David Feil-Seifer and Maja J Mataric, *Defining socially assistive robotics*, Rehabilitation Robotics, 2005. ICORR 2005. 9th International Conference on, IEEE, 2005, pp. 465–468.

[45] Javier Felip, Jose Bernabé, and Antonio Morales, *Contact-based blind grasping of unknown objects*, Humanoid Robots (Humanoids), 2012 12th IEEE-RAS International Conference on, IEEE, 2012, pp. 396–401.

[46] Marshal F Folstein, Susan E Folstein, and Paul R McHugh, *"mini-mental state": a practical method for grading the cognitive state of patients for the clinician*, Journal of psychiatric research **12** (1975), no. 3, 189–198.

[47] Zhao Gong, Songwen Jiang, Qizhi Meng, Yanlei Ye, Peng Li, Fugui Xie, Huichan Zhao, Chunzhe Lv, Xiaojie Wang, and Xinjun Liu, *Shuyu robot: An automatic rapid temperature screening system*, Chinese Journal of Mechanical Engineering **33** (2020), no. 1, 1–4.

[48] Ulla H Graneheim and Berit Lundman, *Qualitative content analysis in nursing research: concepts, procedures and measures to achieve trustworthiness*, Nurse education today **24** (2004), no. 2, 105–112.

[49] H-M Gross, Ch Schroeter, Steffen Mueller, Michael Volkhardt, Erik Einhorn, Andreas Bley, Ch Martin, Tim Langner, and Matthias Merten, *Progress in developing a socially assistive mobile home robot companion for the elderly with mild cognitive impairment*, Intelligent Robots and Systems (IROS), 2011 IEEE/RSJ International Conference on, IEEE, 2011, pp. 2430–2437.

[50] Jianglong Guo, Chaoqun Xiang, and Jonathan Rossiter, *A soft and shape-adaptive electroadhesive composite gripper with proprioceptive and exteroceptive capabilities*, Materials & Design **156** (2018), 586–587.

[51] Joseph R Hageman, *The coronavirus disease 2019 (covid-19)*, 2020.

[52] Li Han and Jeffrey C Trinkle, *Dextrous manipulation by rolling and finger gaiting*, Robotics and Automation, 1998. Proceedings. 1998 IEEE International Conference on, vol. 1, IEEE, 1998, pp. 730–735.

[53] Kensuke Harada and Makoto Kaneko, *Enveloping grasp for multiple objects*, Journal of the Robotics Society of Japan **16** (1998), no. 6, 860–867.

[54] Kensuke Harada, Makoto Kaneko, and T Tsujii, *Rolling-based manipulation for multiple objects*, IEEE Transactions on robotics and automation **16** (2000), no. 5, 457–468.

[55] Marcel Heerink, *Exploring the influence of age, gender, education and computer experience on robot acceptance by older adults*, Proceedings of the 6th international conference on Human-robot interaction, ACM, 2011, pp. 147–148.

[56] Marcel Heerink, Ben Krose, Vanessa Evers, and Bob Wielinga, *The influence of a robot's social abilities on acceptance by elderly users*, ROMAN 2006-The 15th IEEE International Symposium on Robot and Human Interactive Communication, IEEE, 2006, pp. 521–526.

[57] Marcel Heerink, Ben Kröse, Vanessa Evers, and Bob Wielinga, *Assessing acceptance of assistive social agent technology by older adults: the almere model*, International journal of social robotics **2** (2010), no. 4, 361–375.

[58] Shigeo Hirose and Yoji Umetani, *The development of soft gripper for the versatile robot hand*, Mechanism and machine theory **13** (1978), no. 3, 351–359.

[59] W Stamps Howard and Vijay Kumar, *On the stability of grasped objects*, Robotics and Automation, IEEE Transactions on **12** (1996), no. 6, 904–917.

[60] Hsiu-Fang Hsieh and Sarah E Shannon, *Three approaches to qualitative content analysis*, Qualitative health research **15** (2005), no. 9, 1277–1288.

[61] Justin Huang, Tessa Lau, and Maya Cakmak, *Design and evaluation of a rapid programming system for service robots*, The Eleventh ACM/IEEE International Conference on Human Robot Interaction, IEEE Press, 2016, pp. 295–302.

[62] Wesley H Huang and Gregory F Holden, *Nonprehensile palmar manipulation with a mobile robot*, Intelligent Robots and Systems, 2001. Proceedings. 2001 IEEE/RSJ International Conference on, vol. 1, IEEE, 2001, pp. 114–119.

[63] Nicolas Hudson, Thomas Howard, Jeremy Ma, Abhinandan Jain, Max Bajracharya, Steven Myint, Calvin Kuo, Larry Matthies, Paul Backes, Paul Hebert, et al., *End-to-end dexterous manipulation with deliberate interactive estimation*, Robotics and Automation (ICRA), 2012 IEEE International Conference on, IEEE, 2012, pp. 2371–2378.

[64] Kenneth Henderson Hunt, *Kinematic geometry of mechanisms*, vol. 7, Oxford University Press, USA, 1978.

[65] C Jayawardena, I Kuo, C Datta, RQ Stafford, E Broadbent, and BA MacDonald, *Design, implementation and field tests of a socially assistive robot for the elderly: Healthbot version 2*, Biomedical Robotics and Biomechatronics (BioRob), 2012 4th IEEE RAS & EMBS International Conference on, IEEE, 2012, pp. 1837–1842.

[66] Chandimal Jayawardena, I-Han Kuo, Elizabeth Broadbent, and Bruce A MacDonald, *Socially assistive robot healthbot: Design, implementation, and field trials*, IEEE Systems Journal **10** (2016), no. 3, 1056–1067.

[67] Hyunhwan Jeong and Joono Cheong, *Independent contact region (icr) based in-hand motion planning algorithm with guaranteed grasp quality margin*, 2012 IEEE International Conference on Automation Science and Engineering (CASE), IEEE, 2012, pp. 1089–1094.

[68] Holly Jimison and Misha Pavel, *Embedded assessment algorithms within home-based cognitive computer game exercises for elders*, Engineering in Medicine and Biology Society, 2006. EMBS'06. 28th Annual International Conference of the IEEE, IEEE, 2006, pp. 6101–6104.

[69] Michelle J Johnson, Megan A Johnson, Justine S Sefcik, Pamela Z Cacchione, Caio Mucchiani, Tessa Lau, and Mark Yim, *Task and design requirements for an affordable mobile service robot for elder care in an all-inclusive care for elders assisted-living setting*, International Journal of Social Robotics (2017), 1–20.

[70] Reza Kachouie, Sima Sedighadeli, Rajiv Khosla, and Mei-Tai Chu, *Socially assistive robots in elderly care: A mixed-method systematic literature review*, International Journal of Humanâ€"Computer Interaction **30** (2014), no. 5, 369–393.

[71] Makoto Kaneko, Kensuke Harada, and Toshio Tsuji, *A sufficient condition for manipulation of envelope family*, Proceedings 2000 ICRA. Millennium Conference. IEEE International Conference on Robotics and Automation. Symposia Proceedings (Cat. No. 00CH37065), vol. 2, IEEE, 2000, pp. 1060–1067.

[72] Yuzo Kaneshige, Misato Nihei, and Masakatsu G Fujie, *Development of new mobility assistive robot for elderly people with body functional control*, Biomedical Robotics and Biomechatronics, 2006. BioRob 2006. The First IEEE/RAS-EMBS International Conference on, IEEE, 2006, pp. 118–123.

[73] Robert Katzman, Theodore Brown, Paula Fuld, Arthur Peck, Ruben Schechter, and Herbert Schimmel, *Validation of a short orientation-memory-concentration test of cognitive impairment.*, The American journal of psychiatry (1983).

[74] Monroe Kennedy, Kendall Queen, Dinesh Thakur, Kostas Daniilidis, and Vijay Kumar, *Precise Dispensing of Liquids Using Visual Feedback*, IEEE/RSJ 2017 International Conference on Intelligent Robots and Systems, IROS 2017 - Conference Proceedings (2017).

[75] Zeashan Hameed Khan, Afifa Siddique, and Chang Won Lee, *Robotics utilization for healthcare digitization in global covid-19 management*, International journal of environmental research and public health **17** (2020), no. 11, 3819.

[76] Rainer Kimmig, René HM Verheijen, Martin Rudnicki, et al., *Robot assisted surgery during the covid-19 pandemic, especially for gynecological cancer: a statement of the society of european robotic gynaecological surgery (sergs)*, Journal of gynecologic oncology **31** (2020), no. 3.

[77] Chih-Hung King, Tiffany L Chen, Advait Jain, and Charles C Kemp, *Towards an assistive robot that autonomously performs bed baths for patient hygiene*, Intelligent Robots and Systems (IROS), 2010 IEEE/RSJ International Conference on, IEEE, 2010, pp. 319–324.

[78] Vikash Kumar, Yuval Tassa, Tom Erez, and Emanuel Todorov, *Real-time behaviour synthesis for dynamic hand-manipulation*, 2014 IEEE International Conference on Robotics and Automation (ICRA), IEEE, 2014, pp. 6808–6815.

[79] Kenji Kurakata, Tazu Mizunami, Hiroshi Sato, and Yukio Inukai, *Effect of ageing on hearing thresholds in the low frequency region*, Journal of low frequency noise, vibration and active control **27** (2008), no. 3, 175–184.

[80] Zexiang Li, Ping Hsu, and Shankar Sastry, *Grasping and coordinated manipulation by a multifingered robot hand*, The International Journal of Robotics Research **8** (1989), no. 4, 33–50.

[81] Zheng Li, Jan Feiling, Hongliang Ren, and Haoyong Yu, *A novel tele-operated flexible robot targeted for minimally invasive robotic surgery*, Engineering **1** (2015), no. 1, 073–078.

[82] Alexander Libin and Jiska Cohen-Mansfield, *Therapeutic robocat for nursing home residents with dementia: preliminary inquiry*, American Journal of Alzheimer's Disease & Other Dementias® **19** (2004), no. 2, 111–116.

[83] Jong Hyun Lim, Andong Zhan, JeongGil Ko, Andreas Terzis, Sarah Szanton, and Laura Gitlin, *A closed-loop approach for improving the wellness of low-income elders at home using game consoles*, IEEE Communications Magazine **50** (2012), no. 1.

[84] Wing-Yue Geoffrey Louie, Jacob Li, Tiago Vaquero, and Goldie Nejat, *A focus group study on the design considerations and impressions of a socially assistive robot for long-term care*, Robot and Human Interactive Communication, 2014 RO-MAN: The 23rd IEEE International Symposium on, IEEE, 2014, pp. 237–242.

[85] F Lunardini, N Basilico, E Ambrosini, J Essenziale, R Mainetti, A Pedrocchi, K Daniele, M Marcucci, D Mari, S Ferrante, et al., *Exergaming for balance training, transparent monitoring, and social inclusion of community-dwelling elderly*, Research and Technologies for Society and Industry (RTSI), 2017 IEEE 3rd International Forum on, IEEE, 2017, pp. 1–5.

[86] John Lygeros, Claire Tomlin, and Shankar Sastry, *Hybrid systems: modeling, analysis and control*, Electronic Research Laboratory, University of California, Berkeley, CA, Tech. Rep. UCB/ERL M (1999).

[87] Kevin M Lynch, *Nonprehensile robotic manipulation: Controllability and planning*, Citeseer, 1996.

[88] ———, *Toppling manipulation*, Robotics and Automation, IEEE International Conference on, vol. 4, IEEE, 1999, pp. 2551–2557.

[89] Kevin M Lynch and Matthew T Mason, *Stable pushing: Mechanics, controllability, and planning*, The International Journal of Robotics Research **15** (1996), no. 6, 533–556.

[90] ———, *Dynamic manipulation with a one joint robot*, Proceedings of International Conference on Robotics and Automation, vol. 1, IEEE, 1997, pp. 359–366.

[91] ———, *Dynamic nonprehensile manipulation: Controllability, planning, and experiments*, The International Journal of Robotics Research **18** (1999), no. 1, 64–92.

[92] K.M. Lynch and F.C. Park, *Modern robotics*, Cambridge University Press, 2017.

[93] Raymond R Ma, Lael U Odhner, and Aaron M Dollar, *A modular, open-source 3d printed underactuated hand*, 2013 IEEE International Conference on Robotics and Automation, IEEE, 2013, pp. 2737–2743.

[94] Roshena MacPherson, Benjamin Hockman, Andrew Bylard, Matthew A Estrada, Mark R Cutkosky, and Marco Pavone, *Trajectory optimization for dynamic grasping in space using adhesive grippers*, Field and Service Robotics, Springer, 2018, pp. 49–64.

[95] Ronald Martin, Jaime Williams, Thomas Hadjistavropoulos, Heather D Hadjistavropoulos, and Michael MacLean, *A qualitative investigation of seniors' and caregivers' views on pain assessment and management.*, The Canadian journal of nursing research = Revue canadienne de recherche en sciences infirmières **37** (2005), no. 2, 142–64.

[96] Naresh Marturi, Marek Kopicki, Alireza Rastegarpanah, Vijaykumar Rajasekaran, Maxime Adjigble, Rustam Stolkin, Aleš Leonardis, and Yasemin Bekiroglu, *Dynamic grasp and trajectory planning for moving objects*, Autonomous Robots **43** (2019), no. 5, 1241–1256.

[97] Matthew T. Mason , *Mechanics of robotic manipulation*, MIT Press, Cambridge, MA, August 2001.

[98] Matthew T Mason, *Mechanics of robotic manipulation*, MIT press, 2001.

[99] Matthew T Mason and Kevin M Lynch, *Dynamic manipulation*, Proceedings of 1993 IEEE/RSJ International Conference on Intelligent Robots and Systems (IROS'93), vol. 1, IEEE, 1993, pp. 152–159.

[100] Matthew T Mason, Alberto Rodriguez, Siddhartha S Srinivasa, and Andrés S Vazquez, *Autonomous manipulation with a general-purpose simple hand*, The International Journal of Robotics Research **31** (2012), no. 5, 688–703.

[101] Rob McCarney, James Warner, Steve Iliffe, Robbert Van Haselen, Mark Griffin, and Peter Fisher, *The hawthorne effect: a randomised, controlled trial*, BMC medical research methodology **7** (2007), no. 1, 30.

[102] Derek McColl and Goldie Nejat, *Meal-time with a socially assistive robot and older adults at a long-term care facility*, Journal of Human-Robot Interaction **2** (2013), no. 1, 152–171.

[103] Ross Mead, Mark Yim, MJ Matarić, Simon Kim, and Braden McDorman, *Quori: A community-driven modular social robot platform for human-robot interaction*, 2015 International Conference on Social Robotics (ICSR 2015) Robot Design Competition, 2015.

[104] Janet C Mentes, *A typology of oral hydration problems exhibited by frail nursing home residents.*, Journal of gerontological nursing **32** (2006), no. 1, 13–9; quiz 20–1.

[105] Tekin Meriçli, Manuela Veloso, and H Levent Akın, *Push-manipulation of complex passive mobile objects using experimentally acquired motion models*, Autonomous Robots **38** (2015), no. 3, 317–329.

[106] Tekin A Mericli, Manuela Veloso, and H Levent Akin, *Achievable push-manipulation for complex passive mobile objects using past experience*, Proceedings of the 2013 international conference on Autonomous agents and multi-agent systems, 2013, pp. 71–78.

[107] Samer AL Moubayed, Gabriel Skantze, and Jonas Beskow, *The furhat back-projected humanoid head–lip reading, gaze and multi-party interaction*, International Journal of Humanoid Robotics **10** (2013), no. 01, 1350005.

[108] Caio Mucchiani, Monroe Kennedy, Mark Yim, and Jungwon Seo, *Object picking through in-hand manipulation using passive end-effectors with zero mobility*, IEEE Robotics and Automation Letters **3** (2018), no. 2, 1096–1103.

[109] Caio Mucchiani, Suneet Sharma, Megan Johnson, Justine Sefcik, Nicholas Vivio, Justin Huang, Pamela Cacchione, Michelle Johnson, Roshan Rai, Adrian Canoso, et al., *Evaluating older adults' interaction with a mobile assistive robot*, IEEE/RSJ International Conference on Intelligent Robots and Systems, IROS, 2017.

[110] Richard M Murray, *A mathematical introduction to robotic manipulation*, CRC press, 2017.

[111] Richard M Murray, Zexiang Li, and S Shankar Sastry, *A mathematical introduction to robotic manipulation*, CRC, 1994.

[112] Van-Duc Nguyen, *Constructing force- closure grasps*, The International Journal of Robotics Research **7** (1988), no. 3, 3–16.

[113] Van-Duc Nguyen, *Constructing force-closure grasps*, The International Journal of Robotics Research **7** (1988), no. 3, 3–16.

[114] _____, *Constructing force-closure grasps*, The International Journal of Robotics Research **7** (1988), no. 3, 3–16.

[115] Lael U Odhner, Leif P Jentoft, Mark R Claffee, Nicholas Corson, Yaroslav Tenzer, Raymond R Ma, Martin Buehler, Robert Kohout, Robert D Howe, and Aaron M Dollar, *A compliant, underactuated hand for robust manipulation*, The International Journal of Robotics Research **33** (2014), no. 5, 736–752.

[116] Department of Justice, *Ada standards for accessible design*, Title III regulation **28** (2010).

[117] Jennifer M Ortman, Victoria A Velkoff, Howard Hogan, et al., *An aging nation: the older population in the united states*, United States Census Bureau, Economics and Statistics Administration, US Department of Commerce, 2014.

[118] Matthew Piccoli and Mark Yim, *Anticogging: Torque ripple suppression, modeling, and parameter selection*, The International Journal of Robotics Research **35** (2016), no. 1-3, 148–160.

[119] Brennand Pierce, Takaaki Kuratate, Christian Vogl, and Gordon Cheng, *"mask-bot 2i": An active customisable robotic head with interchangeable face*, 2012 12th IEEE-RAS International Conference on Humanoid Robots (Humanoids 2012), IEEE, 2012, pp. 520–525.

[120] Joelle Pineau, Michael Montemerlo, Martha Pollack, Nicholas Roy, and Sebastian Thrun, *Towards robotic assistants in nursing homes: Challenges and results*, Robotics and autonomous systems **42** (2003), no. 3-4, 271–281.

[121] Nancy S Pollard, *Closure and quality equivalence for efficient synthesis of grasps from examples*, The International Journal of Robotics Research **23** (2004), no. 6, 595–613.

[122] Kathleen B Rager, *Self-care and the qualitative researcher: When collecting data can break your heart*, Educational Researcher **34** (2005), no. 4, 23–27.

[123] Kantilal P Rane, *Design and development of low cost humanoid robot with thermal temperature scanner for covid-19 virus preliminary identification*, International Journal **9** (2020), no. 3.

[124] Giovanni Rateni, Matteo Cianchetti, Gastone Ciuti, Arianna Menciassi, and Cecilia Laschi, *Design and development of a soft robotic gripper for manipulation in minimally invasive surgery: a proof of concept*, Meccanica **50** (2015), no. 11, 2855–2863.

[125] U. Reiser, C. Connette, J. Fischer, J. Kubacki, A. Bubeck, F. Weisshardt, T. Jacobs, C. Parlitz, M. Hägele, and A. Verl, *Care-o-bot®3 - creating a product vision for service robot applications by integrating design and technology*, 2009 IEEE/RSJ International Conference on Intelligent Robots and Systems, Oct 2009, pp. 1992–1998.

[126] Anthony Remazeilles, Christophe Leroux, and Gérard Chalubert, *Sam: a robotic butler for handicapped people*, Robot and Human Interactive Communication, 2008. RO-MAN 2008. The 17th IEEE International Symposium on, IEEE, 2008, pp. 315–321.

[127] Alfred A Rizzi and Daniel E Koditschek, *Progress in spatial robot juggling*, Robotics and Automation, 1992. Proceedings., 1992 IEEE International Conference on, IEEE, 1992, pp. 775–780.

[128] Máximo A Roa and Raúl Suárez, *Grasp quality measures: review and performance*, Autonomous robots **38** (2015), no. 1, 65–88.

[129] Máximo A Roa, Raúl Suárez, and Jan Rosell, *Grasp space generation using sampling and computation of independent regions*, 2008 IEEE/RSJ International Conference on Intelligent Robots and Systems, IEEE, 2008, pp. 2258–2263.

[130] Hayley Robinson, Bruce MacDonald, Ngaire Kerse, and Elizabeth Broadbent, *The psychosocial effects of a companion robot: a randomized controlled trial*, Journal of the American Medical Directors Association **14** (2013), no. 9, 661–667.

[131] A. Rodriguez, M.T. Mason, and S. Ferry, *From caging to grasping*, The International Journal of Robotics Research **31** (2012), no. 7, 886–900.

[132] Selma Sabanovic, Casey C Bennett, Wan-Ling Chang, and Lesa Huber, *Paro robot affects diverse interaction modalities in group sensory therapy for older adults with dementia*, Rehabilitation Robotics (ICORR), 2013 IEEE International Conference on, IEEE, 2013, pp. 1–6.

[133] Takeshi Sakaguchi, Masahiro Fujita, Hiroshi Watanabe, and Fumio Miyazaki, *Motion planning and control for a robot performer*, [1993] Proceedings IEEE International Conference on Robotics and Automation, IEEE, 1993, pp. 925–931.

[134] J Kenneth Salisbury and John J Craig, *Articulated hands: Force control and kinematic issues*, The International journal of Robotics research **1** (1982), no. 1, 4–17.

[135] Ashutosh Saxena, Justin Driemeyer, and Andrew Y Ng, *Robotic grasping of novel objects using vision*, The International Journal of Robotics Research **27** (2008), no. 2, 157–173.

[136] Philip Sedgwick, *The hawthorne effect*, Bmj **344** (2012).

[137] Justine S Sefcik, Michelle J Johnson, Mark Yim, Tessa Lau, Nicholas Vivio, Caio Mucchiani, and Pamela Z Cacchione, *Stakeholders' perceptions sought to inform the development of a low-cost mobile robot for older adults: A qualitative descriptive study*, Clinical Nursing Research **27** (2018), no. 1, 61–80.

[138] Jungwon Seo, Mark Yim, and Vijay Kumar, *A theory on grasping objects using effectors with curved contact surfaces and its application to whole-arm grasping*, The International Journal of Robotics Research **35** (2016), no. 9, 1080–1102.

[139] Zainab Shahid, Ricci Kalayanamitra, Brendan McClafferty, Douglas Kepko, Devyani Ramgobin, Ravi Patel, Chander Shekher Aggarwal, Ramarao Vunnam, Nitasa Sahu, Dhirisha Bhatt, et al., *Covid-19 and older adults: what we know*, Journal of the American Geriatrics Society **68** (2020), no. 5, 926–929.

[140] Yang Shen, Dejun Guo, Fei Long, Luis A Mateos, Houzhu Ding, Zhen Xiu, Randall B Hellman, Adam King, Shixun Chen, Chengkun Zhang, et al., *Robots under covid-19 pandemic: A comprehensive survey*, IEEE Access (2020).

[141] Feng-Ru Sheu, Yun-Lin Lee, Hsiu-Tao Hsu, and Nian-Shing Chen, *Effects of gesture-based fitness games on functional fitness of the elders*, Advanced Learning Technologies (ICALT), 2015 IEEE 15th International Conference on, IEEE, 2015, pp. 158–160.

[142] Jian Shi, J Zachary Woodruff, Paul B Umbanhowar, and Kevin M Lynch, *Dynamic in-hand sliding manipulation*, IEEE Transactions on Robotics **33** (2017), no. 4, 778–795.

[143] Karun B Shimoga, *Robot grasp synthesis algorithms: A survey*, The International Journal of Robotics Research **15** (1996), no. 3, 230–266.

[144] Masahiro Shiomi, Takamasa Iio, Koji Kamei, Chandraprakash Sharma, and Norihiro Hagita, *Effectiveness of social behaviors for autonomous wheelchair robot to support elderly people in japan*, PLOS ONE **10** (2015), no. 5, 1–15.

[145] Bruno Siciliano and Oussama Khatib, *Springer handbook of robotics*, Springer, 2016.

[146] Cory-Ann Smarr, Tracy L Mitzner, Jenay M Beer, Akanksha Prakash, Tiffany L Chen, Charles C Kemp, and Wendy A Rogers, *Domestic robots for older adults: attitudes, preferences, and potential*, International journal of social robotics **6** (2014), no. 2, 229–247.

[147] Gordon Smith, Eric Lee, Ken Goldberg, Karl Bohringer, and John Craig, *Computing parallel-jaw grips*, Robotics and Automation, IEEE International Conference on, vol. 3, IEEE, 1999, pp. 1897–1903.

[148] Don Sofge, Lynn Vogel, Yuchi Huang, and John Wentz, *Design and implementation of a multi-use manipulator system to improve shipyard manufacturing processes*, Journal of ship production **17** (2001), no. 3, 130–134.

[149] Jorge Solis, Teshome D Teshome, and Jose Pablo De la Rosa, *Towards developing a multipurpose assistive vehicle robot capable of providing assistance to caregivers and support to elderly people*, Automation Science and Engineering (CASE), 2015 IEEE International Conference on, IEEE, 2015, pp. 1145–1150.

[150] Andrew Specian, Nick Eckenstein, Mark Yim, Ross Mead, Braden McDorman, Simon Kim, and Maja Matarić, *Preliminary system and hardware design for quori, a low-cost, modular, socially interactive robot*, Workshop on social robots in the wild, 2018.

[151] Jeroen Spijker and John MacInnes, *Population ageing: the timebomb that isn't?*, Bmj **347** (2013), f6598.

[152] Will Taggart, Sherry Turkle, and Cory D Kidd, *An interactive robot in a nursing home: Preliminary remarks*, Towards Social Mechanisms of Android Science (2005), 56–61.

[153] Tapio Taipalus and Kazuhiro Kosuge, *Development of service robot for fetching objects in home environment*, Computational Intelligence in Robotics and Automation, 2005. CIRA 2005. Proceedings. 2005 IEEE International Symposium on, IEEE, 2005, pp. 451–456.

[154] Motoki Takagi, Yoshiyuki Takahashi, and Takashi Komeda, *A universal mobile robot for assistive tasks*, Rehabilitation Robotics, 2009. ICORR 2009. IEEE International Conference on, IEEE, 2009, pp. 524–528.

[155] Adriana Tapus, Cristian Tapus, and Maja Mataric, *Music therapist robot for people suffering from dementia: Longitudinal study*, Alzheimer's & Dementia: The Journal of the Alzheimer's Association **5** (2009), no. 4, P338.

[156] Adriana Tapus, Cristian Tapus, and Maja J Mataric, *The use of socially assistive robots in the design of intelligent cognitive therapies for people with dementia*, Rehabilitation Robotics, 2009. ICORR 2009. IEEE International Conference on, IEEE, 2009, pp. 924–929.

[157] Priyesh Tiwari, Jim Warren, Karen Day, Bruce A. MacDonald, Chandimal Jayawardena, I. Han Kuo, Aleksandar Igic, and Chandan Datta, *Feasibility study of a robotic medication assistant for the elderly*, AUIC, 2011.

[158] Pierre Tournassoud, Tomás Lozano-Pérez, and Emmanuel Mazer, *Regrasping*, Robotics and Automation. Proceedings. 1987 IEEE International Conference on, vol. 4, IEEE, 1987, pp. 1924–1928.

[159] K Tracht, S Hogreve, and S Bosse, *Intelligent interpretation of multiaxial gripper force sensors*, Proceedings of CIRP Conference on Assembly Technologies, CATS, vol. 2012, 2012.

[160] Jeffrey C Trinkle, *On the stability and instantaneous velocity of grasped frictionless objects*, Robotics and Automation, IEEE Transactions on **8** (1992), no. 5, 560–572.

[161] N Ulrich, *Grasping using fingers with coupled joints*, ASME Publ. DE-15-3, Trends and Developments in Mechanisms, Machines and Robotics, Proc. Mechanisms Conf., Kissimmee, 1988.

[162] M. Vahedi and A.F. van der Stappen, *Caging polygons with two and three fingers*, The International Journal of Robotics Research **27** (2008), no. 11-12, 1308–1324.

[163] HF Machiel Van der Loos, J Joseph Wagner, Niels Smaby, K Chang, Oscar Madrigal, Larry J Leifer, and Oussama Khatib, *Provar assistive robot system architecture*, Robotics and Automation, 1999. Proceedings. 1999 IEEE International Conference on, vol. 1, IEEE, 1999, pp. 741–746.

[164] A Frank Van der Stappen, Chantal Wentink, and Mark H Overmars, *Computing form-closure configurations*, Robotics and Automation, 1999. Proceedings. 1999 IEEE International Conference on, vol. 3, IEEE, 1999, pp. 1837–1842.

[165] Meaghann S Weaver, Brittany Wichman, Sue Bace, Denice Schroeder, Catherine Vail, Chris Wichman, and Andrew Macfadyen, *Measuring the impact of the home health nursing shortage on family caregivers of children receiving palliative care*, Journal of Hospice and Palliative Nursing **20** (2018), no. 3, 260.

[166] Robert J Webster III and Bryan A Jones, *Design and kinematic modeling of constant curvature continuum robots: A review*, The International Journal of Robotics Research **29** (2010), no. 13, 1661–1683.

[167] Wenqi Wei, Jianzong Wang, Jiteng Ma, Ning Cheng, and Jing Xiao, *A real-time robot-based auxiliary system for risk evaluation of covid-19 infection*, arXiv preprint arXiv:2008.07695 (2020).

[168] J Zachary Woodruff and Kevin M Lynch, *Planning and control for dynamic, nonprehensile, and hybrid manipulation tasks*, 2017 IEEE International Conference on Robotics and Automation (ICRA), IEEE, 2017, pp. 4066–4073.

[169] Takayoshi Yamada, Toshinori Ooba, Tomoya Yamamoto, Nobuharu Mimura, and Yasuyuki Funahashi, *Grasp stability analysis of two objects in two dimensions*, Proceedings of the 2005 IEEE International Conference on Robotics and Automation, IEEE, 2005, pp. 760–765.

[170] Takayoshi Yamada, Toshiya Taki, Manabu Yamada, and Hidehiko Yamamoto, *Grasp stability analysis of two objects by considering contact surface geometry in 3d*, 2011 IEEE International Conference on Robotics and Biomimetics, IEEE, 2011, pp. 1108–1115.

[171] Ajmal Zemmar, Andres M Lozano, and Bradley J Nelson, *The rise of robots in surgical environments during covid-19*, Nature Machine Intelligence **2** (2020), no. 10, 566–572.